Microcirculatory aspects of bisphosphonate-related osteonecrosis of the jaw

Ágnes Janovszky, M.D.

Ph.D. Thesis

Department of Oral and Maxillofacial Surgery,
Institute of Surgical Research,
University of Szeged, Hungary

Szeged, 2014

LIST OF PAPERS RELATED TO THE SUBJECT OF THE THESIS

I. Varga R, **Janovszky A**, Szabó A, Garab D, Bodnár D, Boros M, Neunzehn J, Wiesmann HP, Piffkó J. A novel method for *in vivo* visualization of the microcirculation of the mandibular periosteum in rats. Microcirculation. 2014;21(6):524-31. **IF: 2.763**

II. **Janovszky A**, Szabó A, Vereb T, Piffkó J. Current approaches for early detection and treatment of medication-related osteonecrosis of jaw. Orv Hetil. 2014 (in press). **IF: 0.14**

III. **Janovszky A**, Szabó A, Varga R, Garab D, Boros M, Mester C, Beretka N, Zombori T, Wiesmann HP, Bernhardt R, Ocsovszki I, Balázs P, Piffkó J. Periosteal microcirculatory reactions in a zoledronate-induced osteonecrosis model of the jaw in rats. Clin Oral Invest. 2014 (in press). **IF: 2.285**

ABSTRACT RELATED TO THE SUBJECTS OF THE THESIS

IV. **A Janovszky**, R Varga, A Szabó, D Garab, M Boros, J Piffkó. Microcirculatory consequences of chronic bisphosphonate treatment after tooth extraction in a rat model. Int J Oral Maxillo Surg. 2013;42:(11)1187.

CONTENTS

LIST OF ABBREVIATIONS

ANOVA	analysis of variance
BIS	bisphosphonate
CLSM	confocal laser scanning microscopy
CT	computer tomography
FITC	fluorescein isothiocyanate
H&E	hematoxylin-eosin
IL	interleukin
i.p.	intraperitoneally
i.v.	intravenously
IVM	intravital videomicroscopy
MRONJ	medication-related osteonecrosis of the jaw
OPS	orthogonal polarization spectral imaging
PMN	polymorphonuclear leukocyte
RANK	receptor activator of nuclear factor-κB
RANKL	receptor activator of nuclear factor-κB ligand
RBCV	red blood cell velocity
TNF-alpha	tumor necrosis factor-alpha
VEGF	vascular endothelial growth factor
ZOL	zoledronate

SUMMARY OF THE THESIS

Bisphosphonates (BISs) are widely used for the treatment of osteoporosis and tumors with bone metastasis to inhibit osteoclast activity and bone resorption. Although BIS treatment undoubtedly improves the quality of life, osteonecrosis is a rare, but serious adverse effect that occurs mainly after invasive dental procedures, e.g. tooth extraction, with an increased incidence particularly after the use of third-generation BISs (e.g. zoledronate, ZOL). BISs together with other antiresorptive and antiangiogenic drugs induce necrosis of the oral bones, usually referred to as medication-related osteonecrosis of the jaw (MRONJ), but bone destruction is also seen less frequently in other bones of the skeleton. We hypothesized that a disturbed mandibular microcirculation may play a role in the pathogenesis of MRONJ. In this context, we designed a rat model where chronic BIS treatment was combined with an invasive dental procedure and where the processes of mucosal healing and bone destruction resembled the clinical manifestations of MRONJ. ZOL was applied intravenously (in a dose of 80 μg/kg/week) over 8 weeks, the first two right mandibular molar teeth were extracted in the third week, and various systemic and local parameters of the inflammatory cascade were investigated 6 weeks after tooth extraction. The incidence and severity of the gingival lesions were determined on the basis of a new scoring system, while jaw osteonecrosis was diagnosed by means of computed micro tomography. We also developed a method by which the mandibular periosteum can be visualized relatively simply and highly reproducibly by means of different microscopy methods (fluorescence intravital microscopy, orthogonal spectral imaging and confocal laser scanning microscopy) in rats. Furthermore, we compared the effects of chronic ZOL administration on the mandibular and tibial periosteal microcirculatory reactions (with or without tooth extraction). Intravital fluorescence videomicroscopy revealed significantly increased leukocyte–endothelial interactions (leukocyte rolling and adhesion on the endothelial surface) in the mandibular periosteum, but not in the tibia. Only the leukocyte count and NADPH-oxidase activity of the leukocytes displayes significant reductions, the other systemic inflammatory parameters not being affected by ZOL. We conclude that chronic ZOL treatment causes a distinct microcirculatory inflammatory reaction in the mandibular periosteum, but not in the tibia. The local reaction in the absence of augmented systemic leukocyte inflammatory activity suggests that topically different, endothelium-specific changes may play a critical role in the pathogenesis of MRONJ.

1. INTRODUCTION

1.1. Inflammatory processes in the oral and maxillofacial region. The potential role of periosteal reactions

The oral cavity is particularly prone to inflammatory complications (e.g. periodontitis or abscesses), as it can be sensitively exposed to the external environment in the immediate vicinity of the teeth. The propagation of various infection-related inflammatory reactions within the soft tissues (e.g. sinusitis, phlegmon or intracranial abscesses) is at least partially due to the rich blood supply of the oral and maxillofacial region, favoring the spread of these inflammatory processes. A special nutritive aspect of the jaw (i.e. it is predominantly supplied by the periosteal circulation) also predisposes to various pathological conditions of the bones, ranging from abscess formation to the more severe osteomyelitis and osteonecrosis [Scoletta M 2010]. The present thesis is based on the assumption that morphological and functional changes in the microcirculation in the periosteum play a decisive role in the pathogenesis of various mandibular pathologies.

In general, the role of the periosteal integrity in bone physiology is well recognized, not only as it relates to the maintenance of the vascular supply, but also from the aspect of the active regulation of the bone metabolism and regeneration. It is similarly well known that successful healing after fractures requires the regeneration of the peri- and endosteal circulations [Macnab I 1974]. Likewise, periosteal damage leads to perturbed bone healing with consequent delayed union or pseudoarthrosis formation [Utvag SE 1998, Gustilo RB 1990, Esterhai JL 1991]. With regard to the mandible, clinical observations show that defective angiogenesis of the mandibular mucoperiosteal tissues is evoked by long-term treatment with bisphosphonate (BIS), resulting in severe conditions such as osteonecrosis of the jaw [Wehrhan F 2011]. It follows that periosteal microvascular alterations can be of importance in the pathomechanism of oral diseases associated with a deterioration of tissue perfusion and with inflammatory complications.

1.2. Special features of the jaw bones with respect to the blood and nerve supply and bone remodeling

The continuous blood supply of the bones is necessary in order to ensure physiological bone remodeling, metabolism and regeneration, but differences are observed within the skeletal system. While the appendicular long bones receive their vascular supply from the nutritive arteries, the epiphyseal and metaphyseal vessels [Hooper 1987, Johnson EO 2004, Findlay DM 2007], the circulation of the maxillofacial bones, and especially the

lower jaw, is provided by the mucoperiosteal tissue through the inferior alveolar and sublingual arteries [Huelke DF 1965, Shannon J 2011]. This underlines the role of the periosteum in the bone remodeling and regeneration processes of the jawbones [Støre G 1999, Elshahat A 2004]. The innervation pattern of the mandible also differs from that of appendicular long bones such as the tibia. The mandibular nerve, the third and inferior division of the trigeminal nerve, provides the innervation of the lower third of the maxillofacial region, containing both afferent and efferent fibers [Rodella LF 2012]. While networks of nerves spread across the surface of the mandible, the tibial periosteum displays a longitudinal orientation. Vasoactive intestinal polypeptide-positive nerve fibers also form small networks with individual fine varicose fibers in the mandibular periosteum, whereas larger networks are to be seen at the tibia. These fine fibers are associated with both vascular and nonvascular elements, suggesting specific functions in the mandibular periosteum [Hill EL 1991].

The jaw region additionally possesses particular regeneration and remodeling characteristics. As opposed to long bone fractures, which heal mainly through endochondral ossification, intramembranous ossification has a higher impact in the mandible [Yu YY 2012]. In line with this, periosteum-derived stem cells, which play an important role in the bony regeneration processes, have been shown to possess the highest osteogenic potential in the mandible, while tibial periosteum or bone marrow stem cells are superior in terms of chondrogenesis [Park JB 2012]. Further, mandible bone marrow stem cells have been demonstrated to have a marked capacity to induce bone formation both *in vitro* and *in vivo* [Aghaloo TL 2010]. The fact that this phenomenon may be observed *in vivo* [Schmidt BL 2002, Ueno T 2002] indicates that the mandible possesses a particularly high degree of osteogenesis potential among the different anatomical locations [Solheim E 1995]. It was recently shown that distinct differences in the expression pattern of bone development-related genes exist between mandibular and tibial osteoblasts [Reichert JC 2013]. Systemic disorders such as osteoporosis have also been reported to influence bone remodeling differently in the mandible and the tibia, the mandible being significantly less affected in experimental osteoporosis [Yamashiro T 1998, Mavropoulos A 2007, Liu H 2014]. Intense mechanical loading of the alveolar process during mastication may protect the alveolar bone from the osteoporosis-related bone loss observed at other skeletal sites [Mavropoulos A 2007].

BISs also exert unique effects on the bones in the maxillofacial region. The regional BIS uptake reaches a higher concentration in the mandible in comparison with the

appendicular and other axial bones [Wen D 2011]. The receptor activator of nuclear factor κB (RANK)/receptor activator of nuclear factor κB ligand (RANKL)/osteoprotegerin axis, a signaling pathway that regulates osteoclast differentiation and activation, is also diversely affected by BIS, causing a decrease in RANKL values in the mandible and the opposite effect in the tibia [Çankaya M 2013]. Furthermore, BIS treatment exerts site differential effects during the early healing processes of tibial and mandibular fractures by delaying callus, cartilage and bone remodeling specifically in the mandible [Yu YY 2012]. The potential regional differences in microcirculatory reactions, however, are less well clarified.

1.3. Microcirculatory inflammatory reactions

Acute inflammation is a complex biological response of the cells, tissues and organs to harmful stimuli, such as pathogens, damaged cells or irritants. Almost all of the cardinal symptoms (redness/*rubor*, swelling/*tumor*, increased heat/*calor*, pain/*dolor*, and loss of function/*functio laesa*) can be linked to changes in the microcirculation. Behind these symptoms, characteristic changes within the microcirculation can be evidenced such as (1) an impaired vasomotor function, (2) decreased capillary perfusion, (3) increased microvascular permeability, (4) activation of the coagulation cascade and enhanced thrombosis, and (5) the adherence of leukocytes and platelets.

Tissue trauma or ischemia–reperfusion brings about a very complex antigen-dependent or independent activation of the immune system. Briefly, infection, oxido-reductive stress or tissue disintegration (usually caused by free radical-mediated injury) creates noxious signals which lead to the release of pro-inflammatory cytokines such as complements, tumor necrosis factor-alpha (TNF-alpha) and interleukin-1 (IL-1) and -6 (IL-6) and also induce direct endothelial injury [Serrick C 1994, Kurose I 1997, Carden DL 2000, Loukas M 2008]. In the initial phase, a local hyperemic reaction occurs as a result of the rapid release of vasoactive mediators (histamine, bradykinin, neuropeptides, prostaglandins and nitric oxide) produced by inflammatory cells (mast cells, macrophages, fibroblasts, parenchymal and endothelial cells) [Cooper D 2002]. These changes are also associated with an increase in microvascular permeability/edema formation promoted by various mediators (histamine, bradykinin, leukotrienes, platelet activating factor, substance P and the vascular endothelial growth factor (VEGF)), the activation of neutrophil leukocytes resulting in further tissue injury through the transmigration of polymorphonuclear leukocytes (PMN) [for a review, see Kvietys PR 2012].

A complex activation of the inflammatory cascade is initiated through the release of chemoattractants, leading to the activation of PMNs and promoting their accumulation within and around the injured tissue. These processes result in the enhanced expression of various adhesion molecules on the surface of leukocytes and endothelial cells, such as immunoglobin-like adhesion receptors (intercellular adhesion molecule-1, platelet–endothelial cell adhesion molecule-1 and vascular cell adhesion molecule-1), integrins (CD11/CD18), and selectins (E-, P- and L-selectin) [Springer TA 1990, Eppihimer MJ 1997]. This is followed by the adhesion of PMNs and platelets to the activated endothelium, with the resultant development of cell-to-cell interactions (rolling, sticking and migration of PMNs) [Wanner GA 1996, Loukas M 2008]. The PMNs produce further reactive oxygen species via NADPH-oxidase and myeloperoxidase and release the lysosomal enzymes elastase, collagenase and phospholipase, which promote tissue necrosis and apoptosis [Cooper D 2002]. The propagation of inflammatory processes toward remote organs is mediated by activated PMNs or the spreading of pro-inflammatory cytokines [Springer TA 1990, Eltzschig HK 2004, Tapuria N 2008].

Free radicals, nitric oxide and PMNs have been shown to play a role in various oral inflammatory and neoplastic diseases [Battino M 1999, Scott DA 2012, Choudhari SK 2013]. Furthermore, inflammatory processes play a part not only in oral pathologies, but also in bone healing [Thomas MV 2011]. An increased release of pro-inflammatory cytokines has been demonstrated in chronically BIS-treated patients [Sharma D 2013].

1.4. Assessment of the periosteal microcirculatory reactions in intraoral and systemic diseases

Studies of the microcirculation in the oral region attracted considerable attention when the predictive value of mucosal perfusion deficits was demonstrated in septic shock patients [Verdant CL 2009, Top AP 2011]. Another intraoral manifestation of a systemic menace was revealed during cardiac surgery [Bauer A 2007] and the intraoral microcirculation proved to correlate well with the gastrointestinal perfusion changes [Verdant CL 2009]. On the other hand, oral infection may also exert systemic effects as the blood-borne oral lipopolysaccharides and oral bacteria have been shown to provoke the release of the cytokines (e.g. IL-6 and TNF-alpha), which in turn brings about an acute phase response [Williams RC 2005]. The periosteal microcirculatory aspects of systemic and intraoral diseases, however, have been far less well clarified.

The vascular architecture of the intraoral region, including the periosteum, can be examined by imaging methods such as computer tomography (CT), magnetic resonance imaging and to some extent scintigraphy or histology [Berggren A 1982, Nobuto T 1989, Bhatt R 2000, Fayad LM 2005].

Nevertheless, these tools are not relevant when dynamic changes or functional aspects of the periosteal microcirculation are to be investigated. The methods utilized for examinations of the functional characteristics of the microcirculation, such as hemoglobin absorptiometry combined with laser-Doppler flowmetry, may provide information on tissue oxygenation and perfusion, but in this case the tissue mass is rather robust, e.g. the gingival [Milstein DM 2013]. If more accurate detection or improved spatial resolution of the microcirculation is needed, fluorescence intravital microscopy (IVM) can provide an opportunity for real-time examination of the microcirculation of superficial layers of different organs. Conventional fluorescence IVM has many advantages. It can visualize not only changes in the efficacy of microvascular perfusion, but also leukocyte–endothelial interactions (such as rolling and adhesion), metabolic variables or signs of apoptosis [Horie Y 1996, Abshagen K 2006].

For observation of the microcirculation of superficial tissue layers, nonfluorescence techniques such as orthogonal polarization spectral imaging (OPS) [Groner W 1999] and sidestream dark-field imaging have also been developed [Milstein DM 2010]. These methods have the advantage that the use of fluorescence markers is not necessary and this allows the possibility of human applications in the oral cavity [Milstein DM 2010, De Backer D 2013]. Observation of the periosteal compartment would still necessitate surgical exposure, but the imaging of individual vessels and cells is possible without disturbing their functional characteristics.

The calvarian periosteum can be visualized in experimental settings [Stuehmer C 2009], but examination of the microcirculation of the jaw bones runs into many technical difficulties. We earlier developed methods suitable for visualization of the tibial periosteum and the synovial membrane in the knee joint in rats [Varga R 2008, Hartmann P 2012], but such approaches were not available for the exposure and *in vivo* investigation of the mandibular periosteum. We therefore considered it important to address this issue, in part to solve the technical problems and in part because the physiology or the pathophysiological reactions of the jaw may differ from those in other bones of the skeleton. Specifically, BISs have been demonstrated to cause osteonecrosis in the jaw after invasive dental procedures, but such reactions do not occur in the bones of the appendicular

skeleton [Stadelmann VA 2008, Blazsek J 2009]. This observation suggests that potentially different microcirculatory reactions may evolve in the periosteum at different anatomical locations. For this reason, in Study 1 we set out to compare the microcirculatory characteristics of the mandibular and the tibial periosteum through the use of a microsurgical approach and microscopic methods that are suitable for the *in vivo* visualization of individual microvessels.

1.5. Medication-related osteonecrosis of the jaw (MRONJ)

1.5.1. Pharmacology of BISs

BISs are widely used for the treatment of rheumatologic and oncological diseases with bone metastasis and are commonly administered in osteolytic conditions (e.g. Paget's disease and myeloma multiplex) [Ruggiero SL 2014].

BISs are pyrophosphate analogs in which oxygen is replaced by a carbon atom, resulting in a backbone P-C-P which is stable against enzymes with hydrolytic activity. Although BISs have a similar core structure, they also contain two side-chains or groups, R1 and R2, attached to the central carbon atom. All the recently developed BISs contain a hydroxy side-group at position R1, increasing their binding to bone. Differences in the physicochemical and biological properties of BISs are due to the differences in the R2 side-group, where the presence of nitrogen and its orientation within the R2 side-chain can influence their overall potency [Luckman SP 1998, Rodan GA 1998, Mönkkönen H 2006, Ebetino FH 2011, Rogers MJ 2011].

The BISs are generally classified as first- (e.g. etidronate, clodronate), second- (e.g. alendronate and pamidronate) or third-generation (e.g. zoledronate (ZOL), olpadronate and neridronate) compounds. The taxonomy of BISs based on their chemical structure, such as their nitrogen content, is clinically more relevant as more severe side-effects (i.e. osteonecrosis) have been attributed to BISs containing nitrogen [Marx RE 2003, Ruggiero SL 2014]. The main therapeutic effect of BISs is linked to the inhibition of the activity and apoptosis induction of osteoclasts altering the bone metabolism (Figure 1) [Rodan GA 1998, Brozoski MA 2012]. This leads to the inhibition of bone resorption and a reduction of bone turnover [Borozoski MA 2012], but the mechanism of action shows differences as a function of the nitrogen content. Non-nitrogen-containing BISs (etidronate and clodronate) are intracellularly incorporated, their accumulation leading to osteoclast apoptosis by inhibiting ATP-dependent enzymes [Rodan GA 1998, Rogers MJ 2011]. The more potent nitrogen-containing BISs (alendronate, ZOL and pamidronate) inhibit farnesyl

diphosphate synthase, which is responsible for an enzymatic process during the mevalonate pathway (cholesterol synthesis), inducing apoptosis and decreasing the functional activity of osteoclasts [Luckman SP 1998, Rodan GA 1998, Mönkkönen H 2006, Ebetino FH 2011, Rogers MJ 2011].

Depending on the therapeutic indication and the severity of the skeletal disorders, these drugs can be administered orally or intravenously (i.v.) in different doses and frequencies. However the biological utilization during gastrointestinal absorption is not appropriate (~ 1%), while 60% of i.v. administered BISs can bind to the bone surface [Ezra A 2000]. Owing to their long half-life (~ 10 years), the effects of BISs on bone remodeling can be evidenced for several years [Brozoski MA 2012].

Antiangiogenic effects of BISs are also known. This feature is particularly favorable in oncological cases, where this adjuvant treatment reduces tumor invasion and the progression of bone metastases. Antiangiogenic effects of BISs brought about by the modification of VEGF or VEGF receptor expressions or by other factors have been observed in both *in vitro* [Wood J 2002, Ziebart T 2013] and *in vivo* studies [Fournier P 2002, Bigi MM 2010, Guevarra CS 2013, Smidt-Hansen T 2013, Ohba T 2014, Pabst AM 2014]. BISs can inhibit the migration of different cell types, influencing regeneration [Koch FP 2011, Ziebart T 2013, Hagelauer N, 2014, Ohba T 2014], and also modulate immunological processes [Fujimura T 2013, Sasaki O 2013, Kalyan S 2014].

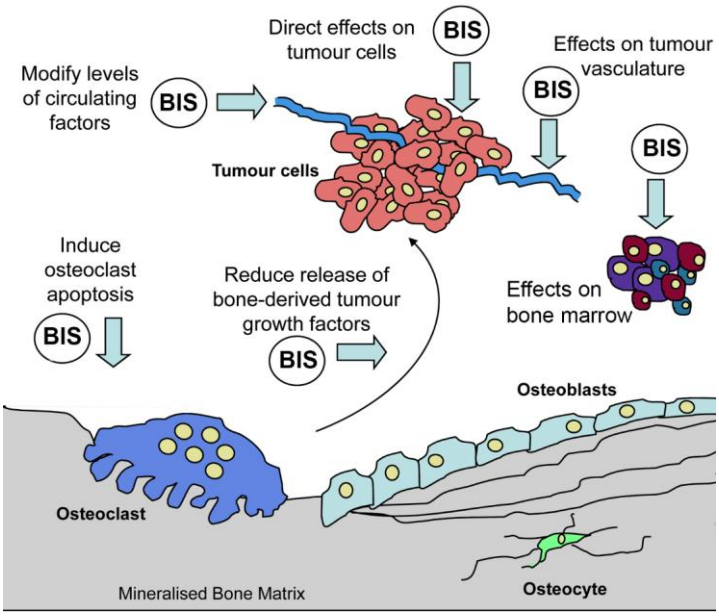

Figure 1. The effects of BIS [based on Holen I 2010]

1.5.2. Side-effects of BISs. Osteonecrosis of the jaw

Treatment with BISs induces various side-effects with relatively high incidence. These include influenza-like symptoms after the first BIS administration, but mucosal irritation, hypocalcemia, cardiac conduction disturbances and an impaired renal function have also been reported [Bunyaratavej N 2009, Han GY 2009, Rossini M 2013].

Although BIS treatment undoubtedly improves the quality of life of the patients [Endo N 2012, Kerschan-Schindl K 2012, Wilson S 2012], osteonecrosis is a serious adverse effect in a number of cases [Kühl S 2012, Yamashita J 2012]. BIS-related osteonecrosis of the jaw was first reported in 2003 [Marx RE 2003], but it was later proven that other antiresorptive (e.g. denosumab) [Aghaloo TL 2010, Niibe K 2014, O'Halloran M 2014, Vyas S 2014] and antiangiogenic (e.g. bevacizumab or sunitinib) drugs [Serra E 2009, Van Poznak C 2010, Koch FP 2011] also bring about MRONJ [Ruggiero SL 2014]. This occurs mainly after invasive dental procedures, e.g. tooth extraction or a periodontal disorder [Kang B 2013, Ruggiero SL 2014], with an increased incidence particularly after the use of third-generation BISs (e.g. ZOL) [Drozdzowska B 2011, Brozoski MA 2012]. MRONJ occurs predominantly in molar and premolar regions in the mandible [Ruggiero SL 2009, Otto S 2012].

The most recently position paper published by the American Association of Oral and Maxillofacial Surgeons specifies that MRONJ can be divided into the following stages with (a)typical symptoms (Table 1) [Ruggiero SL 2014]:

Stages	Common complaints of the patient	Clinical manifestations	Radiological findings
Patients at risk	no apparent necrotic bone in asymptomatic patients treated orally or i.v. with an antiresorptive or antiangiogenic drug		
0	atypical symptoms (odontalgia, dull, aching bone pain, sinus pain)	no necrotic bone, loosening of teeth, periapical/periodontal fistula without pulpal necrosis	alveolar bone loss, changes in trabecular pattern, osteosclerosis, periodontal ligament thickening (Figure 2A)
1	no symptoms	exposed and necrotic bone, or fistula without signs of infection	see above
2	pain	see above + infection	see above
3	pain	see above + osteolysis (Figure 2B)	see above

Table 1. Stages of MRONJ [Ruggiero SL 2014].

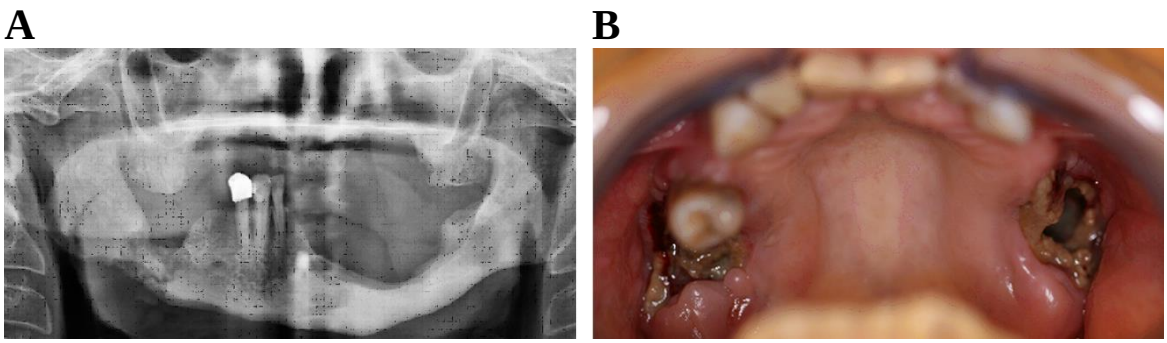

Figure 2. Radiological manifestation of the osteonecrosis on the right side of the mandible in a BIS-treated patient (A). Clinical manifestation of bilateral, extended osteonecrosis of the maxilla in another BIS-treated patient (B).

Many theories and risk factors have been taken into account during examinations of the pathogenesis of MRONJ [Mehrotra B 2006]. The epidemiological data on MRONJ are often not comparable because of its multifactorial etiology [Yamashita J 2010]; insomuch as it can be influenced by the administered drug (orally or i.v., non-/nitrogen-containing BIS), the duration of the therapy, the indication of BIS administration (osteoporosis, oncological reason or other), co-morbidities, the concomitant use of other drugs (corticosteroids or chemotherapeutic drugs), poor oral hygiene, genetic factors (CYP2C8) [Sarasquete ME 2009], age, an invasive dental procedure and other conditions [Drozdzowska B 2011, Brozoski MA 2012, Ruggiero SL 2014]. Local contamination and infection evoked by invasive dental procedures in the presence of BIS treatment have also been emphasized in the development of MRONJ [Mawardi H 2011, Wei X 2012], since BISs can take part in the development of biofilm formation [Sedghizadeh PP 2008, Kumar SK 2010]. Osteonecrosis, however, can develop several years later, which may be explained by the long half-lives of these medications [Brozoski MA 2012] and not by the acute infectious induction. Moreover, BIS treatment has been shown to cause sterile inflammatory reactions such as aseptic peritonitis [Calligeros D 1993, Norton JT 2011] and an enhancement of leukocyte–endothelial cell interactions in the knee joint [Zysk SP 2003]. These effects may be linked to an upregulation of pro-inflammatory cytokines such as IL-1 and TNF-alpha [Zysk SP 2003, Norton JT 2011, Anastasilakis AD 2012] in response to BIS administration. The effects of BIS also show spatial differences, because certain inflammatory reactions were confined to the mandible, but were not present in the femur [Senel FC 2010]. In another model, the stability of femoral implants was even enhanced after BIS treatment [Stadelmann VA 2008]. Nevertheless, the exact pathomechanism of

MRONJ has not yet been clarified, and the possibilities of its prevention or the use of curative modalities are also limited.

Tooth extraction is normally accompanied by tissue ischemia, which initiates a cascade of inflammatory reactions promoting the expression of different hypoxia-induced angiogenic substances [Sharma D 2013]. Among these factors, a considerable contribution of VEGF in the pathogenesis of MRONJ can be presumed. Specifically, antibodies against VEGF alone induce osteonecrosis of the mandible [Pakosch D 2012] and bevacizumab increases the incidence of MRONJ [Aragon-Ching JB 2009]. The predictive value of plasma VEGF levels regarding the risk of MRONJ has also been assumed [Vincenzi B 2012]. Further, BIS treatment has been shown to downregulate the expression of angiogenic factors, with the simultaneous upregulation of inflammatory cytokines [Mozzati M 2012]. This is supported by the fact that BIS treatment combined with an anti-angiogenic drug (bevacizumab) can also increase the prevalence of MRONJ [Aragon-Ching JB 2009].

The periosteal perfusion significantly influences bone healing and determines the prognosis of adjacent soft tissue traumas as well [Schaser KD 2003]. However, little is known about the microcirculatory effects of BIS, and especially the microcirculation of the mandible. Likewise, no data are available to date on the periosteal changes after invasive dental procedures involving BIS treatment. In Study 2, we hypothesized that a disturbed mandibular microcirculation may play a role in the pathogenesis of MRONJ.

2. MAIN GOALS

The main goals of the present studies were:

1. To develop a novel microsurgical procedure for the *in vivo* visualization of the mandibular periosteal microcirculation through the use of different microscopy methods (fluorescence IVM, OPS and confocal laser scanning microscopy (CLSM)) in rats.
2. To examine the systemic and local mandibular periosteal inflammatory microcirculatory reactions in comparison with those in the tibia in a clinically relevant model of BIS-induced MRONJ in rats.

3. MATERIALS AND METHODS

All chemicals were purchased from Sigma Aldrich (St. Louis, MO, USA) unless indicated otherwise. The study was performed in accordance with the Guidelines laid down by the National Institutes of Health (NIH) in the USA regarding the care and use of animals for experimental procedures, and with the 2010/63/EU Directive and was approved by the Animal Welfare Committee of the University of Szeged (V/1639/2013).

3.1. Microsurgical exposure of the mandibular and tibial periosteum for *in vivo* microscopic examinations

Sprague-Dawley rats (their average weight at the time of the experiment was 320 ± 10 g) were anesthetized intraperitoneally (i.p.) with an initial dose of sodium pentobarbital (45 mg/kg). After cannulation of the trachea, the penile vein was cannulated to administer fluids and drugs (supplementary dose of sodium pentobarbital: 5 mg/kg). During preparation and microcirculatory investigations, the rats were placed in a supine position on a heating pad to maintain the body temperature at 36-37 °C.

For *in vivo* examination of the mandibular periosteum, the fur of the animals in the mandibular region was shaved, and a lateral incision parallel to the incisor tooth was made in the facial skin and the underlying subcutaneous tissue, using a careful microsurgical approach under an operating microscope (6x magnification; Carl Zeiss GmbH, Jena, Germany). The masseter muscle consists of superficial and deep parts, the latter being further divided into anterior and posterior sections in rats [Cox PG 2011]. The fascia between the anterior part of the deep masseter and the anterior superficial masseter was cut with microscissors (Figure 3A). By this means, the periosteal membrane covering the corpus of the mandible laterally to the incisor tooth was reached and it was gently separated from the covering thin connective tissue (Figure 3B). Stitches with 7.0 monofilament polypropylene microsurgical thread were placed into the surrounding masseter muscles for retraction and better exposure of the region of interest. We applied this surgical approach on both sides of the lower jaw. With this preparation technique, the periosteal microcirculation of the mandible could be examined by *in vivo* microscopic methods at the anterior margin of the molar region.

The medial/anterior surface of the tibia was exposed by complete transection of the anterior gracilis muscle with microscissors, and careful atraumatic microsurgical removal of the connective tissue covering the tibial periosteum (Figure 3C,D) [Varga R 2008].

3.2. Experimental protocols

3.2.1. Protocol for *in vivo* examination of the microcirculatory characteristics of the mandibular periosteum using different microscopic approaches in rats

In Study 1, 10 male Sprague-Dawley rats were used. After the surgical procedures and exposure of the mandibular and tibial periosteum on both sides, recordings were performed on the right side with OPS, which does not require any fluorescence labeling. After this, the animals received i.v. injections of fluorescein isothiocyanate (FITC)-labeled erythrocytes (0.2 mL; Sigma Aldrich) (Figure 5A,B) [Ruh J 1998] and rhodamine-6G (0.2%, 0.1 mL; Sigma Aldrich) for the staining of leukocytes (Figure 3C,D), and IVM recording was performed at the previous locations. Subsequently, 50 μL of the nuclear dye acriflavin (1 mM) was applied topically to the tibial periosteal surface on the left side, and rinsed off with warm physiological saline solution after an exposure time of 1 min, and CLSM recording was then performed (Figure 6B). The same staining procedure was carried out for the mandible on the left side (Figure 6A). This was followed by an i.v. injection of the plasma dye FITC-dextran 150 kDa (0.3 mL, 20 mg/mL solution dissolved in saline; Sigma Aldrich), and CLSM (Figure 6C,D) and IVM recordings (Figure 5E,F) were made on the tibia and the mandible on the right side 5 min after the injection of the tracer.

The exposed periosteum of the corpus of the mandible or the tibial periosteum on the right side was positioned horizontally on an adjustable stage and superfused with 37 °C saline. The periosteal membranes were first visualized with an OPS device (Cytoscan™, Cytometrics, PA, USA), which provides optimal imaging of the microvascular structures at a chosen focus level (penetration depth: approx. 200 μm [Groner W 1999]) (Figure 4A,B). This technique utilizes epi-illumination with linearly polarized light at 548 nm (which is the isobestic point of oxy- and deoxyhemoglobin) to visualize hemoglobin-containing structures without the additional use of a fluorochrome. Images were recorded on a SVHS video recorder (Panasonic AG-MD 830; Matsushita Electric Industrial Co., Tokyo, Japan) and a personal computer.

Confocal imaging of the surface of the mandibular and tibial periosteum was performed with a Five1 Optiscan device (Optiscan Pty. Ltd., Melbourne, Victoria, Australia) (Figure 6). *In vivo* histology was employed by placing the Optiscan probe on the surface of the periosteal membranes and by changing the focus level through virtual sections of 7 μm during the confocal imaging (penetration depth: 0-250 μm). Cell nuclei were first stained with topically applied acriflavin (see above) on the left side, and this was

followed by recordings on the contralateral side after i.v. injection of the intravascular tracer FITC-dextran (see above). Images were stored on a personal computer provided by the manufacturer.

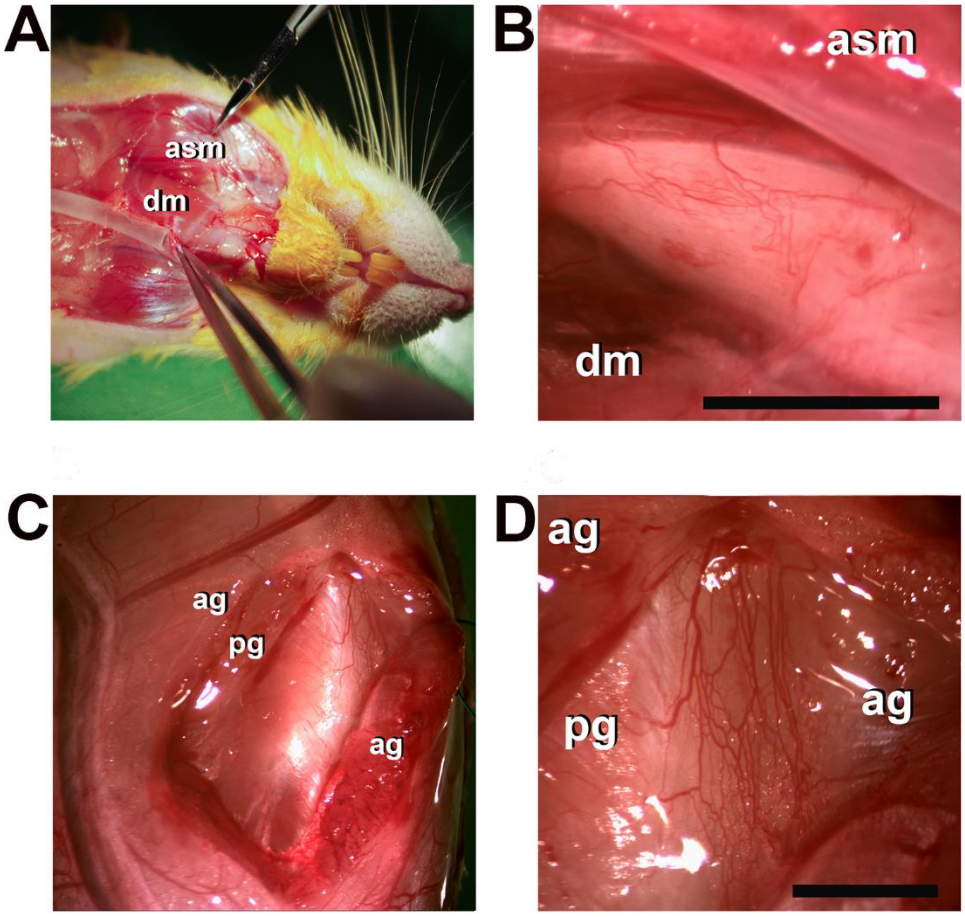

Figure 3. Exposure of the mandibular and tibial periosteum for *in vivo* microscopic examinations. Access to the mandibular periosteum was achieved by making a lateral incision parallel to the incisor tooth in the facial skin and the underlying subcutaneous tissue, which was followed by gentle separation of the fascia between the anterior part of the deep masseter (dm) and the anterior superficial masseter (asm) muscles (A, B). Finally, the thin connective tissue covering the periosteum was gently incised with microscissors. By this means, the periosteal membrane covering the corpus of the mandible laterally to the incisor tooth was reached. The tibial periosteum was reached by transecting the anterior gracilis (ag) muscle completely in the middle (and a part of the posterior gracilis muscle (pg) too) and gently removing the thin connective tissue covering the periosteum (C, D). The bar denotes 2,500 μm.

3.2.2. Protocol for the induction of BIS-induced osteonecrosis and examination of its periosteal microcirculatory consequences in rats

In Study 2, 20 male Sprague-Dawley rats were randomly allocated to saline vehicle-treated control (n=10), or i.v. ZOL-treated (n=10, ZOL) groups. ZOL (Zometa®; Novartis Europharm, Budapest, Hungary) was administered through a tail vein in a dose of 80 μg/kg

once a week for 8 weeks. At the end of the 3rd week of the protocol, the first and second molar teeth on the right side were extracted from the mandible under ketamine and xylazine (i.p. 25 and 75 mg/kg, respectively) anesthesia. The teeth were luxated with an 18G needle and the extraction was performed with extraction forceps. The roots were also removed with a dental drill under a Zeiss operating microscope (6x magnification, Carl Zeiss GmbH, Jena, Germany). By these means, the defect was equal in size and severity in all rats. For pain relief, intramuscular ketoprofen (Ketodex Forte, Berlin-Chemie AG, Berlin, Germany; 5 mg/kg) and oral metamizole sodium (Algopyrin, Sanofi-Aventis, Budapest, Hungary; 75 mg/kg) were administered for 3 days. Mucosal healing processes were monitored continuously throughout the experimental period. Through fluorescence IVM, the microcirculatory variables were compared in the mandibular and tibial periosteum in the 9th week of the protocol. FITC-labeled erythrocytes (0.2 mL i.v.) were used to stain red blood cells, and rhodamine-6G (0.2%, 0.1 mL i.v.) to stain leukocytes. Leukocyte function/activation and inflammation were examined by assessing the NADPH-oxidase activity of neutrophil leukocytes, whole blood free radical production, the expression of CD11b adhesion molecule on neutrophil leukocytes and the plasma TNF-alpha content. The incidence and severity of mucosal lesions were also assessed. Mandibular osteonecrosis was evidenced by computed microCT analysis and standard histology (see later).

3.3. Methods for the visualization of the mandibular and tibial periosteal microcirculation

3.3.1. OPS technique

In Study 1, the periosteal membranes were first visualized with an OPS device (Cytoscan™, Cytometrics, Philadelphia, PA, USA), which provides optimal imaging of the microvascular structures at a chosen focus level (penetration depth: approx. 200 μm; [Groner W 1999]) (Figure 4 A,B). This technique utilizes epi-illumination with linearly polarized light at 548 nm (which is the isobestic point of oxy- and deoxyhemoglobin) to visualize hemoglobin-containing structures without the additional use of a fluorochrome. Images were recorded on a SVHS video recorder (Panasonic AG-MD 830; Matsushita Electric Industrial Co., Tokyo, Japan) and a personal computer.

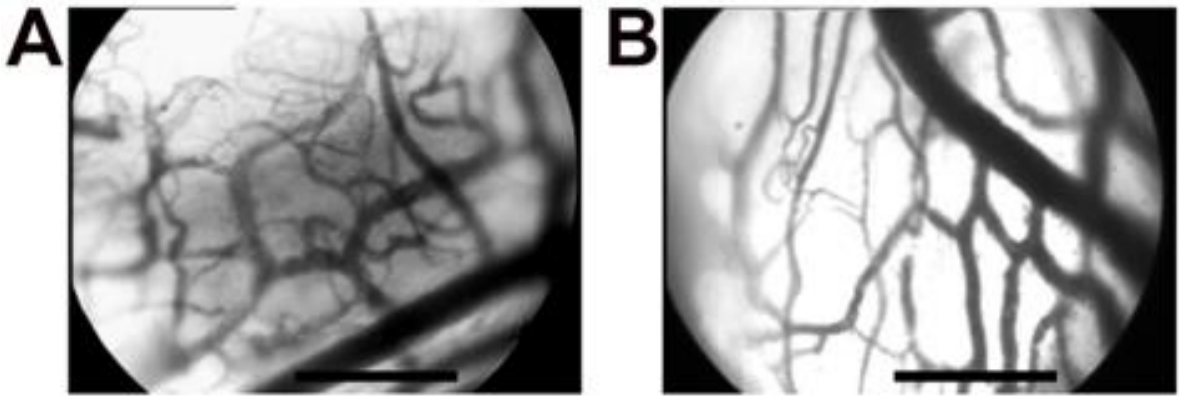

Figure 4. Micrographs showing the mandibular (A) and tibial (B) periosteum, made with the OPS imaging technique. The bar denotes 200 μm.

3.3.2. Fluorescence IVM

In both studies, the periosteal microcirculation was visualized by IVM (penetration depth: approx. 250 μm; Zeiss Axiotech Vario 100HD microscope; 100-W HBO mercury lamp; Acroplan 20 x / 0.5 N.A. W, Carl Zeiss GmbH, Jena, Germany). Images from 3 or 4 fields of the mandibular and the tibial periosteum (Figure 5) were recorded with a charge-coupled device video camera (Teli CS8320Bi, Toshiba Teli Corporation, Osaka, Japan) attached to an S-VHS video-recorder (Panasonic AG-MD 830; Matsushita Electric Industrial Co., Tokyo, Japan) and a personal computer (see the labeling techniques above).

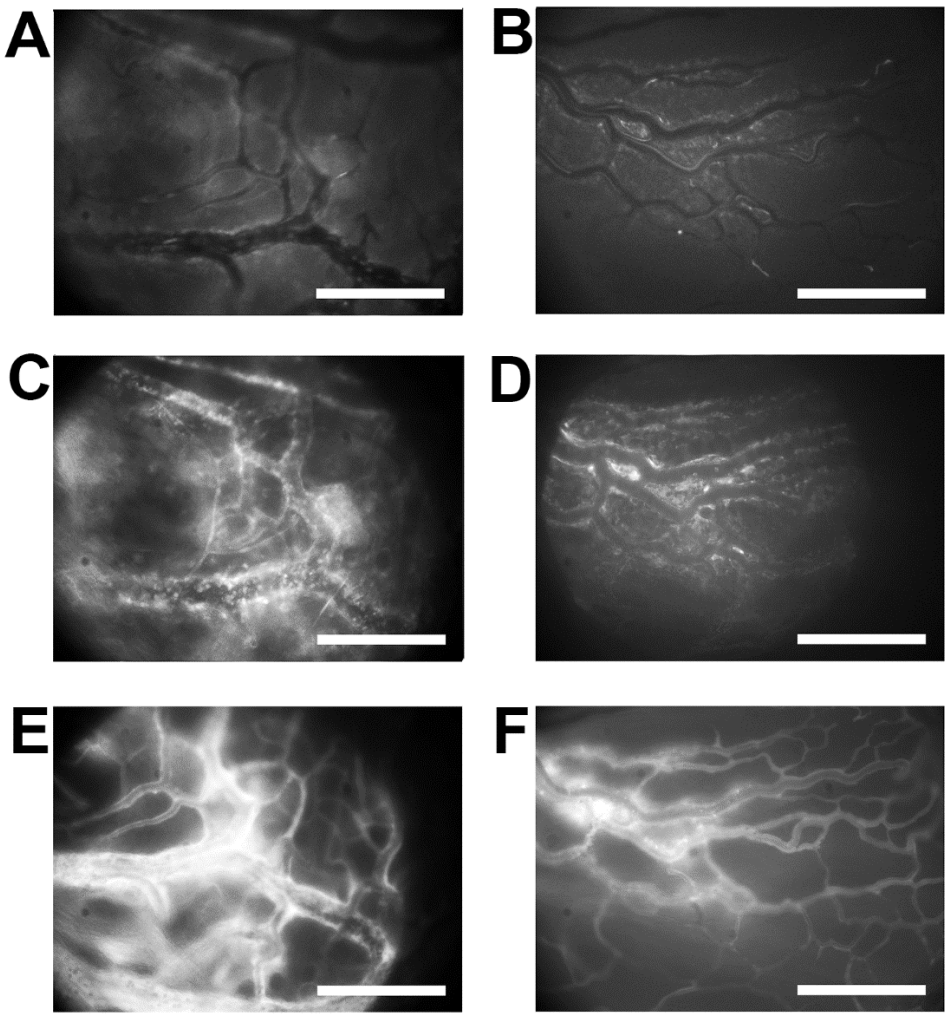

Figure 5. Fluorescence IVM images of the mandibular (A, C, E) and the tibial (B, D, F) periosteum, involving FITC-labeled erythrocytes (A, B), rhodamine 6G-labeled neutrophil leukocytes (C, D) and FITC-dextran-labeled plasma (E, F). The bar denotes 200 μm.

3.3.3. Fluorescence CLSM

In Study 1, confocal imaging of the surface of the mandibular and tibial periosteum was performed with a Five1 Optiscan device (Optiscan Pty. Ltd., Melbourne, Victoria, Australia) (Figure 6). *In vivo* histology was employed by placing the Optiscan probe on the surface of the periosteal membranes and by changing the focus level through virtual sections of 7 μm during the confocal imaging (penetration depth: 0-250 μm). Cell nuclei were first stained with topically applied acriflavin (see above) on the left side, and this was followed by recordings on the contralateral side after i.v. injection of the intravascular tracer FITC-dextran (see above). Images were stored on a personal computer provided by the manufacturer.

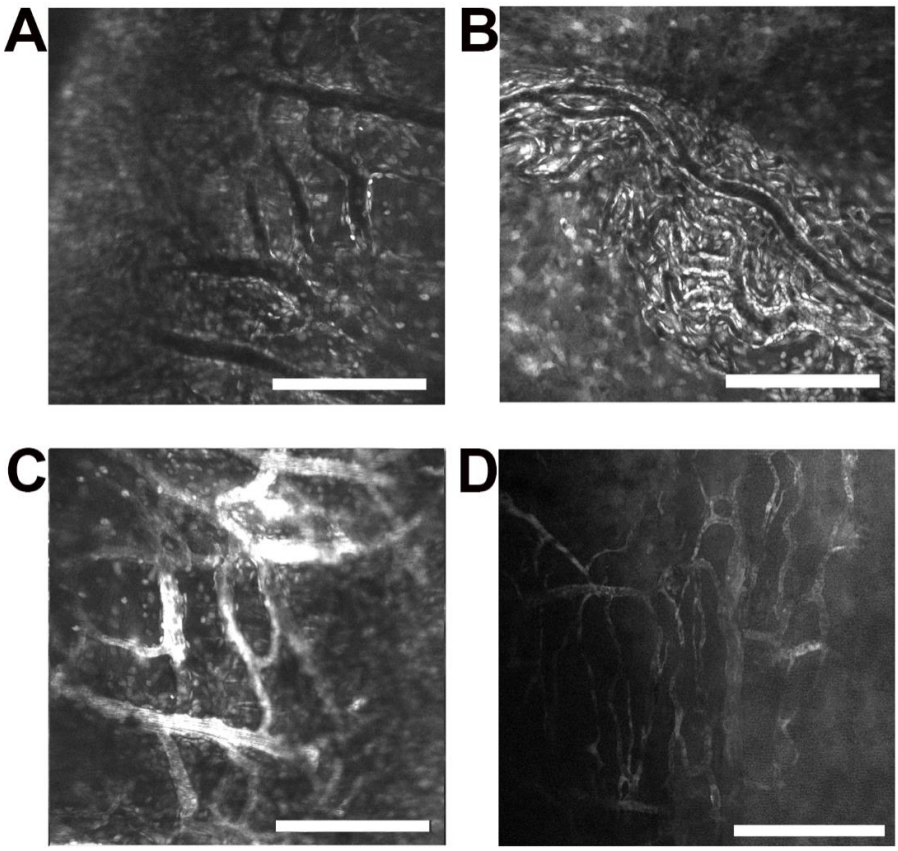

Figure 6. CLSM images of the mandibular (A, C) and tibial (B, D) periosteum. Cell nuclei were labeled by the topical application of acriflavin (left side) (A, B). Images were also taken at both structures on the right sides after the i.v. injection of FITC-dextran (C, D). The bar denotes 200 μm.

3.3.4. Video analysis

Quantitative evaluation of the microcirculatory parameters was performed off-line by frame-to-frame analysis of the videotaped images taken for IVM and OPS (IVM Software; Pictron Ltd, Budapest, Hungary). Leukocyte–endothelial cell interactions were analyzed in at least in 4 postcapillary venules per rat. Rolling leukocytes were defined as cells moving with a velocity less than 40% of that of the erythrocytes in the centerline of the microvessel and passing through the observed vessel segment within 30 s, and are given as the number of cells per second per vessel circumference. Adherent leukocytes were defined as cells that did not move or detach from the endothelial lining within an observation period of 30 s and are given as the number of cells per mm^2 of endothelial surface, calculated from the diameter and length of the vessel segment. Red blood cell velocity (RBCV, μm/s) was determined by frame-to-frame analysis of 5-6 consecutive video-captured images taken after labeling of the erythrocytes (see above).

3.4. Measurement of systemic inflammatory parameters

3.4.1. Leukocyte count

1.5 mL of blood was collected from the penile vein in a tube with EDTA and was held on ice. 100 μL was mixed with Turks solution (0.2 mg gentian violet in 1 mL of glacial acetic acid, 6.25% v/v) in 1:20 dilution. Leukocytes were determined as monomorphonuclear cells and PMNs in a hematocytometer.

3.4.2. Flow cytometric analysis of CD11b expression changes

The surface expression of CD11b on the peripheral blood granulocytes was determined by flow cytometric analysis as detailed elsewhere [Szabó A 2011]. One-hundred μL of whole blood was incubated with 20 μL of FITC-conjugated mouse anti-rat CD11b monoclonal antibody (BD Pharmingen, San Jose, CA, USA) for 20 min. Negative controls were obtained by omitting the antibody. The cells were then washed twice in Hanks buffer and centrifuged at 13,500 rpm for 5 min and the pellet was resuspended. The erythrocytes were lyzed with a Lysing kit (Biodesign, Saco, ME, USA), after which the cells were washed twice again (6,000 rpm, 5 min) and resuspended in 750 μL of Hanks buffer. Computer-assisted FACStar Plus Becton-Dickinson equipment was used for cytometry; the granulocytes were gated on the basis of their characteristic forward and side-scatter features. Generally, 10,000 events per sample were collected and recorded; the percentage of labeled (activated) granulocytes (relative to the overall marker-bearing cells) and the mean fluorescence intensity (average marker density) were calculated [Szabó A 2011]

3.4.3. Leukocyte NADPH-oxidase activity

The NADPH-oxidase activity of isolated leukocytes was determined by a modified chemiluminometric procedure [Bencsik P 2010]. Blood was drawn from the femoral artery into EDTA-containing tubes, and the erythrocytes in 100 μL of whole blood were lyzed in a hypotonic solution and centrifuged at 2,000 g. The pellet was resuspended and washed twice in Dulbecco's phosphate-buffered saline solution. Twenty μL of resuspended pellet was incubated for 3 min at 37 °C in a Dulbecco's solution containing lucigenin (1 mM), EGTA (1 mM) and saccharose (140 mM). NADPH-oxidase activity was determined via the NADPH-dependent increase in luminescence elicited by adding 100 mM NADPH (in 20 μL) with an FB12 Single Tube Luminometer (Berthold Detection Systems GmbH, Bad Wildbad, Germany). Samples incubated in the presence of nitroblue tetrazolium served as

controls. The measurements were performed in triplicates and were normalized for protein content.

3.4.4. Free radical-producing capacity of the blood

10 µL of blood dissolved in Hanks buffer was incubated for 20 min at 37 °C in lucigenin (5 mM; dissolved in Hanks buffer) or luminol (15 mM; dissolved in Hanks buffer) solutions in the presence or absence of zymozan (190 µM, dissolved in Hanks buffer). Superoxide and hydrogen peroxide productions were estimated via the rate of zymozan-induced increase in chemiluminescence (measured with the above luminometer) and normalized for leukocyte counts in the peripheral blood.

3.4.5. Plasma TNF-alpha levels

Blood samples were centrifuged at 13,500 rpm for 5 min at 4 °C and then stored at -70 °C until assay. Plasma TNF-alpha concentration were determined in duplicate by means of a commercially available enzyme-linked immunosorbent assay kit (R&D Systems, Minneapolis, MN, USA).

3.5. Assessment of morphological changes

3.5.1. Detection of gingival healing processes

Healing of the gingiva at the end of the study period (6 weeks after the tooth extraction) was determined on the basis of the osteonecrosis staging system provided by the American Association of Oral and Maxillofacial Surgeons [Ruggiero SL 2014]; this was adapted for rats (see Table 2). The examination was performed under an operating microscope (6x magnification; Carl Zeiss GmbH, Jena, Germany) by an independent maxillofacial surgeon. The incidence and the severity of the gingival healing disorder were evaluated simultaneously.

Score	Exposed bone	Inflammation/infection	Fistula formation
Score 0	-	-	-
Score 1	+	-	-
Score 2	+	+	-
Score 3	+	+	+

Table 2. Scoring of macroscopic signs of the BIS-related healing processes after tooth extraction (adopted from the staging of MRONJ by Ruggiero et al. [Ruggiero SL 2014])

3.5.2. Detection of osteonecrosis through the use of microCT

Mandibles fixed with formaldehyde were used for micro-CT imaging (SCANCO vivaCT 75, Scanco Medical, Brüttisellen, Switzerland); subsequent analysis was performed on 2D sections in the coronal view of the images, the section being chosen that showed the highest degree of tissue defect at the earlier extraction site. The mean density of the bone was estimated via the calculated percentage of the radiolucent area of the alveolar portion of the bone.

3.5.3. Detection of osteonecrosis through the use of histological analysis

The specimens were fixed in 6% neutral buffered formalin for 10 days, then rinsed in phosphate-buffered saline and decalcified in 5% EDTA for 7 days. The decalcified specimens were embedded in paraffin and cut into 20 semi-serial sections with a microtome (Shandon Finesse 325, Thermo Scientific, Waltham, MA, USA), and routine hematoxylin and eosin (H&E) staining was performed. The sections were examined under a light microscope at 4-40x magnification (Modell CHT, Olympos, Hamburg, Germany). The incidence of osteonecrosis of the jaw was determined on the basis of characteristic signs of necrosis, such as missing nuclear staining, the development of sequester formation and inflammatory infiltration.

3.6. Statistical analyses

The statistical analyses were performed with a statistical software package (SigmaStat for Windows, Jandel Scientific, Erkrath, Germany). For the analysis of microcirculatory parameters, changes in variables within and between groups (with respect to location and treatment, separately) were analyzed by the two-way analysis of varience (ANOVA) test, followed by the Holm–Sidak test. Differences between groups (other inflammatory parameters, and scores) were analyzed with Student’s t-test. Data are presented as mean values and SEM in all Figures and Tables. P values < 0.05 were considered significant.

4. RESULTS

4.1. Morphological and functional characteristics of the mandibular and tibial periosteal microcirculation

With the reported preparation technique, the anterior surface of the tibial periosteum provides a larger observation field (ranging between 8.89 and 9.88 mm^2) (Figure 3D) than that of the exposed mandibular region (ranging between 8.03 and 9.18 mm^2) (Figure 3B). Furthermore, the entire exposed tibial periosteal surface can be examined by the different *in vivo* microscopic methods, whereas only approximately one third of the mandibular periosteum (i.e. its anterior part) can easily be reached by the relatively robust objectives. The vascular density reached 0.0182±0.0011/μm in the case of the tibia, and was 0.0193±0.0008/μm in the mandibular periosteum. The arterioles, capillaries and venules can be distinguished on the basis of the vessel diameters and the direction of flow of the moving elements (plasma or red blood cells) within them. Within the mandibular periosteum, the vascular network consisted mainly of arterioles and venules, but a few capillaries and mostly venules were present in the tibial periosteum (as depicted in Figures 4-6).

IVM demonstrated that the RBCV values were similar in the two capillary beds (827.5±30.1 μm/s in the mandibular and 739.0±37.7 μm/s in the tibial periosteum) (Table 3). The OPS technique revealed similar RBCV values (data not shown). The IVM data did not indicate any significant differences in the magnitude of the leukocyte-endothelial cell interactions between the two locations (Table 3).

Periosteum	RBCV	Rolling	Sticking
Mandible	827.5 ± 30.1	46.6 ± 5.8	13.4 ± 4.4
Tibia	739.0 ± 37.7	56.9 ± 11.5	18.5 ± 3.9

Table 3. Microcirculatory parameters: RBCV (μm/s) in the capillaries, and PMN rolling (1/mm/s) and sticking (1/mm^2) in the postcapillary venules of the mandibular and tibial periosteum in rats. Mean values ± SEM are presented.

The CLSM method was applied to stain the cell nuclei of the vascular compartment (Figure 6 A,B). The vascular organization was also visualized when intravascular dye (FITC-dextran) was employed (Figure 6 C,D).

4.2. Periosteal microcirculatory reactions in the mandible in rats treated chronically with ZOL

IVM recordings of the microcirculation were performed in a mandibular periosteal region just adjacent to the site of the earlier tooth extraction and also on the contralateral side 6 weeks after tooth extraction. The data were compared with those on the tibial periosteum.

In vivo microscopy revealed homogenous microvascular perfusion in all of the periosteal tissues examined; the RBCVs were similar in the mandibular and tibial capillary beds (827.5 ± 30.1 μm/s and 739.0 ± 37.7 μm/s, respectively). The data were similar on the two sides of the mandible and were not influenced by chronic ZOL treatment (data not shown).

However, the leukocyte rolling in the postcapillary venules of the mandible in the ZOL-treated group was significantly higher than in the saline-treated group both at the site of tooth extraction and on the contralateral side; the differences between the sites were not statistically significant (Figure 7).

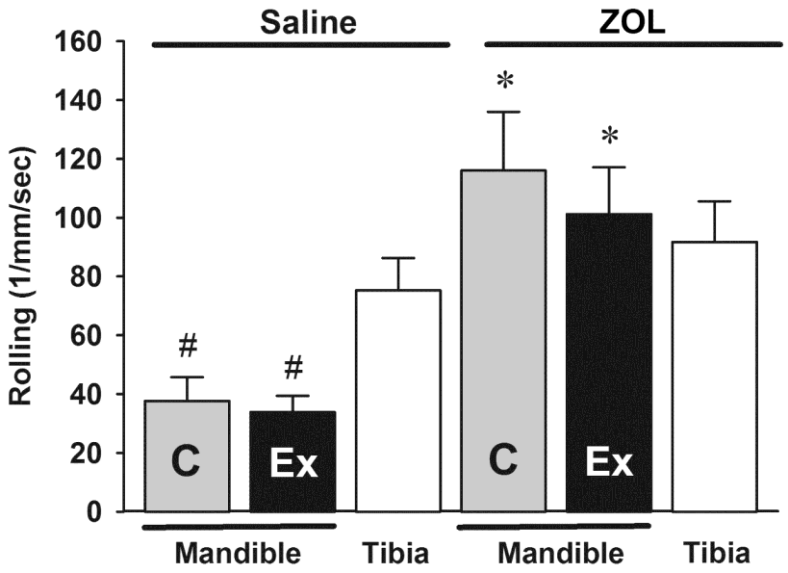

Figure 7. Periosteal primary leukocyte–endothelial cell interactions (rolling) in saline- and ZOL-treated animals in the postcapillary venules of the mandible on the tooth extraction (Ex) and the contralateral (C) sides and in the tibia. Data are presented as means ± SEM. * $P < 0.01$ vs the corresponding saline-treated group. $^{\#}P < 0.05$ vs the tibia. Two-way ANOVA was followed by the Holm–Sidak test.

Similar differences were observed in the leukocyte adhesion values after ZOL, which revealed a statistically significant enhancement in the mandibular periosteum as compared with the tibial periosteum (Figure 8).

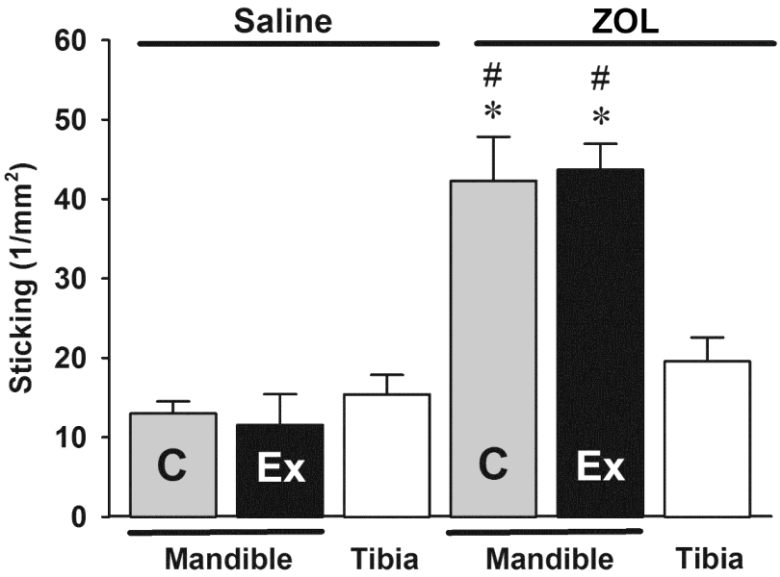

Figure 8. Periosteal secondary leukocyte–endothelial cell interactions (sticking) in the postcapillary venules of the mandible on the tooth extraction (Ex) and the contralateral (C) sides and in the tibia in saline- and ZOL-treated animals. Data are presented as means±SEM. * $P < 0.01$ vs the corresponding saline-treated group. # $P < 0.01$ vs the tibia. Two-way ANOVA was followed by the Holm–Sidak test.

ZOL evoked similar rolling and adhesion values irrespectively of the presence of MRONJ (data not shown). The tibial microcirculation was characterized by higher leukocyte rolling, but similar adhesion in comparison with the data obtained for the mandible in the saline-treated animals; none of them were influenced by ZOL at this location.

4.3. Gingival and mucosal healing of the mandible in rats treated chronically with ZOL

Six weeks after the tooth extraction, intact mucosa could be observed in 8/10 of the control animals (the average healing score was 0.25 ± 0.25), but different degrees of mucosal healing disorders were detected in all (10/10) of the ZOL-treated animals. The severity of the healing disorders reached a score of 1.83 ± 0.18 in this group ($P < 0.01$).

Normal bony regeneration with a radiolucent areas of 12.09 ± 1.91% of the alveolar bone could be detected at the site of the earlier tooth extraction in all (10/10) of the saline-

treated animals. In contrast, a certain degree of discontinuity of the cortical and spongious bone regions was found in 7/10 of the ZOL-treated animals. This higher incidence of impaired bony regeneration was accompanied by a significantly lower average bone density in this group (39.51 ± 7.18% of the alveolar area) as compared with that in the saline-treated group ($P < 0.01$) (Figure 9).

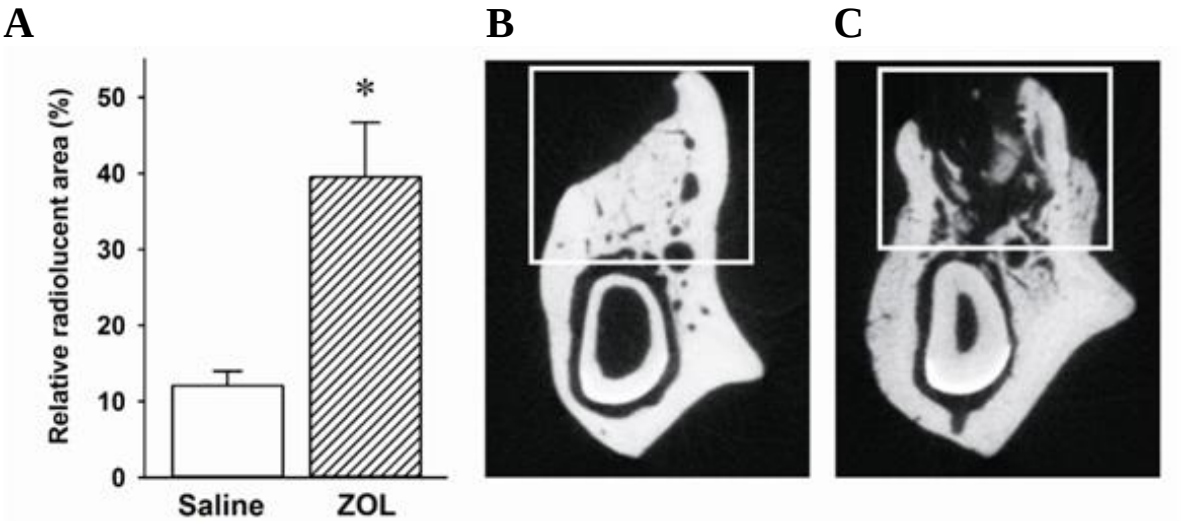

Figure 9. Bone density differences expressed as a percentage of the radiolucent area of the alveolar bone (marked with a rectangle) in saline- and BIS-treated animals 6 weeks after tooth extraction (section A). Data are presented as means ± SEM. * $P < 0.05$ vs saline, Student's t-test. Micro-CT scans show representative images of the mandibular cross-sections in saline- and ZOL-treated rats (sections B and C, respectively).

The radiological diagnosis of mandibular osteonecrosis was confirmed by standard histological examinations (Figure 10). Findings of missing nuclear staining in the osteocytes, increased inflammatory infiltration and granulation tissue formation around the necrotic area, and occasional sequester formation were made in 6/10 of the ZOL-treated animals, whereas nearly normal bone regeneration was observed in the other rats.

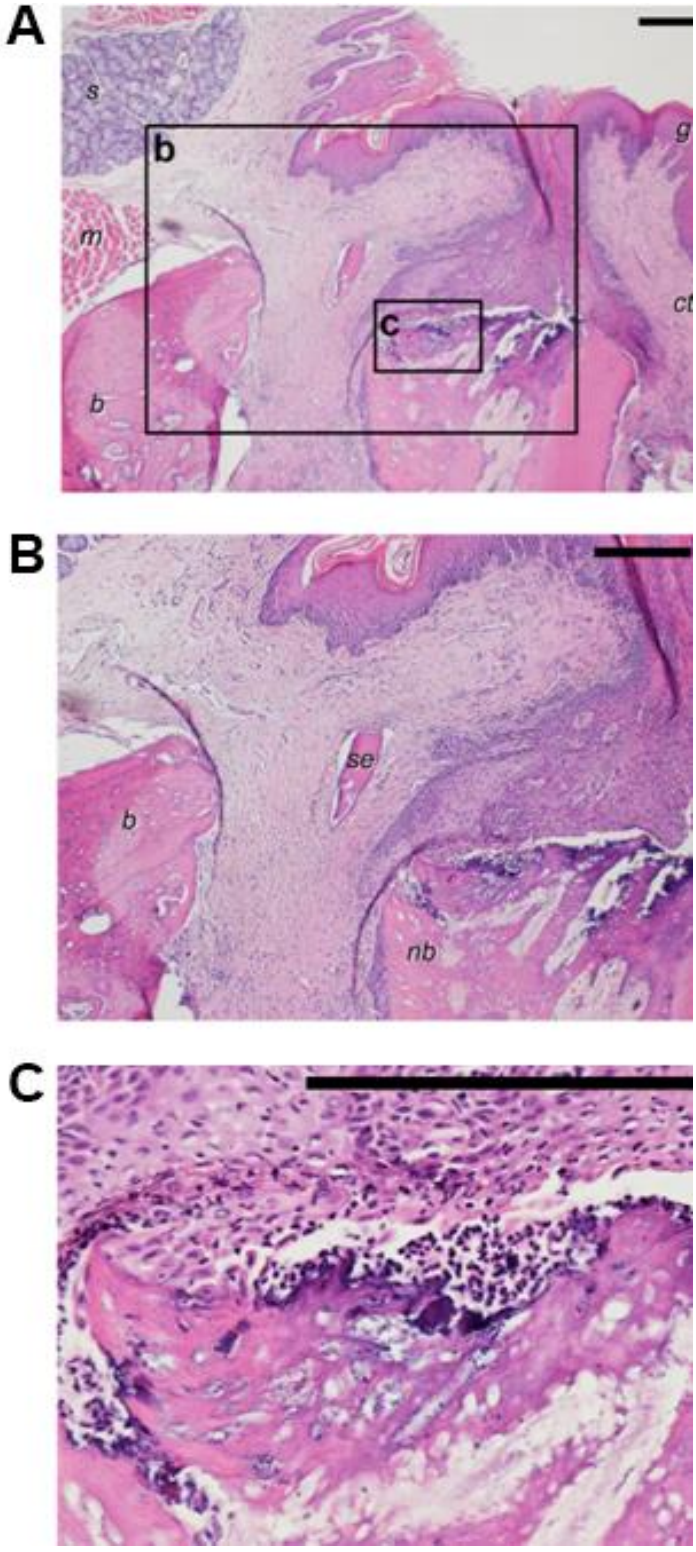

Figure 10. Representative micrograph (H&E staining) showing regeneration processes in a ZOL-treated animal 6 weeks after tooth extraction (magnification 4x) (section A). s: salivary gland, m: muscle b: bone, g: gingiva, ct: connective tissue. Sequester formation (se) and lack of nuclear staining of the necrotic bone (nb), and PMN granulocyte infiltration around the necrotic area (center of the section) can be seen at higher magnifications (magnifications 10x and 40x) (sections B and C, respectively). The bar denotes 200 μm.

4.4. Consequences of chronic ZOL treatment on systemic inflammatory parameters

To exclude the possibility of increased leukocyte counts behind the increased PMN rolling and adhesion after ZOL treatment, the number of PMNs was determined with the conventional Türk solution staining method and using a hemocytometer 6 weeks after tooth extraction. As expected, the number of PMNs was not higher (but rather even lower) in the rats chronically treated with ZOL (Table 4).

Parameter	Saline	ZOL	*P* values
PMN count in the blood (cells/μL)	4513 ± 250	3731 ± 215	< 0.05
CD11b expression (mean fluorescence intensity)	1.57 ± 0.21	1.37 ± 0.09	n.s.
TNF-alpha (pg/mL)	2.65 ± 0.49	2.33 ± 0.39	n.s.

Table 4. The effects of chronic ZOL treatment on the leukocyte count, neutrophil-derived CD11b adhesion molecule expression and plasma TNF-alpha levels. Data are presented as mean ± SEM. *P* < 0.05 vs saline, Student's t-test.

As evidenced by the mean fluorescence values of the adhesion molecule CD11b within the leukocyte population (as measured by flow cytometry), no significant differences was detected between the saline- and ZOL-treated animals (Table 4). There were no differences between the saline- and ZOL-treated experimental groups with respect to the plasma TNF-alpha levels either (n=6 and n=5, respectively) (Table 4).

The NADPH-oxidase activity of the neutrophil leukocytes harvested from the ZOL-treated animals was significantly lower than that for the control animals (Figure 11A). The free radical-derived chemiluminescence of the whole blood (as determined by the superoxide and hydroxyl radical-dependent chemiluminescence measurements) indicated no differences between the two experimental groups (Figure 11B).

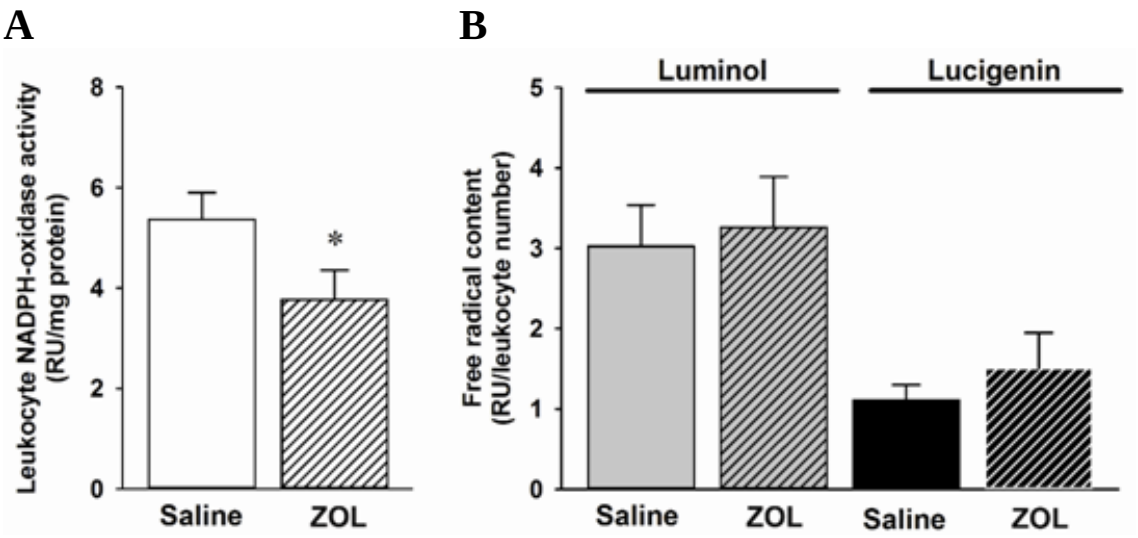

Figure 11. The effects of chronic ZOL treatment on leukocyte NADPH-oxidase activity (**A**) and whole blood free radical production (**B**) (the latter shown by chemiluminescence in the presence of lucigenin and luminol to detect superoxide anion and hydroxyl radical production, respectively). Data are presented as means ± SEM. * $P < 0.05$ vs saline, Student's t-test.

5. DISCUSSION

5.1. The importance of mandibular periosteal microcirculatory examinations in various maxillofacial diseases

As a major source of osteoprogenitor cells, the periosteum of the jaw bones has a high impact in the pathogenesis of various orofacial diseases, but specific, real-time examination of its microcirculation can be performed only after surgical exposure of this structure. As a result, the periosteal microcirculation has been examined in only a relatively limited number of studies of the tibia [Rücker M 1998, Schaser KD 2003, Zhang L 2003, Varga R 2008] or the calvaria [Stuehmer C 2009], and we are aware of only one study in the maxilla-mandibular region, in rabbits [Rücker M 2005]. All of these latter studies involved the use of conventional fluorescence IVM which (as opposed to OPS) also makes possible the investigation of microcirculatory perfusion, permeability and leukocyte–endothelial interactions. In Study 1, we developed a surgical approach to the mandibular periosteum. When a rodent model is to be established, similarities to the human anatomy should first be ascertained. The most accessible region, where the periosteum is situated most superficially, is the area medial to the parotideomasseteric region [Cox PG 2011]. This region, between the superficial masseter muscles and the mentum, just laterally to the ever-growing incisor tooth of the rat, can be approached by incising the skin and subcutaneous tissue. We gained access to the periosteum next to the anterior part of the superficial masseter muscle in the area where this muscle adheres to the ventral margin of the mandible. It was considered important to proceed laterally to the continuously growing incisor teeth so as to avoid any potential functional dissimilarities to the human characteristics.

The fluorescence IVM data revealed that the mandibular microcirculatory variables are similar to those seen in the tibia. It should be added that the preparation was stable for approximately 4 h in preliminary experiments, when only IVM was employed (data not shown). In the case of CLSM, the potential toxic effects of topically-applied nuclear dyes would probably influence the microcirculation in the long run, and examination may therefore preferably be restricted to one time point only. As regards the periosteal microcirculation, examination of the effects of surgical trauma of the tibia [Zhang L 2003] and the maxilla [Rücker M 2005] is a possible target for IVM methods. Such questions can also be answered by using the present exposure technique. Moreover, the consequences of tooth extraction (particularly of first molars) and the subsequent osteogenesis on the

periosteal microcirculatory reactions may also be examined. In previous studies, osteogenesis-related capillary density changes (by OPS) [Lindeboom JA 2008] and leukocyte–endothelial interactions in experimental peridontitis (by IVM) [Carvalho RR 2009] were examined in the mucosa, but never in the periosteum. Furthermore, the present model appears suitable for CLSM; the penetration of intranuclear dyes for the examination of angiogenesis and apoptosis is also possible. CLSM has previously been employed in the oral mucosa to visualize intraoral mucosal lesions, tumors [Franz M 2007], borders of malignancies and resection margins [Capodiferro S 2008, Scivetti M 2009, Haxel BR 2010].

The IVM approach can be a particularly valuable tool for the examination of oral inflammatory processes. In consequence of the relatively high penetration depth of laser light, laser-Doppler flowmetry has been used for the detection of mucosal/gingival inflammatory processes. As examples, the consequences of periodontal access flap surgery and inflammation have been detected in the gingiva [Kerdvongbundit V 2003, Retzepi M 2007] and in the pulpar blood flow [Verdickt GM 2001]. With use of the proposed method, such inflammatory complications could also be examined by using the mandibular periosteum.

Study 1 demonstrated certain differences in architecture in the mandibular and the tibial periosteum. Specifically, the venules proved to be the predominant structures in the examined anteromedial surface of the tibia, whereas arterioles were also detected in the mandible. Differences within the skeletal system were earlier reported, when it was found that the jaw microcirculation has a higher number of anastomoses and a greater impact of the centromedullar circulation as opposed to the long bones of the skeleton [Chanavaz M 1995]. A corrosion cast study similarly revealed lower numbers of capillaries and arterioles in the periosteal compartment than in the gingival compartment, which is characterized by a rich capillary network [Nobuto T 1989]. At the present stage, the impact of our observations cannot be fully assessed and potential regional differences should also be taken into account: we earlier demonstrated [Greksa F 2012] that the anterolateral side of the tibia (which has been used in a myocutaneous flap model [Rücker M 1998]) has more capillaries than on the anteromedial side. We consider that the higher density of venules may predispose to microcirculatory inflammatory complications, e.g. the transmigration of neutrophil leukocytes through the postcapillary venules.

In summary, the new microsurgical approach presented provides access to the periosteal microcirculation in the rat mandible. We compared the mandibular

microcirculatory variables with those of a standard and stable tibial model by using fluorescence IVM to ascertain that this new technique does not cause microcirculatory disturbances or inflammatory complications. It was demonstrated that this exposure procedure makes the mandibular periosteum accessible for OPS and CLSM examinations. It is anticipated that this model and the investigation of mandibular microcirculatory alterations may contribute to a better understanding of maxillofacial or dentoalveolar diseases.

5.2. Periosteal microcirculatory inflammatory processes playing a potential role in the pathogenesis of MRONJ

In Study 2, via the chronic administration of high i.v. doses of ZOL in combination with an invasive dental intervention, a high prevalence of mucosal healing disorders (~ 100%) was achieved together with a relatively high osteonecrosis rate (70%; as revealed by micro-CT and histological analyses). This protocol was based on a modified literature method [Biasotto M 2010]. BIS doses in the range 20-2250 μg/kg with different frequencies and different administration routes have been administered by others (for a meta-analysis, see Barba-Recreo P 2013). The relatively high dose applied here (80 μg/kg/week) is still well tolerated in rats and, although it was also administered in a higher frequency than on human use, it produced symptoms and radiological evidence similar to those observed in humans. Apart from the dose of ZOL, the relatively high incidence of MRONJ in this study can be explained by the triggering effect of the applied dental extraction (the importance of which has been demonstrated in MRONJ patients) [Ruggiero SL 2014]), and the use of the mandibular site (there is a higher prevalence of osteonecrosis at this localization in humans) [Marx RE 2007].

It is reasonable to assume that impaired regeneration processes contribute to the pathophysiology of MRONJ. From a functional aspect, bony regeneration processes depend not only on the functional activity of the osteoblasts and osteoclasts, but also on the blood supply and angiogenesis. BISs have been shown to influence all of these processes. As such, the inhibition of osteoclast recruitment to the bone surface [Rodan GA 1996] and shortening of the osteoclast life span are the main effects of BISs that are brought about directly or indirectly (via the osteoprotegerin-RANKL pathway) [Maruotti N 2012]. Accordingly, delayed bone healing [Kobayashi Y 2010, Yamashita J 2011], together with decreased bone formation and vascularity in the extraction socket, have been detected in ZOL-treated rats [Aguirre JI 2012]. Numerous studies have elucidated the antiangiogenic

effects of BIS both *in vitro* [Wood J 2002] and *in vivo* [Kobayashi Y 2010, Pabst AM 2014]. Furthermore, thicker and less connected/ordered blood vessels in the alveolar bone of the mandible were found in ZOL-treated rats after tooth extraction [Guevarra CS 2013].

The periosteum contains a population of stem/osteoprogenitor cells playing key roles in bone repair [Brighton CT 1992, Allen MR 2004, Xie C 2008, Chappuis V 2012]. BISs bound to a bone surface can affect adjacent cells and inhibit their growth [Cornish J 2011]. A critical concentration of BIS in the mandible [Kimmel DB 2007, Reid IR 2007, Wen D 2011], and the direct toxic and related inflammatory effects in the periosteum may also contribute to the development of MRONJ. BISs exert toxic effects on many different cell types (fibroblasts, osteoblasts, and endothelial and epithelial cells), manifested in diminished cell proliferation and decreased collagen production, ZOL being the most inhibitory in this respect [Reid IR 2007, Naidu A 2008, Scheper MA 2009, Agis H 2010, Açil Y 2012].

Marked inflammatory reactions are attributed to BISs through the induction of peritonitis via the activation of immunological pathways after i.p. administration [Calligeros D 1993, Yamaguchi K 2000, Norton JT 2011]. Enhanced leukocyte–endothelial interactions have been demonstrated by means of IVM after BIS treatment in an arthritis model in mice [Zysk SP 2003]. BIS-associated inflammatory bony changes have also been detected in the mandible [Senel FC, 2010]. Interestingly, these inflammatory changes were limited to the mandible, and were not seen in the femur or the tibia [Senel FC 2010, Yu YY 2012]. High-dose ZOL exacerbates the inflammatory response in a periodontitis model, where the bone lesions strikingly resemble MRONJ [Aguirre JI 2012]. In the present study, pro-inflammatory aspects of chronic BIS treatment could also be traced in the mandibular periosteum, and histological analysis supported the infiltration of the tissue by leukocytes in the neighboring necrotic zone.

In this microsurgical model, the periosteal microcirculation of the mandible can be visualized relatively easily in the molar region, which is likewise a cardinal localization of MRONJ [Ruggiero SL 2014]. Apart from nutritive considerations, the periosteum is important for its osteoprogenitor cell content during bone regeneration. Although BISs exert effects on osteoblast proliferation, differentiation and migration in the entire skeleton [Koch FP 2011], their action seems to depend on the anatomical location, with the jaw bones as highly frequent sites of osteonecrosis. After prolonged use, BISs are known to accumulate in the skeleton, reaching the highest concentration in the mandible [Reid IR 2007, Wen D 2011], which may explain their potential toxic effects predominantly in the

jaw bones. Furthermore, osteoblasts have different proliferation properties at different locations (appendicular vs axial bones) under physiological circumstances, and this phenomenon is also critically influenced by BIS treatment [Marolt D 2012]. The functional activity of the osteocytes too differs between the mandible and the tibia [Çankaya M 2013], and the aggravating effects of BISs on bone healing are confined to the jaw [Kuroshima S 2014]. Although the above findings reveal certain potential factors contributing to the higher incidence of osteonecrosis of the jaw bones, the exact pathomechanism is unknown.

As opposed to the microcirculatory consequences of bone injury (i.e. fractures) [Zhang L 2003], the effects of tooth extraction on the microcirculatory derangement and local inflammation are less commonly described, due to methodological constraints. We focus here on the microcirculatory aspects of chronic ZOL treatment combined with an earlier local trauma of the jaw (tooth extraction). IVM data were obtained in the proximity of the injury and from a contralateral (intact) site on the mandibular periosteum and were compared with those relating to the intact tibia. After chronic ZOL treatment, increased degrees of leukocyte–endothelial interactions (rolling and adhesion) were observed in the mandibular periosteum, both at the site of the earlier tooth extraction and at the contralateral site, but the corresponding interactions in the tibia were less extensive. It is still an unanswered question why the examined cell-to-cell interactions are higher in the postcapillary venules of the mandible, irrespectively of the proximity of the tooth extraction site and the presence of MRONJ in the ZOL-treated group. In preliminary studies, we did not observe inflammatory complications in the mandibular periosteum without tooth extraction, which demonstrated the triggering effect of the trauma in this region. This observation was supported by further findings, when more intense inflammatory reactions of ZOL were evolved in the acute phase after tooth extraction (data not shown). The inflammatory processes were similarly shown in an IVM study to be aggravated by a BIS in an arthritis model in mice [Zysk SP 2003]. Elevated levels of the pro-inflammatory cytokine TNF-alpha have been reported in human patients in response to certain types of BISs [Katz J 2011, Anastasilakis AD 2012, Tzermpos F 2013], but were not detected after the chronic administration of ZOL in our study. Furthermore, the number and functional activity (free radical-producing capacity) of PMNs were moderately reduced here. Such effects on the free radical-producing potential of PMNs (including NADPH-oxidase and myeloperoxidase activity) have also been demonstrated by others [Yamagishi S 2005, Salvolini E 2009, Kuiper JW 2012]. It has been suggested that the compromised neutrophil functions too may be used as potential biomarkers for MRONJ susceptibility

[Favot CL 2013]. Interestingly, others have found impaired neutrophil chemotaxis after BIS exposure in mice [Kuiper JW 2012] and humans [Favot CL 2013], and this parameter is influenced most extensively by ZOL among the different types of BISs [Hagelauer N 2014]. For leukocyte-endothelial interactions (as seen in our study), an enhanced expression of adhesion molecules is required on the surface of the endothelial cells and/or neutrophil leukocytes [Eppihimer MJ 1997]. Interestingly, the expression of the neutrophil-derived adhesion molecule CD11b (responsible for leukocyte adherence) was not found to be influenced by chronic ZOL treatment here or in other studies. The extents of these inflammatory reactions, however, differed in the jaw and the tibial regions. Minodronate was reported to inhibit the VEGF-induced expression of intercellular adhesion molecule-1 in endothelial cells [Yamagishi S 2004] and a similar finding was revealed by local administration of clodronate-liposomes in the synovial lining of rheumatoid arthritis patients [Barrera P 2000]. Regional differences might therefore be explained by different degrees of endothelium-derived adhesion molecule expression at the different anatomical locations.

6. SUMMARY OF NEW FINDINGS

1. We have developed a novel microsurgical approach which provides a simple and reproducible approach to the mandibular periosteum of the rat, where morphological and functional features of the microvasculature can be assessed by different *in vivo* visualization techniques (IVM, OPS and CLSM methods). This access to the mandibular periosteum offers an excellent opportunity for investigations of microcirculatory manifestations of dentoalveolar and maxillofacial diseases.
2. Microvascular processes were explored after chronic ZOL treatment for the first time in the mandibular periosteum in rats.
3. Chronic BIS treatment in combination with tooth extraction induced:

   - gingival healing disorders and radiologically determined osteonecrosis in the mandible, which resembles the clinical signs of MRONJ;

   - periosteal microcirculatory inflammatory reactions confined to the mandible (not present in the tibial periosteum).
4. Regional differences between the mandibular and tibial periosteum might be explained by different degrees of endothelium-derived adhesion molecule expression at the different anatomical locations after chronic ZOL treatment. This observation may contribute to a better understanding of the pathomechanism and the development of strategies to counteract BIS-induced side-effects.

7. ACKNOWLEDGMENTS

I am grateful to Professor József Piffkó for initiating my scientific career and for providing me with the opportunity to carry out my scientific work in the Institute of Surgical Research under his scientific guidance and with his help.

I am indebted to Dr. Andrea Szabó, who helped me acquire the basic experimental and microsurgical skills and granted me unlimited daily assistance in performing the studies and writing publications.

I am also grateful to Professor Mihály Boros, Director of the Institute of Surgical Research, who supported my research work from the beginnings and provided the infrastructural background for my scientific work.

I thank Professor Béla Iványi and Dr. Tamás Zombori for their cooperation in the histological investigations.

My special thanks are due to all the technical staff at the Institute of Surgical Research for their skillful assistance.

This thesis is supported by the European Union and co-funded by the European Social Fund. Project title: “Telemedicine-focused research activities in the field of Mathematics, Informatics and Medical Sciences”. Project number: TÁMOP-4.2.2.A-11/1/KONV-2012-0073. Further supporting research grants: TÁMOP 4.2.2A-11/1/KONV-2012-0035, TÁMOP 4.2.4.A/2-11-1-2012-0001 and OTKA – 109388.

8. REFERENCES

1. **Abshagen K**, Eipel C, Menger MD, Vollmar B. Comprehensive analysis of the regenerating mouse liver: an in vivo fluorescence microscopic and immunohistological study. J Surg Res. 2006;134(2):354-362.
2. **Açil Y**, Möller B, Niehoff P, Rachko K, Gassling V, Wiltfang J, Simon MJ. The cytotoxic effects of three different bisphosphonates in-vitro on human gingival fibroblasts, osteoblasts and osteogenic sarcoma cells. J Craniomaxillofac Surg. 2012;40(8):e229-e235.
3. **Aghaloo TL**, Chaichanasakul T, Bezouglaia O, Kang B, Franco R, Dry SM, Atti E, Tetradis S. Osteogenic potential of mandibular vs. long-bone marrow stromal cells. J Dent Res. 2010;89(11):1293-1298.
4. **Agis H**, Blei J, Watzek G, Gruber R. Is zoledronate toxic to human periodontal fibroblasts? J Dent Res. 2010;89(1):40-45.
5. **Aguirre JI**, Akhter MP, Kimmel DB, Pingel JE, Williams A, Jorgensen M, Kesavalu L, Wronski TJ. Oncologic doses of zoledronic acid induce osteonecrosis of the jaw-like lesions in rice rats (Oryzomys palustris) with periodontitis. J Bone Miner Res. 2012;27(10):2130-2143.
6. **Allen MR**, Hock JM, Burr DB. Periosteum: biology, regulation, and response to osteoporosis therapies. Bone. 2004;35(5):1003-1012.
7. **Anastasilakis AD**, Polyzos SA, Delaroudis S, Bisbinas I, Sakellariou GT, Gkiomisi A, Papadopoulou E, Gerou S, Makras P. The role of cytokines and adipocytokines in zoledronate-induced acute phase reaction in postmenopausal women with low bone mass. Clin Endocrinol (Oxf). 2012;77(6):816-822.
8. **Aragon-Ching JB**, Ning YM, Chen CC, Latham L, Guadagnini JP, Gulley JL, Arlen PM, Wright JJ, Parnes H, Figg WD, Dahut WL. Higher incidence of Osteonecrosis of the Jaw (ONJ) in patients with metastatic castration resistant prostate cancer treated with anti-angiogenic agents. Cancer Invest. 2009;27(2):221-226.
9. **Barba-Recreo P**, Del Castillo Pardo de Vera JL, García-Arranz M, Yébenes L, Burgueño M. Zoledronic acid - Related osteonecrosis of the jaws. Experimental model with dental extractions in rats. J Craniomaxillofac Surg. 2013. pii: S1010-5182(13)00304-1.
10. **Barrera P**, Blom A, van Lent PL, van Bloois L, Beijnen JH, van Rooijen N, de Waal Malefijt MC, van de Putte LB, Storm G, van den Berg WB. Synovial macrophage

depletion with clodronate-containing liposomes in rheumatoid arthritis. Arthritis Rheum. 2000;43(9):1951-1959.

11. **Battino M**, Bullon P, Wilson M, Newman H. Oxidative injury and inflammatory periodontal diseases: the challenge of anti-oxidants to free radicals and reactive oxygen species. Crit Rev Oral Biol Med. 1999;10(4):458-476.
12. **Bauer A**, Kofler S, Thiel M, Eifert S, Christ F. Monitoring of the sublingual microcirculation in cardiac surgery using orthogonal polarization spectral imaging: preliminary results. Anesthesiology. 2000;107(6):939-945.
13. **Biasotto M**, Chiandussi S, Zacchigna S, Moimas S, Dore F, Pozzato G, Cavalli F, Zanconati F, Contardo L, Giacca M, Di Lenarda R. A novel animal model to study non-spontaneous bisphosphonates osteonecrosis of jaw. J Oral Pathol Med. 2010;39(5):390-396.
14. **Bencsik P**, Kupai K, Giricz Z, Görbe A, Pipis J, Murlasits Z, Kocsis GF, Varga-Orvos Z, Puskás LG, Csonka C, Csont T, Ferdinandy P. Role of iNOS and peroxynitrite-matrix metalloproteinase-2 signaling in myocardial late preconditioning in rats. Am J Physiol Heart Circ Physiol. 2010;299(2):H512-H518.
15. **Berggren A**, Weiland AJ, Ostrup LT, Dorfman H. Microvascular free bone transfer with revascularization of the medullary and periosteal circulation or the periosteal circulation alone. A comparative experimental study. J Bone Joint Surg Am. 1982;64(1):73-87.
16. **Bhatt R**, Lauder I, Finlay DB, Allen MJ, Belton IP. Correlation of bone scintigraphy and histological findings in medial tibial syndrome. Br J Sports Med. 2000;34(1):49-53.
17. **Blazsek J**, Dobó Nagy C, Blazsek I, Varga R, Vecsei B, Fejérdy P, Varga G. Aminobisphosphonate stimulates bone regeneration and enforces consolidation of titanium implant into a new rat caudal vertebrae model. Pathol Oncol Res. 2009;15(4):567-577.
18. **Bigi MM**, Escudero ND, Ubios AM, Mandalunis PM. Evaluation of vascular endothelial growth factor (VEGF) in interradicular bone marrow in olpadronate treated animals. Acta Odontol Latinoam. 2010;23(3):265-269.
19. **Brighton CT**, Lorich DG, Kupcha R, Reilly TM, Jones AR, Woodbury RA 2nd. The pericyte as a possible osteoblast progenitor cell. Clin Orthop Relat Res. 1992;(275):287-299.

20. **Brozoski MA**, Traina AA, Deboni MC, Marques MM, Naclério-Homem Mda G. Bisphosphonate-related osteonecrosis of the jaw. Rev Bras Reumatol. 2012;52(2):265-270.
21. **Bunyaratavej N**, Wajanavisit W, Pauvilai P, Kitumnuoypong T, Kittimanon N, Lektrakoon S. Safety and antisorptive power of Ibandronate applied in the real-life setting. J Med Assoc Thai. 2009;92 Suppl5:S72-S75.
22. **Calligeros D**, Douglas P, Abeygunasekera S, Smith G. Aseptic peritonitis in association with the use of pamidronate. Med J Aust. 1993;159(2):144.
23. **Çankaya M**, Cizmeci Şenel F, Kadioglu Duman M, Muci E, Dayisoylu EH, Balaban F. The effects of chronic zoledronate usage on the jaw and long bones evaluated using RANKL and osteoprotegerin levels in an animal model. Int J Oral Maxillofac Surg. 2013;42(9):1134-1139.
24. **Capodiferro S**, Maiorano E, Loiudice AM, Scarpelli F, Favia G. Oral laser surgical pathology: a preliminary study on the clinical advantages of diode laser and on the histopathological features of specimens evaluated by conventional and confocal laser scanning microscopy. Minerva Stomatol. 2008;57(1-2):1-6,6-7.
25. **Carden DL**, Granger DN. Pathophysiology of ischaemia-reperfusion injury. J Pathol. 2000;190(3):255-66.
26. **Carvalho RR**, Pellizzon CH, Justulin L Jr, Felisbino SL, Vilegas W, Bruni F, Lopes-Ferreira M, Hiruma-Lima CA. Effect of mangiferin on the development of periodontal disease: involvement of lipoxin A4, anti-chemotaxic action in leukocyte rolling. Chem Biol Interact. 2009;179(2-3):344-350.
27. **Chanavaz M**. Anatomy and histophysiology of the periosteum: quantification of the periosteal blood supply to the adjacent bone with 85Sr and gamma spectrometry. J Oral Implantol. 1995;21(3):214-219.
28. **Chappuis V**, Gamer L, Cox K, Lowery JW, Bosshardt DD, Rosen V. Periosteal BMP2 activity drives bone graft healing. Bone. 2012;51(4):800-809.
29. **Choudhari SK**, Chaudhary M, Bagde S, Gadbail AR, Joshi V. Nitric oxide and cancer: a review. World J Surg Oncol. 2013;11:118.
30. **Cooper D**, Stokes KY, Tailor A, Granger DN. Oxidative stress promotes blood cell-endothelial cell interactions in the microcirculation. Cardiovasc Toxicol. 2002;2(3):165-180.
31. **Cornish J**, Bava U, Callon KE, Bai J, Naot D, Reid IR. Bone-bound bisphosphonate inhibits growth of adjacent non-bone cells. Bone. 2011;49(4):710-716.

32. **Cox PG**, Jeffery N. Reviewing the morphology of the jaw-closing musculature in squirrels, rats, and guinea pigs with contrast-enhanced microCT. Anat Rec (Hoboken) 2011;294(6): 915-928.

33. **De Backer D**, Donadello K, Sakr Y, Ospina-Tascon G, Salgado D, Scolletta S, Vincent JL. Microcirculatory alterations in patients with severe sepsis: impact of time of assessment and relationship with outcome. Crit Care Med. 2013;41(3):791-799.

34. **Drozdzowska B**. Osteonecrosis of the jaw. Endokrynol Pol. 2011;62 Suppl 3:4-9.

35. **Ebetino FH**, Hogan AM, Sun S, Tsoumpra MK, Duan X, Triffitt JT, Kwaasi AA, Dunford JE, Barnett BL, Oppermann U, Lundy MW, Boyde A, Kashemirov BA, McKenna CE, Russell RG. The relationship between the chemistry and biological activity of the bisphosphonates. Bone. 2011;49(1):20-33.

36. **Elshahat A**, Inoue N, Marti G, Safe I, Manson P, Vanderkolk C. Role of guided bone regeneration principle in preventing fibrous healing in distraction osteogenesis at high speed: experimental study in rabbit mandibles. J Craniofac Surg. 2004;15(6):916-921.

37. **Eltzschig HK**, Collard CD. Vascular ischaemia and reperfusion injury. Br Med Bull. 2004;70:71-86.

38. **Endo N**. QOL evaluation for osteoporosis. Clin Calcium. 2012;22(6):845-851.

39. **Eppihimer MJ**, Granger DN. Ischemia/reperfusion-induced leukocyte-endothelial interactions in postcapillary venules. Shock. 1997;8(1):16-25.

40. **Esterhai JL Jr**, Queenan J. Management of soft tissue wounds associated with type III open fractures. Orthop Clin North Am. 1991;22(3):427-432.

41. **Ezra A**, Golomb G. Administration routes and delivery systems of bisphosphonates for the treatment of bone resorption. Adv Drug Deliv Rev. 2000;42(3):175-195.

42. **Favot CL**, Forster C, Glogauer M. The effect of bisphosphonate therapy on neutrophil function: a potential biomarker. Int J Oral Maxillofac Surg. 2013;42(5):619-626.

43. **Fayad LM**, Kamel IR, Kawamoto S, Bluemke DA, Frassica FJ, Fishman EK. Distinguishing stress fractures from pathologic fractures: a multimodality approach. Skeletal Radiol. 2005;34(5):245-259.

44. **Findlay DM**. Vascular pathology and osteoarthritis. Rheumatology (Oxford). 2007;46:1763-1768.

45. **Foolen J**, van Donkelaar C, Nowlan N, Murphy P, Huiskes R, Ito K. Collagen orientation in periosteum and perichondrium is aligned with preferential directions of tissue growth. J Orthop Res. 2008;26(9):1263-1268.

46. **Fournier P**, Boissier S, Filleur S, Guglielmi J, Cabon F, Colombel M, Clézardin P. Bisphosphonates inhibit angiogenesis in vitro and testosterone-stimulated vascular regrowth in the ventral prostate in castrated rats. Cancer Res. 2002;62(22):6538-6544.

47. **Franz M**, Hansen T, Borsi L, Geier C, Hyckel P, Schleier P, Richter P, Altendorf-Hofmann A, Kosmehl H, Berndt A. A quantitative co-localization analysis of large unspliced tenascin-C(L) and laminin-5/gamma2-chain in basement membranes of oral squamous cell carcinoma by confocal laser scanning microscopy. J Oral Pathol Med. 2007;36(1):6-11.

48. **Fujimura T**, Kambayashi Y, Furudate S, Kakizaki A, Aiba S. Immunomodulatory effect of bisphosphonate risedronate sodium on CD163+ arginase 1+ M2 macrophages: the development of a possible supportive therapy for angiosarcoma. Clin Dev Immunol. 2013;2013:325412.

49. **Goto T**, Yamaza T, Kido MA, Tanaka T. Light- and electron-microscopic study of the distribution of axons containing substance P and the localization of neurokinin-1 receptor in bone. Cell Tissue Res. 1998;293(1):87-93.

50. **Greksa F**, Tóth K, Boros M, Szabó A. Periosteal microvascular reorganization after tibial reaming and intramedullary nailing in rats. J Orthop Sci. 2012;17(4):477-483.

51. **Groner W**, Winkelman JW, Harris AG, Ince C, Bouma GJ, Messmer K, Nadeau RG. Orthogonal polarization spectral imaging: a new method for study of the microcirculation. Nat Med. 1999;5(10):1209-1012.

52. **Guevarra CS**, Borke JL, Stevens MR, Bisch FC, Zakhary I, Messer R, Gerlach RC, Elsalanty ME. Vascular alterations in the Sprague-Dawley rat mandible during intravenous bisphosphonate therapy. J Oral Implantol. 2013 Dec 2. [Epub ahead of print]

53. **Gustilo RB**, Merkow RL, Templeman D. The management of open fractures. J Bone Joint Surg Am. 1990;72(2):299-304.

54. **Hagelauer N**, Pabst AM, Ziebart T, Ulbrich H, Walter C. In vitro effects of bisphosphonates on chemotaxis, phagocytosis, and oxidative burst of neutrophil granulocytes. Clin Oral Investig. 2014 Mar 26. [Epub ahead of print]

55. **Han GY**, Wang O, Xing XP, Meng XW, Lian XL, Guan H, Ye W, Xia WB, Li M, Jiang Y, Hu YY, Liu HC, Cui QC. The efficacy and safety of intravenous bisphosphonates in the treatment of primary hyperparathyroidism complicated by hypercalcemia crisis. Zhonghua Nei Ke Za Zhi. 2009;48(9):729-733.

56. **Hartmann P**, Erős G, Varga R, Kaszaki J, Garab D, Németh I, Rázga Z, Boros M, Szabó A. Limb ischemia-reperfusion differentially affects the periosteal and synovial microcirculation. J Surg Res. 2012;178(1):216-222.

57. **Haxel BR**, Goetz M, Kiesslich R, Gosepath J. Confocal endomicroscopy: a novel application for imaging of oral and oropharyngeal mucosa in human. Eur Arch Otorhinolaryngol. 2010;267(3):443-448.

58. **Hill EL**, Elde R. Distribution of CGRP-, VIP-, D beta H-, SP-, and NPY-immunoreactive nerves in the periosteum of the rat. Cell Tissue Res. 1991;264(3):469-480.

59. **Holen I**, Coleman RE. Anti-tumour activity of bisphosphonates in preclinical models of breast cancer. Breast Cancer Res. 2010;12(6):214.

60. **Hooper G**. Bone as a tissue In: Orthopedics. The principles and practice of musculoskeletal surgery. Chapter 1:3-15. Editors: Hughes SPF, Benson MKD'A, Colton CL. Churchill Livingstone 1987 (Edinburgh, London, Melbourne, New York)

61. **Horie Y**, Wolf R, Miyasaka M, Anderson DC, Granger DN. Leukocyte adhesion and hepatic microvascular responses to intestinal ischemia/reperfusion in rats. Gastroenterology. 1996;111(3):666-673.

62. **Huelke DF**, Castelli WA. The blood supply of the rat mandible. Anat Rec. 1965;153(4):335-341.

63. **Johnson EO**, Soultanis K, Soucacos PN. Vascular anatomy and microcirculation of skeletal zones vulnerable to osteonecrosis: vascularization of the femoral head. Orthop Clin North Am. 2004;35:285-291.

64. **Kalyan S**, Chandrasekaran V, Quabius ES, Lindhorst TK, Kabelitz D. Neutrophil uptake of nitrogen-bisphosphonates leads to the suppression of human peripheral blood γδ T cells. Cell Mol Life Sci. 2014;71(12):2335-2346.

65. **Katz J**, Gong Y, Salmasinia D, Hou W, Burkley B, Ferreira P, Casanova O, Langaee TY, Moreb JS. Genetic polymorphisms and other risk factors associated with bisphosphonate induced osteonecrosis of the jaw. Int J Oral Maxillofac Surg. 2011;40(6):605-611.

66. **Kerdvongbundit V**, Vongsavan N, Soo-Ampon S, Hasegawa A. Microcirculation and micromorphology of healthy and inflamed gingivae. Odontology. 2003;91(1):19-25.

67. **Kerschan-Schindl K**, Patsch J, Kudlacek S, Gleiss A, Pietschmann P. Measuring quality of life with the German Osteoporosis Quality of Life Questionnaire in women with osteoporosis. Wien Klin Wochenschr. 2012;124(15-16):532-537.

68. **Kimmel DB**. Mechanism of action, pharmacokinetic and pharmacodynamic profile, and clinical applications of nitrogen-containing bisphosphonates. J Dent Res. 2007;86(11):1022-1033.

69. **Kobayashi Y**, Hiraga T, Ueda A, Wang L, Matsumoto-Nakano M, Hata K, Yatani H, Yoneda T. Zoledronic acid delays wound healing of the tooth extraction socket, inhibits oral epithelial cell migration, and promotes proliferation and adhesion to hydroxyapatite of oral bacteria, without causing osteonecrosis of the jaw, in mice. J Bone Miner Metab. 2010;28(2):165-175.

70. **Koch FP**, Wunsch A, Merkel C, Ziebart T, Pabst A, Yekta SS, Blessmann M, Smeets R. The influence of bisphosphonates on human osteoblast migration and integrin aVb3/tenascin C gene expression in vitro. Head Face Med. 2011;7(1):4.

71. **Koch FP**, Walter C, Hansen T, Jäger E, Wagner W. Osteonecrosis of the jaw related to sunitinib. Oral Maxillofac Surg. 2011;15(1):63-66.

72. **Kowada T**, Kikuta J, Kubo A, Ishii M, Maeda H, Mizukami S, Kikuchi K. In vivo fluorescence imaging of bone-resorbing osteoclasts. J Am Chem Soc. 2011;133(44):17772-17776.

73. **Kuiper JW**, Forster C, Sun C, Peel S, Glogauer M. Zoledronate and pamidronate depress neutrophil functions and survival in mice. Br J Pharmacol. 2012;165(2):532-539.

74. **Kumar SK**, Gorur A, Schaudinn C, Shuler CF, Costerton JW, Sedghizadeh PP. The role of microbial biofilms in osteonecrosis of the jaw associated with bisphosphonate therapy. Curr Osteoporos Rep. 2010;8(1):40-48.

75. **Kurose I**, Argenbright LW, Wolf R, Lianxi L, Granger DN. Ischemia/reperfusion-induced microvascular dysfunction: role of oxidants and lipid mediators. Am J Physiol. 1997;272(6 Pt 2):H2976-H2982.

76. **Kuroshima S**, Entezami P, McCauley LK, Yamashita J. Early effects of parathyroid hormone on bisphosphonate/steroid-associated compromised osseous wound healing. Osteoporos Int. 2014;25(3):1141-1150.

77. **Kühl S**, Walter C, Acham S, Pfeffer R, Lambrecht JT. Bisphosphonate-related osteonecrosis of the jaws--a review. Oral Oncol. 2012;48(10):938-947.

78. **Kvietys PR**, Granger DN. Role of reactive oxygen and nitrogen species in the vascular responses to inflammation. Free Radic Biol Med. 2012;52(3):556-592

79. **Lindeboom JA**, Mathura KR, Milstein DM, Ince C. Microvascular soft tissue changes in alveolar distraction osteogenesis. Oral Surg Oral Med Oral Pathol Oral Radiol Endod. 2008;106(3):350-355.

80. **Liu H**, Gao K, Lin H, Zhang Y, Li B. Relative Skeletal Effects in Different Sites of the Mandible with the Proximal Tibia during Ovariectomy and the Subsequent Estrogen Treatment. J Oral Implantol. 2014 Jun 10. [Epub ahead of print]

81. **Loukas M**, Kinsella CR Jr, Kapos T, Tubbs RS, Ramachandra S. Anatomical variation in arterial supply of the mandible with special regard to implant placement. Int J Oral Maxillofac Surg. 2008;37(4):367-371.

82. **Luckman SP**, Hughes DE, Coxon FP, Graham R, Russell G, Rogers MJ. Nitrogen-containing bisphosphonates inhibit the mevalonate pathway and prevent post-translational prenylation of GTP-binding proteins, including Ras. J Bone Miner Res. 1998;13(4):581-589.

83. **Macnab I**, Dehoas WG. The role of periosteal blood supply in the healing of fractures of the tibia. Clin Orthop. 1974;105:27-33.

84. **Marolt D**, Cozin M, Vunjak-Novakovic G, Cremers S, Landesberg R. Effects of pamidronate on human alveolar osteoblasts in vitro. J Oral Maxillofac Surg. 2012;70(5):1081-1092.

85. **Maruotti N**, Corrado A, Neve A, Cantatore FP. Bisphosphonates: effects on osteoblast. Eur J Clin Pharmacol. 2012;68(7):1013-1018.

86. **Marx RE**. Pamidronate (Aredia) and zoledronate (Zometa) induced avascular necrosis of the jaws: a growing epidemic. J Oral Maxillofac Surg. 2003;61(9):1115-1117.

87. **Marx RE**, Cillo JE Jr, Ulloa JJ: Oral bisphosphonate-induced osteonecrosis: risk factors, prediction of risk using serum CTX testing, prevention, and treatment. J Oral Maxillofac Surg., 2007;65(12):2397-2410.

88. **Mavropoulos A**, Rizzoli R, Ammann P. Different responsiveness of alveolar and tibial bone to bone loss stimuli. J Bone Miner Res. 2007;22(3):403-410.

89. **Mawardi H**, Giro G, Kajiya M, Ohta K, Almazrooa S, Alshwaimi E, Woo SB, Nishimura I, Kawai T. A role of oral bacteria in bisphosphonate-induced osteonecrosis of the jaw. J Dent Res. 2011;90(11):1339-1345.

90. **Mehrotra B**, Ruggiero S. Bisphosphonate complications including osteonecrosis of the jaw. Hematology Am Soc Hematol Educ Program. 2006:356-360, 515.

91. **Milstein DM**, Cheung YW, Žiūkaitė L, Ince C, van den Akker HP, Lindeboom JA. An integrative approach for comparing microcirculation between normal and alveolar cleft gingiva in children scheduled for secondary bone grafting procedures. Oral Surg Oral Med Oral Pathol Oral Radiol. 2013;115(3):304-309.

92. **Milstein DM**, Lindeboom JA, Ince C. Intravital sidestream dark-field (SDF) imaging is used in a rabbit model for continuous noninvasive monitoring and quantification of mucosal capillary regeneration during wound healing in the oral cavity: a pilot study. Arch Oral Biol. 2010;55(5):343-349.

93. **Mönkkönen H**, Auriola S, Lehenkari P, Kellinsalmi M, Hassinen IE, Vepsäläinen J, Mönkkönen J. A new endogenous ATP analog (ApppI) inhibits the mitochondrial adenine nucleotide translocase (ANT) and is responsible for the apoptosis induced by nitrogen-containing bisphosphonates. Br J Pharmacol. 2006;147(4):437-445.

94. **Mozzati M**, Martinasso G, Maggiora M, Scoletta M, Zambelli M, Carossa S, Oraldi M, Muzio G, Canuto RA. Oral mucosa produces cytokines and factors influencing osteoclast activity and endothelial cell proliferation, in patients with osteonecrosis of jaw after treatment with zoledronic acid. Clin Oral Investig. 2013;17(4):1259-1266.

95. **Naidu A**, Dechow PC, Spears R, Wright JM, Kessler HP, Opperman LA. The effects of bisphosphonates on osteoblasts in vitro. Oral Surg Oral Med Oral Pathol Oral Radiol Endod. 2008;106(1):5-13.

96. **Niibe K**, Ouchi T, Iwasaki R, Nakagawa T, Horie N. Osteonecrosis of the jaw in patients with dental prostheses being treated with bisphosphonates or denosumab. J Prosthodont Res. 2014. pii: S1883-1958(14)00091-7.

97. **Nobuto T**, Yanagihara K, Teranishi Y, Minamibayashi S, Imai H, Yamaoka A. Periosteal microvasculature in the dog alveolar process. J Periodontol. 1989;60(12):709-715.

98. **Norton JT**, Hayashi T, Crain B, Corr M, Carson DA. Role of IL-1 receptor-associated kinase-M (IRAK-M) in priming of immune and inflammatory responses by nitrogen bisphosphonates. Proc Natl Acad Sci U S A. 2011;108(27):11163-11168.

99. **O'Halloran M**, Boyd N, Smith A. Denosumab and osteonecrosis of the jaws - the pharmacology, pathogenesis and a report of two cases. Aust Dent J. 2014 Aug 16. doi: 10.1111/adj.12217. [Epub ahead of print]

100. **Ohba T**, Cates JM, Cole HA, Slosky DA, Haro H, Ichikawa J, Ando T, Schwartz HS, Schoenecker JG. Pleiotropic effects of bisphosphonates on osteosarcoma. Bone. 2014;63:110-120.

101. **Otto S**, Schreyer C, Hafner S, Mast G, Ehrenfeld M, Stürzenbaum S, Pautke C. Bisphosphonate-related osteonecrosis of the jaws - characteristics, risk factors, clinical features, localization and impact on oncological treatment. J Craniomaxillofac Surg. 2012;40(4):303-309.

102. **Pabst AM**, Ziebart T, Ackermann M, Konerding MA, Walter C. Bisphosphonates' antiangiogenic potency in the development of bisphosphonate-associated osteonecrosis of the jaws: influence on microvessel sprouting in an in vivo 3D Matrigel assay. Clin Oral Investig. 2014;18(3):1015-1022.

103. **Pakosch D**, Papadimas D, Munding J, Kawa D, Kriwalsky MS. Osteonecrosis of the mandible due to anti-angiogenic agent, bevacizumab. Oral Maxillofac Surg. 2013;17(4):303-306.

104. **Park JB**, Bae SS, Lee PW, Lee W, Park HY, Kim H, Lee KH, Kim IK. Comparison of stem cells derived from periosteum and bone marrow of jaw bone and long bone in rabbit models. J Tissue Eng Regen Med. 2012;9(4):224-230.

105. **Reichert JC**, Gohlke J, Friis TE, Quent VM, Hutmacher DW. Mesodermal and neural crest derived ovine tibial and mandibular osteoblasts display distinct molecular differences. Gene. 2013;525(1):99-106.

106. **Reid IR**, Bolland MJ, Grey AB. Is bisphosphonate-associated osteonecrosis of the jaw caused by soft tissue toxicity? Bone. 2007;41(3):318-320.

107. **Retzepi M**, Tonetti M, Donos N. Gingival blood flow changes following periodontal access flap surgery using laser Doppler flowmetry. J Clin Periodontol. 2007;34(5):437-443.

108. **Rodan GA**. Mechanisms of action of bisphosphonates. Annu Rev Pharmacol Toxicol. 1998;38:375-388.

109. **Rodella LF**, Buffoli B, Labanca M, Rezzani R. A review of the mandibular and maxillary nerve supplies and their clinical relevance. Arch Oral Biol. 2012;57(4):323-334.

110. **Rogers MJ**, Crockett JC, Coxon FP, Mönkkönen J. Biochemical and molecular mechanisms of action of bisphosphonates. Bone. 2011;49(1):34-41.

111. **Rossini M**, Adami S, Viapiana O, Tripi G, Zanotti R, Ortolani R, Vella A, Troplini S, Gatti D. Acute phase response after zoledronic acid is associated with long-term effects on white blood cells. Calcif Tissue Int. 2013;93(3):249-252.

112. **Ruggiero SL**, Dodson TB, Assael LA, Landesberg R, Marx RE, Mehrotra B; Task Force on Bisphosphonate-Related Osteonecrosis of the Jaws, American Association of Oral and Maxillofacial Surgeons. American Association of Oral and Maxillofacial Surgeons position paper on bisphosphonate-related osteonecrosis of the jaw - 2009 update. Aust Endod J. 2009;35(3):119-130.

113. **Ruggiero SL**, Dodson TB, Fantasia J, Gordday R, Aghaloo T, Mehrotra B, O'Ryan F. Medication-Related Osteonecrosis of the Jaw–2014 Update. J Oral Maxillofac Surg. 2014;72(10):1938–1956.

114. **Ruh J**, Ryschich E, Secchi A, Gebhard MM, Glaser F, Klar E, Herfarth C. Measurement of blood flow in the main arteriole of the villi in rat small intestine with FITC-labeled erythrocytes. Microvasc Res. 1998;6(1):62-69.

115. **Rücker M**, Binger T, Deltcheva K, Menger MD. Reduction of midfacial periosteal perfusion failure by subperiosteal versus supraperiosteal dissection. J Oral Maxillofac Surg. 2005;63(1):87-92.

116. **Salvolini E**, Orciani M, Vignini A, Di Primio R, Mazzanti L. The effects of disodium pamidronate on human polymorphonuclear leukocytes and platelets: an in vitro study. Cell Mol Biol Lett. 2009;14(3):457-465.

117. **Sarasquete ME**, González M, San Miguel JF, García-Sanz R. Bisphosphonate-related osteonecrosis: genetic and acquired risk factors. Oral Dis. 2009;15(6):382-387.

118. **Sasaki O**, Imamura M, Yamazumi Y, Harada H, Matsumoto T, Okunishi K, Nakagome K, Tanaka R, Akiyama T, Yamamoto K, Dohi M. Alendronate attenuates eosinophilic airway inflammation associated with suppression of Th2 cytokines, Th17 cytokines, and eotaxin-2. J Immunol. 2013;191(6):2879-2889.

119. **Schaser KD**, Zhang L, Haas NP, Mittlmeier T, Duda G, Bail HJ. Temporal profile of microvascular disturbances in rat tibial periosteum following closed soft tissue trauma. Langenbecks Arch Surg. 2003;388(5):323-330.

120. Scheper MA, Badros A, Chaisuparat R, Cullen KJ, Meiller TF. Effect of zoledronic acid on oral fibroblasts and epithelial cells: a potential mechanism of bisphosphonate-associated osteonecrosis. Br J Haematol. 2009;144(5):667-676.

121. Schmidt BL, Kung L, Jones C, Casap N. Induced osteogenesis by periosteal distraction. J Oral Maxillofac Surg. 2002;60(10):1170-1175.

122. Scivetti M, Lucchese A, Ficarra G, Giuliani M, Lajolo C, Maiorano E, Favia G. Oral pulse granuloma: histological findings by confocal laser scanning microscopy. Ultrastruct Pathol. 2009;33(4):155-159.

123. Sedghizadeh PP, Kumar SK, Gorur A, Schaudinn C, Shuler CF, Costerton JW. Identification of microbial biofilms in osteonecrosis of the jaws secondary to bisphosphonate therapy. J Oral Maxillofac Surg. 2008;66(4):767-775.

124. Senel FC, Kadioglu Duman M, Muci E, Cankaya M, Pampu AA, Ersoz S, Gunhan O. Jaw bone changes in rats after treatment with zoledronate and pamidronate. Oral Surg Oral Med Oral Pathol Oral Radiol Endod. 2010;109(3):385-391.

125. Serra E, Paolantonio M, Spoto G, Mastrangelo F, Tetè S, Dolci M. Bevacizumab-related osteneocrosis of the jaw. Int J Immunopathol Pharmacol. 2009;22(4):1121-1123.

126. Serrick C, Adoumie R, Giaid A, Shennib H. The early release of interleukin-2, tumor necrosis factor-alpha and interferon-gamma after ischemia reperfusion injury in the lung allograft. Transplantation. 1994;58(11):1158-1162.

127. Smidt-Hansen T, Folkmar TB, Fode K, Agerbaek M, Donskov F. Combination of zoledronic Acid and targeted therapy is active but may induce osteonecrosis of the jaw in patients with metastatic renal cell carcinoma. J Oral Maxillofac Surg. 2013;71(9):1532-1540.

128. Scoletta M, Arduino PG, Dalmasso P, Broccoletti R, Mozzati M. Treatment outcomes in patients with bisphosphonate-related osteonecrosis of the jaws: a prospective study. Oral Surg Oral Med Oral Pathol Oral Radiol Endod. 2010;110(1):46-53.

129. Scott DA, Krauss J. Neutrophils in periodontal inflammation. Front Oral Biol. 2012;15:56-83.

130. Shannon J, Shannon J, Modelevsky S, Grippo AA. Bisphosphonates and osteonecrosis of the jaw. J Am Geriatr Soc. 2011;59(12):2350-2355.

131. Sharma D, Ivanovski S, Slevin M, Hamlet S, Pop TS, Brinzaniuc K, Petcu EB, Miroiu RI. Bisphosphonate-related osteonecrosis of jaw (BRONJ): diagnostic criteria

and possible pathogenic mechanisms of an unexpected anti-angiogenic side effect. Vasc Cell. 2013;5(1):1.

132. **Solheim E**, Pinholt EM, Talsnes O, Larsen TB, Kirkeby OJ. Bone formation in cranial, mandibular, tibial and iliac bone grafts in rats. J Craniofac Surg. 1995;6(2):139-142.

133. **Springer TA**. Adhesion receptors of the immune system. Nature. 1990;346(6283):425-434.

134. **Szabó A**, Hartmann P, Varga R, Jánvári K, Lendvai Z, Szalai I, Gomez I, Varga G, Greksa F, Németh I, Rázga Z, Keresztes M, Garab D, Boros M. Periosteal microcirculatory action of chronic estrogen supplementation in osteoporotic rats challenged with tourniquet ischemia. Life Sci. 2011;88(3-4):156-162.

135. **Stadelmann VA**, Gauthier O, Terrier A, Bouler JM, Pioletti DP. Implants delivering bisphosphonate locally increase periprosthetic bone density in an osteoporotic sheep model. A pilot study. Eur Cell Mater. 2008;16:10-16.

136. **Støre G**, Granström G. Osteoradionecrosis of the mandible: a microradiographic study of cortical bone. Scand J Plast Reconstr Surg Hand Surg. 1999;33(3):307-314.

137. **Stuehmer C**, Schumann P, Bormann KH, Laschke MW, Menger MD, Gellrich NC, Rücker M. A new model for chronic in vivo analysis of the periosteal microcirculation. Microvasc Res. 2009;77(2):104-108.

138. **Utvåg SE**, Grundnes O, Reikerås O. Effects of lesion between bone, periosteum and muscle on fracture healing in rats. Acta Orthop Scand. 1998;69(2):177-180.

139. **Tapuria N**, Kumar Y, Habib MM, Abu Amara M, Seifalian AM, Davidson BR. Remote ischemic preconditioning: a novel protective method from ischemia reperfusion injury--a review. J Surg Res. 2008;150(2):304-330.

140. **Thomas MV**, Puleo DA. Infection, inflammation, and bone regeneration: a paradoxical relationship. J Dent Res. 2011;90(9):1052-1061.

141. Top AP, Ince C, de Meij N, van Dijk M, Tibboel D. Persistent low microcirculatory vessel density in nonsurvivors of sepsis in pediatric intensive care. Crit Care Med. 2011;39(1):8-13.

142. **Tzermpos F**, Iatrou I, Papadimas C, Pistiki A, Georgitsi M, Giamarellos-Bourboulis EJ. Function of blood monocytes among patients with orofacial infections. J Craniomaxillofac Surg. 2013;41(2):88-91.

143. **Ueno T**, Kagawa T, Fukunaga J, Mizukawa N, Sugahara T, Yamamoto T. Evaluation of osteogenic/chondrogenic cellular proliferation and differentiation in the xenogeneic periosteal graft. Ann Plast Surg. 2002;48(5):539-545.

144. **Van Poznak C**. Osteonecrosis of the jaw and bevacizumab therapy. Breast Cancer Res Treat. 2010;122(1):189-191.

145. **Varga R**, Török L, Szabó A, Kovács F, Keresztes M, Varga G, Kaszaki J, Boros M. Effects of colloid solutions on ischemia-reperfusion-induced periosteal microcirculatory and inflammatory reactions: comparison of dextran, gelatin, and hydroxyethyl starch. Crit Care Med. 2008;36(10):2828-2837.

146. **Verdant CL**, De Backer D, Bruhn A, Clausi CM, Su F, Wang Z, Rodriguez H, Pries AR, Vincent JL. Evaluation of sublingual and gut mucosal microcirculation in sepsis: a quantitative analysis. Crit Care Med. 2009;37(11):2875-2881.

147. **Verdickt GM**, Abbott PV. Blood flow changes in human dental pulps when capsaicin is applied to the adjacent gingival mucosa. Oral Surg Oral Med Oral Pathol Oral Radiol Endod. 2001;92(5):561-565.

148. **Vincenzi B**, Napolitano A, Zoccoli A, Iuliani M, Pantano F, Papapietro N, Denaro V, Santini D, Tonini G. Serum VEGF levels as predictive marker of bisphosphonate-related osteonecrosis of the jaw. J Hematol Oncol. 2012;5:56.

149. **Vyas S**, Hameed S, Murugaraj V. Denosumab-associated osteonecrosis of the jaw--a case report. Dent Update. 2014;41(5):449-450.

150. **Wanner GA**, Ertel W, Müller P, Höfer Y, Leiderer R, Menger MD, Messmer K. Liver ischemia and reperfusion induces a systemic inflammatory response through Kupffer cell activation. Shock. 1996;5(1):34-40.

151. **Wehrhan F**, Stockmann P, Nkenke E, Schlegel KA, Guentsch A, Wehrhan T, Neukam FW, Amann K. Differential impairment of vascularization and angiogenesis in bisphosphonate-associated osteonecrosis of the jaw-related mucoperiosteal tissue. Oral Surg Oral Med Oral Pathol Oral Radiol Endod. 2011;112(2):216-221.

152. **Wei X**, Pushalkar S, Estilo C, Wong C, Farooki A, Fornier M, Bohle G, Huryn J, Li Y, Doty S, Saxena D. Molecular profiling of oral microbiota in jawbone samples of bisphosphonate-related osteonecrosis of the jaw. Oral Dis. 2012;18(6):602-612.

153. **Wen D**, Qing L, Harrison G, Golub E, Akintoye SO. Anatomic site variability in rat skeletal uptake and desorption of fluorescently labeled bisphosphonate. Oral Dis. 2011;17(4):427-432.

154. **Williams RC Jr**, Harmon ME, Burlingame R, Du Clos TW. Studies of serum C-reactive protein in systemic lupus erythematosus. J Rheumatol. 2005;32(3):454-461.

155. **Wilson S**, Sharp CA, Davie MW. Health-related quality of life in patients with osteoporosis in the absence of vertebral fracture: a systematic review. Osteoporos Int. 2012;23(12):2749-2768.

156. **Wood J**, Bonjean K, Ruetz S, Bellahcène A, Devy L, Foidart JM, Castronovo V, Green JR. Novel antiangiogenic effects of the bisphosphonate compound zoledronic acid. J Pharmacol Exp Ther. 2002;302(3):1055-1061.

157. **Xie C**, Ming X, Wang Q, Schwarz EM, Guldberg RE, O'Keefe RJ, Zhang X. COX-2 from the injury milieu is critical for the initiation of periosteal progenitor cell mediated bone healing. Bone. 2008;43(6):1075-1083.

158. **Yamagishi S**, Abe R, Inagaki Y, Nakamura K, Sugawara H, Inokuma D, Nakamura H, Shimizu T, Takeuchi M, Yoshimura A, Bucala R, Shimizu H, Imaizumi T. Minodronate, a newly developed nitrogen-containing bisphosphonate, suppresses melanoma growth and improves survival in nude mice by blocking vascular endothelial growth factor signaling. Am J Pathol. 2004;165(6):1865-1874.

159. **Yamagishi S**, Matsui T, Nakamura K, Takeuchi M. Minodronate, a nitrogen-containing bisphosphonate, inhibits advanced glycation end product-induced vascular cell adhesion molecule-1 expression in endothelial cells by suppressing reactive oxygen species generation. Int J Tissue React. 2005;27(4):189-195.

160. **Yamaguchi K**, Motegi K, Iwakura Y, Endo Y. Involvement of interleukin-1 in the inflammatory actions of aminobisphosphonates in mice. Br J Pharmacol. 2000;130(7):1646-1654.

161. **Yamashiro T**, Takano-Yamamoto T. Differential responses of mandibular condyle and femur to oestrogen deficiency in young rats. Arch Oral Biol. 1998;43(3):191-195.

162. **Yamashita J**, McCauley LK, Van Poznak C. Updates on osteonecrosis of the jaw. Curr Opin Support Palliat Care. 2010;4(3):200-206.

163. **Yamashita J**, Koi K, Yang DY, McCauley LK. Effect of zoledronate on oral wound healing in rats. Clin Cancer Res. 2011;17(6):1405-1414.

164. **Yamashita J**, McCauley LK. Antiresorptives and osteonecrosis of the jaw. J Evid Based Dent Pract. 2012;12(3 Suppl):233-247.

165. **Yokoyama M**, Atsumi T, Tsuchiya M, Koyama S, Sasaki K. Dynamic changes in bone metabolism in the rat temporomandibular joint after molar extraction using bone scintigraphy. Eur J Oral Sci. 2009;117(4):374-379.

166. **Yu YY**, Lieu S, Hu D, Miclau T, Colnot C. Site specific effects of zoledronic acid during tibial and mandibular fracture repair. PLoS One. 2012;7(2):e31771.

167. **Zhang L**, Bail H, Mittlmeier T, Haas NP, Schaser KD. Immediate microcirculatory derangements in skeletal muscle and periosteum after closed tibial fracture. J Trauma. 2003;54(5):979-985.

168. **Ziebart T**, Ziebart J, Gauss L, Pabst A, Ackermann M, Smeets R, Konerding MA, Walter C. Investigation of inhibitory effects on EPC-mediated neovascularization by different bisphosphonates for cancer therapy. Biomed Rep. 2013;1(5):719-722.

169. **Zysk SP**, Dürr HR, Gebhard HH, Schmitt-Sody M, Refior HJ, Messmer K, Veihelmann A. Effects of ibandronate on inflammation in mouse antigen-induced arthritis. Inflamm Res. 2003;52(5):221-226.

9. ANNEX

I.

Microcirculation
The Official Journal of the Microcirculatory Society, Inc., the British Microcirculation Society, and the Australia & New Zealand Microcirculation Society

DOI:10.1111/micc.12128

Original Article

A Novel Method for *In Vivo* Visualization of the Microcirculation of the Mandibular Periosteum in Rats

RENÁTA VARGA,* ÁGNES JANOVSZKY,*,† ANDREA SZABÓ,† DÉNES GARAB,† DÓRA BODNÁR,† MIHÁLY BOROS,† JÖRG NEUNZEHN,‡ HANS-PETER WIESMANN,‡ AND JÓZSEF PIFFKÓ*

*Department of Oral and Maxillofacial Surgery, University of Szeged, Szeged, Hungary; †Institute of Surgical Research, University of Szeged, Szeged, Hungary; ‡Institute of Materials Science, Max Bergmann Center of Biomaterials, TU Dresden, Dresden, Germany
Address for correspondence: Renáta Varga M.D., Ph.D., Department of Oral and Maxillofacial Surgery, University of Szeged, Kálvária sgt. 57, Szeged H-6725, Hungary. *E-mail:* vargarenata@gmail.com

Received 14 January 2014; accepted 7 March 2014.

ABSTRACT

Objective: The periosteum plays an important role in bone physiology, but observation of its microcirculation is greatly limited by methodological constraints at certain anatomical locations. This study was conducted to develop a microsurgical procedure which provides access to the mandibular periosteum in rats.

Methods: Comparisons of the microcirculatory characteristics with those of the tibial periosteum were performed to confirm the functional integrity of the microvasculature. The mandibular periosteum was reached between the facial muscles and the anterior surface of the superficial masseter muscle at the external surface of the mandibular corpus; the tibial periosteum was prepared by dissecting the covering muscles at the anteromedial surface. Intravital fluorescence microscopy was used to assess the leukocyte–endothelial interactions and the RBCV in the tibial and mandibular periosteum. Both structures were also visualized through OPS and fluorescence CLSM.

Results: The microcirculatory variables in the mandibular periosteum proved similar to those in the tibia, indicating that no microcirculatory failure resulted from the exposure technique.

Conclusion: This novel surgical approach provides simple access to the mandibular periosteum of the rat, offering an excellent opportunity for investigations of microcirculatory manifestations of dentoalveolar and maxillofacial diseases.

Key words: mandibular periosteum, intravital microscopy, orthogonal polarization spectral imaging, confocal laser scanning microscopy, rat

Abbreviations used: CLSM, confocal laser scanning microscopy; FITC, fluorescein isothiocyanate; i.v., intravenous; IVM, intravital microscopy; OPS, orthogonal polarization spectral imaging; RBCV, red blood cell velocity.

Please cite this paper as: Varga R, Janovszky Á, Szabó A, Garab D , Bodnár D, Boros M, Neunzehn J, Wiesmann HP, Piffkó J. A novel method for *in vivo* visualization of the microcirculation of the mandibular periosteum in rats. *Microcirculation* **21**: 524–531, 2014.

INTRODUCTION

The rich blood supply of the maxillofacial region ensures fast healing of the tissues in the oral cavity. On the other hand, these tissues, and the bones of the jaw in particular, are strikingly prone to local inflammatory complications, ranging from abscess formation to osteomyelitis and osteonecrosis [30]. It is reasonable to assume that functional and morphological impairments of the periosteal microcirculation are critically involved in these processes. This assumption is supported by clinical observations where osteonecrosis and defective angiogenesis of the mucoperiosteal tissues were demonstrated in patients receiving chronic bisphosphonate treatment [37]. In general, the role of the periosteal integrity in bone physiology is well recognized, not only as it concerns to the maintenance of the vascular supply but also from the aspect of active regulation of the bone metabolism and regeneration. It is similarly well known that successful healing after fractures requires the regeneration of the peri- and endosteal circulations [20]. It follows that periosteal microvascular alterations can be of importance in the pathomechanism of oral diseases associated with a deterioration of tissue perfusion and with inflammatory complications.

The vascular architecture of the intraoral region, including the periosteum, can be examined by imaging methods such as computer tomography, magnetic resonance imaging and to some extent scintigraphy or histology [3,4,11,23]. Nevertheless, these tools are not relevant when dynamic changes or functional aspects of the periosteal microcirculation are to be

investigated. The methods utilized for examinations of the functional characteristics of the microcirculation, such as hemoglobin absorptiometry combined with laser-Doppler flowmetry, may provide information on tissue oxygenation and perfusion, but in this case the tissue mass is rather robust, e.g., the gingiva [21]. If more accurate detection or improved spatial resolution of the microcirculation is needed, fluorescence IVM can provide an opportunity for real-time examination of the microcirculation of superficial layers of different organs. Conventional fluorescence IVM has many advantages. It can visualize not only changes in the efficacy of microvascular perfusion but also leukocyte–endothelial interactions, metabolic variables, or signs of apoptosis [1,17]. For observation of the microcirculation of superficial tissue layers, nonfluorescence techniques such as OPS [14] and sidestream dark-field imaging have also been developed [22]. These methods have the advantage that the use of fluorescence markers is not necessary and this allows a possibility for human applications also in the oral cavity [10,22]. Observation of the periosteal compartment would still necessitate surgical exposure, but the imaging of individual vessels and cells is possible without disturbing their functional characteristics.

The calvarian periosteum can be visualized in experimental settings [32], but examination of the microcirculation of the jaw bones runs into many technical difficulties. We earlier developed methods suitable for visualization of the tibial periosteum and the synovial membrane in the knee joint in rats [15,34], but such approaches were not available for the exposure and *in vivo* investigation of the mandibular periosteum. We therefore considered it important to address this issue, in part to solve the technical problems and in part because the physiology or the pathophysiological reactions of the jaw may differ from those in other bones of the skeleton. Specifically, bisphosphonates have been demonstrated to cause osteonecrosis in the jaw after invasive dental procedures, but such reactions do not occur in the bones of the appendicular skeleton [5,31]. This observation suggests that potentially different microcirculatory reactions may evolve in the periosteum at different anatomical locations. For this reason, we set out to compare the microcirculatory characteristics of the mandibular and the tibial periosteum through the use of a microsurgical approach and microscopic methods that are suitable for *in vivo* visualization of individual microvessels. Firstly, the functional integrity of the mandibular microcirculation was ascertained by using the OPS method, where the use of fluorescent markers is not required (and sampling for biochemical and molecular biological analyses is therefore possible). We used the "gold standard" fluorescence IVM for the determination of perfusion and leukocyte–endothelial interactions. Finally, CLSM was chosen as it offers an opportunity for determination of the *in vivo* histology of tissues (including microvessels) without sectioning, fixation, and embedding artifacts. The final aim of the study was to provide a comprehensive methodological basis for future investigations targeting the potential microcirculatory manifestations of oral diseases.

MATERIALS AND METHODS

The experiments were performed in full accordance with the NIH Guidelines (Guide for the Care and Use of Laboratory Animals) and approved by the Animal Welfare Committee of the University of Szeged (V/1639/2013).

Animals

Ten male Sprague–Dawley rats were used (the average weight at the time of the experiment was 320 ± 10 g). The animals were anaesthetized intraperitoneally with an initial dose of sodium pentobarbital (45 mg/kg). After cannulation of the trachea, the penile vein was cannulated to administer fluids and drugs (supplementary dose of sodium pentobarbital; 5 mg/kg). During preparation and microcirculatory investigations, the rats were placed in a supine position on a heating pad to maintain the body temperature at 36–37°C.

Surgical Procedures

The fur of the animals in the mandibular region was shaved, and a lateral incision parallel to the incisor tooth was made in the facial skin and the underlying subcutaneous tissue using a careful microsurgical approach under an operating microscope (6× magnification; Carl Zeiss GmbH, Jena, Germany). The masseter muscle consists of superficial and deep parts, the latter being further divided into anterior and posterior sections in rats [9]. The fascia between the anterior part of the deep masseter and the anterior superficial masseter was cut with microscissors (Figure 1A). By this means, the periosteal membrane covering the corpus of the mandible laterally to the incisor tooth was reached and it was gently separated from the covering thin connective tissue (Figure 1B). Stitches with 7.0 monofilament polypropylene microsurgical thread were placed into the surrounding masseter muscles for retraction and better exposure of the region of interest. We applied this surgical approach on both sides of the lower jaw. With this preparation technique, the periosteal microcirculation of the mandible could be examined by *in vivo* microscopic methods at the anterior margin of the molar region.

For comparison of the characteristics of the mandibular microcirculation with those of the tibial periosteum, the medial/anterior surface of the tibia was exposed by complete transection of the anterior gracilis muscle with microscissors, and careful atraumatic microsurgical removal of the connective tissue covering the tibial periosteum (Figure 1C,D) [34]. These dissections were performed on both sides to permit parallel observations of intravascular and topically applied fluorescence tracers (see later).

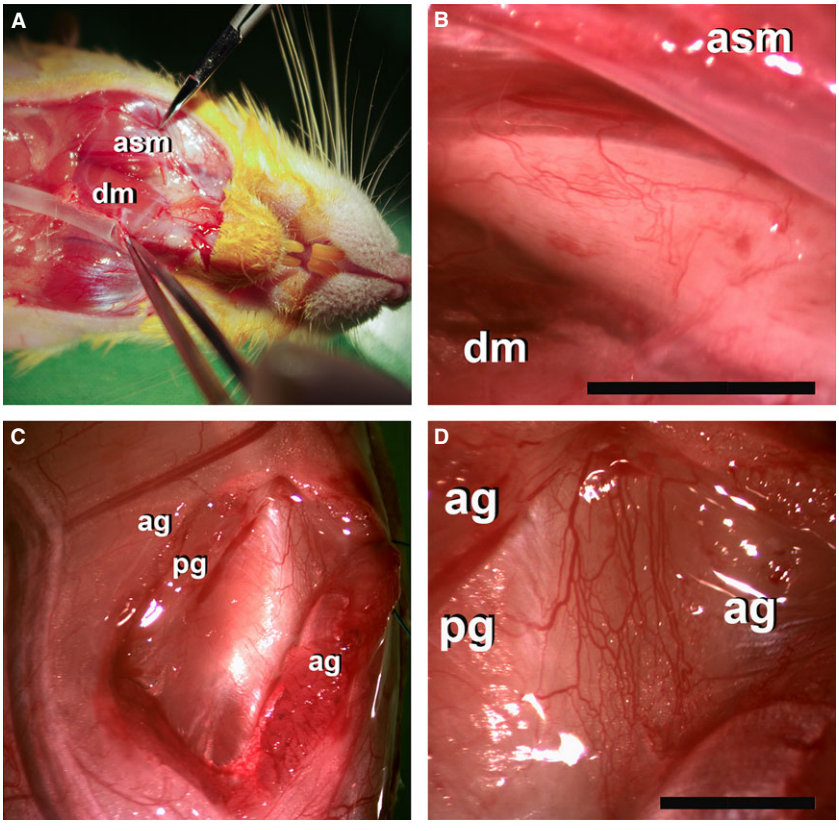

Figure 1. Exposure of the mandibular and tibial periosteum for *in vivo* microscopic examinations. Access to the mandibular periosteum was achieved by making a lateral incision parallel to the incisor tooth in the facial skin and the underlying subcutaneous tissue, which was followed by gentle separation of the fascia between the anterior part of the deep masseter (dm) and the anterior superficial masseter (asm) muscles (**A, B**). Finally, the thin connective tissue covering the periosteum was gently incised with microscissors. By this means, the periosteal membrane covering the corpus of the mandible laterally to the incisor tooth was reached. The tibial periosteum was reached by transecting the anterior gracilis (ag) muscle completely in the middle (and a part of the posterior gracilis muscle [pg] too) and gently removing the thin connective tissue covering the periosteum (**C, D**). The bar denotes 2500 μm.

Experimental Protocol

After surgical exposure of the mandibular and tibial periosteum on both sides, recordings were performed on the right side with OPS, which does not require any fluorescence labeling (see later) (Figure 2A,B). After this, the animals received i.v. injections of FITC-labeled erythrocytes (0.2 mL; Sigma Aldrich, St. Louis, MO, USA) (Figure 3A,B) [27] and rhodamine-6G (0.2%, 0.1 mL; Sigma Aldrich) for the staining of leukocytes (Figure 3C,D), and IVM recording was performed at the previous locations. Subsequently, 50 μL of the nuclear dye acriflavin (1 mM) was applied topically to the tibial periosteal surface on the left side and was rinsed off with warm physiological saline solution after an exposure time of one minute, and then CLSM recording was performed (Figure 4B). The same staining procedure was carried out for the mandible on the left side (Figure 4A). This was followed by an i.v. injection of the plasma dye FITC-dextran 150 kDa (i.v. 0.3 mL, 20 mg/mL solution dissolved in saline; Sigma Aldrich), and CLSM (Figure 4C,D) and IVM recordings (Figure 3E,F) were made on the tibia and the mandible on the right side five minutes after injection of the tracer.

OPS Technique

The exposed periosteum of the corpus of the mandible or the tibial periosteum on the right side was horizontally positioned on an adjustable stage and superfused with 37°C saline. The periosteal membranes were first visualized with

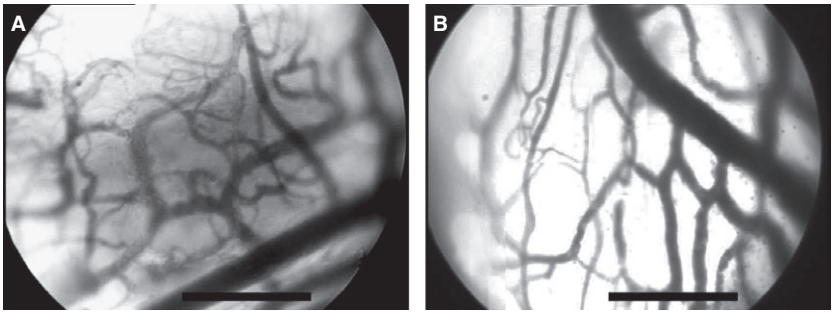

Figure 2. Micrographs showing the mandibular (**A**) and tibial periosteum (**B**) made with the OPS technique. The bar denotes 200 μm.

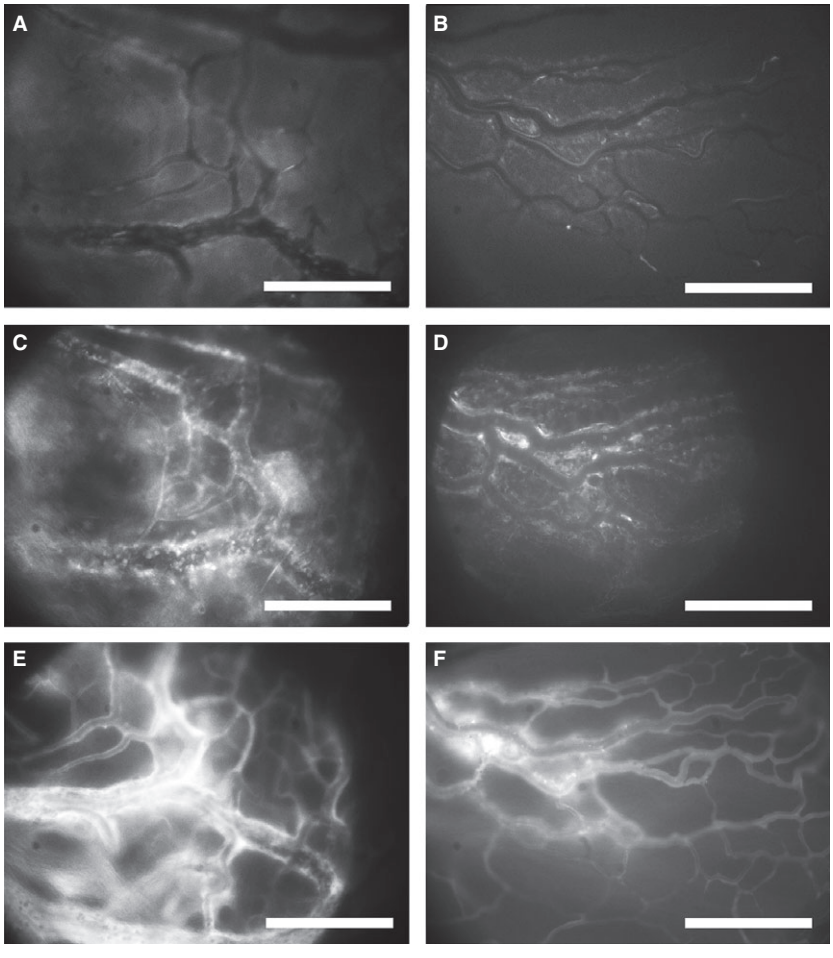

Figure 3. Fluorescence intravital microscopic images of the mandibular (**A, C, E**) and the tibial periosteum (**B, D, F**), involving FITC-labeled erythrocytes (**A, B**), rhodamine 6G-labeled neutrophil leukocytes (**C, D**), and FITC-dextran-labeled plasma (**E, F**). The bar denotes 200 μm.

an OPS device (Cytoscan™; Cytometrics, Philadelphia, PA, USA), which provides optimal imaging of the microvascular structures at a chosen focus level [penetration depth: approx. 200 μm; 11] (Figure 2A,B). This technique utilizes epi-illumination with linearly polarized light at 548 nm (which is the isobestic point of oxy- and deoxyhemoglobin) to visualize hemoglobin-containing structures without the additional use of a fluorochrome. Images were recorded on a SVHS video recorder (Panasonic AG-MD 830; Matsushita Electric Industrial Co., Tokyo, Japan) and a personal computer.

Fluorescence IVM

The periosteal microcirculation was visualized by IVM (penetration depth: approx. 250 μm; Zeiss Axiotech Vario 100HD microscope; 100-W HBO mercury lamp; Acroplan 20× /0.5 N.A. W; Carl Zeiss GmbH, Jena, Germany). Images from three–four fields of the mandibular and the tibial periosteum (Figure 3) were recorded with a charge-coupled device video camera (Teli CS8320Bi; Toshiba Teli Corporation, Osaka, Japan) attached to an S-VHS video recorder (Panasonic AG-MD 830; Matsushita Electric Industrial Co.) and a personal computer (see labeling techniques above).

Fluorescence CLSM

Confocal imaging of the surface of the mandibular and tibial periosteum was performed with a Five1 Optiscan device (Optiscan Pty. Ltd., Melbourne, Vic., Australia) (Figure 4). *In vivo* histology was employed by placing the Optiscan probe on the surface of the periosteal membranes and by changing the focus level through virtual sections of 7 μm during the confocal imaging (penetration depth: 0–250 μm). Cell nuclei were first stained with topically applied acriflavin (see above) on the left side, and this was followed by recordings on the contralateral side after i.v. injection of the intravascular tracer FITC-dextran (see above). Images were stored on a personal computer provided by the manufacturer.

Video Analysis

Quantitative evaluation of the microcirculatory parameters was performed off-line by the frame-to-frame analysis of the

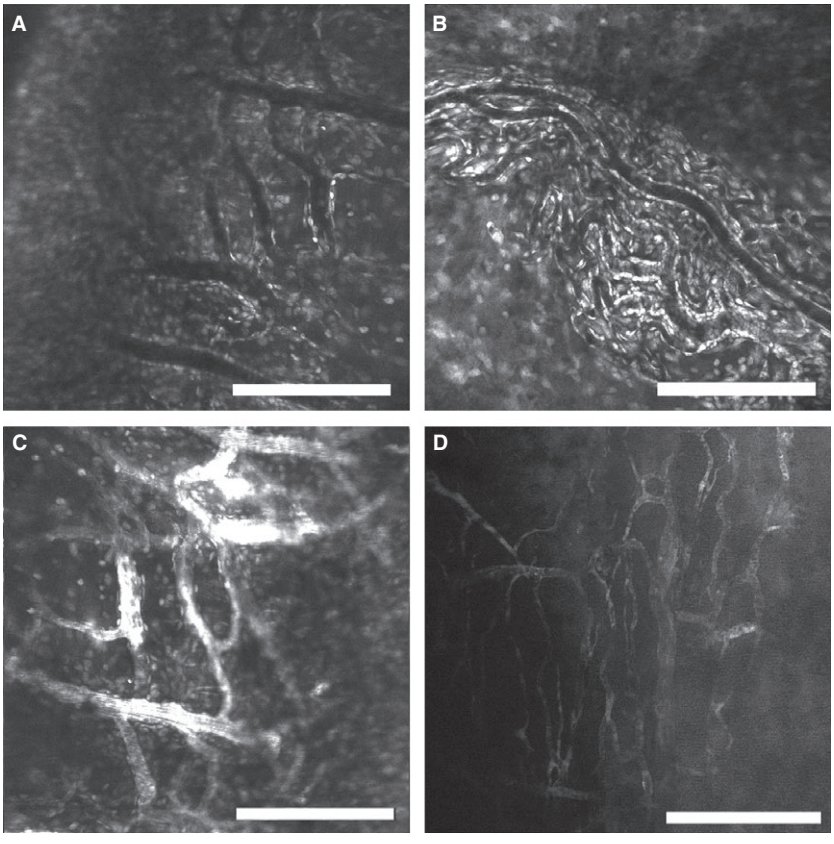

Figure 4. Confocal laser scanning microscopic images of the mandibular (**A, C**) and tibial periosteum (**B, D**). Cell nuclei were labeled by the topical application of acriflavin (left side) (**A, B**). Images were also taken at both structures on the right sides after the i.v. injection of FITC-dextran (**C, D**). The bar denotes 200 μm.

videotaped images taken for IVM and OPS (IVM Software; Pictron Ltd, Budapest, Hungary). Leukocyte–endothelial cell interactions were analyzed at least in four postcapillary venules per rat. Rolling leukocytes were defined as cells moving with a velocity less than 40% of that of the erythrocytes in the centerline of the microvessel and passing through the observed vessel segment within 30 seconds, and are given as the number of cells per second per vessel circumference. Adherent leukocytes were defined as cells that did not move or detach from the endothelial lining within an observation period of 30 seconds and are given as the number of cells per mm^2 of endothelial surface, calculated from the diameter and length of the vessel segment. RBCV (μm/s) was determined by frame-to-frame analysis of 5–6 consecutive video-captured images taken after labeling of the erythrocytes (see above).

Statistical Analysis

The statistical analysis was performed with a statistical software package (SigmaStat for Windows, Jandel Scientific, Erkrath, Germany). Within the IVM data, RBCV values in the capillaries and the extents of rolling and adherence of leukocytes in the postcapillary venules of the mandibular and tibial periosteum were compared by using the Student's *t*-test. Comparisons within the RBCV values measured with IVM and OPS were also made with the Student's *t*-test. p values <0.05 were considered significant.

RESULTS

With the reported preparation technique, the anterior surface of the tibial periosteum provides a larger observation field (ranging between 8.89 and 9.88 mm^2) (Figure 1D) than that of the exposed mandibular region (ranging between 8.03 and 9.18 mm^2) (Figure 1B). Furthermore, the entire exposed tibial periosteal surface can be examined by different *in vivo* microscopic methods, whereas only approximately one third of the mandibular periosteum (i.e., its anterior part) can easily be reached by the relatively robust objectives. The vascular density reached $0.0182 \pm 0.0011/\mu$m in case of the tibia and was $0.0193 \pm 0.0008/\mu$m in the mandibular periosteum. The arterioles, capillaries, and venules can be distinguished on the basis of vessel diameters and the direction of flow of moving elements (plasma or red blood cells) within them. Within the mandibular periosteum, the vascular network consisted mainly of arterioles and venules, but a few capillaries and mostly venules were present in the tibial periosteum (as depicted in Figures 2–4).

IVM demonstrated that the RBCV values were similar in the two capillary beds (827.5 ± 30.1 μm/s in the mandibular

and 739.0 ± 37.7 μm/s in the tibial periosteum) (Table 1). The OPS technique revealed similar RBCV values (data not shown). The IVM data did not indicate any significant differences in the magnitude of the leukocyte–endothelial cell interactions between the two locations (Table 1).

The CLSM method was applied to stain the cell nuclei of the vascular compartment (Figure 4A,B). The vascular organization was also visualized when intravascular dye (FITC-dextran) was employed (Figure 4C,D).

At the end of the experiments, tissue specimens were harvested for histology. The tibial periosteum appeared to be more strongly attached to the underlying bone than that in the mandible.

DISCUSSION

Studies of the microcirculation in the oral region gained considerable attention when the predictive value of mucosal perfusion deficits was demonstrated in septic shock patients [33,35]. Another intraoral manifestation of a systemic menace was revealed during cardiac surgery [2] and the intraoral microcirculation was demonstrated to correlate well with the gastrointestinal perfusion changes [35]. The periosteal microcirculatory aspects of systemic and intraoral diseases, however, have been far less well clarified. These above human observations became possible by the development of methods which provide quantitative information on individual vessels without the need for the use of fluorescent tracers (i.e., OPS or sidestream dark-field methods). High spatial resolution is an advantage of intravital microscopic methods in general, but the relatively low penetration depth restricts the examination to the superficial layers such as the mucosal or gingival/mucosal surfaces in the oral cavity.

As a major source of osteoprogenitor cells, the periosteum of the jaw bones has a high impact in the pathogenesis of various orofacial diseases, but specific, real-time examination of its microcirculation can be performed only after surgical exposure of this structure. As a result, the periosteal microcirculation has been examined in only a relatively limited number of studies of the tibia [26,28,34,38] or the calvaria [32], and we are aware of only one study in the maxilla–mandibular region, in rabbits [25]. All these latter studies involved the use of conventional fluorescence IVM which (as opposed to OPS) also makes possible the investigation of microcirculatory perfusion, permeability, and leukocyte–endothelial interactions. In this study, we developed a surgical approach to the mandibular periosteum. When a rodent model is to be established, similarities to the human anatomy should first be ascertained. The most accessible region, where the periosteum is situated most superficially, is the area medial to the parotideomasseteric region [9]. This region, between the superficial masseter muscles and the mentum, just laterally to the ever-growing incisor tooth of the rat, can be approached by incising the skin and subcutaneous tissue. We gained access to the periosteum next to the anterior part of the superficial masseter muscle in the area where this muscle adheres to the ventral margin of the mandible. It was considered important to proceed laterally to the continuously growing incisor teeth so as to avoid any potential functional dissimilarities to the human characteristics.

The fluorescence IVM data revealed that the mandibular microcirculatory variables are similar to those seen in the tibia. It should be added that the preparation was stable for approximately four hours in preliminary experiments, when only IVM was employed (data not shown). In the case of CLSM, the potential toxic effects of topically applied nuclear dyes would probably influence the microcirculation in the long run, and examination may be therefore preferably be restricted to one time point only. As regards the periosteal microcirculation, examination of the effects of surgical trauma of the tibia [38] and the maxilla [25] is a possible target for IVM methods. Such questions can also be answered by using the present exposure technique. Moreover, the consequences of tooth extraction (particularly of first molars) and the subsequent osteogenesis on the periosteal microcirculatory reactions may also be examined. In previous studies, osteogenesis-related capillary density changes (by OPS) [19] and leukocyte–endothelial interactions in experimental peridontitis (by IVM) [7] were examined in the

Table 1. Microcirculatory parameters: RBCV in the capillaries, and leukocyte rolling, and sticking in the postcapillary venules of the mandibular and tibial periosteum in rats as determined by the OPS technique and fluorescence IVM

Method	OPS	IVM		
Parameter	RBCV (μm/s)	RBCV (μm/s)	Rolling (/mm/s)	Sticking (/mm^2)
Mandible	736.6 ± 26.7	827.5 ± 30.1	46.6 ± 5.8	13.4 ± 4.4
Tibia	723.7 ± 39.2	739.0 ± 37.7	56.9 ± 11.5	18.5 ± 3.9

Mean values ± SEM are presented.

mucosa, but never in the periosteum. Furthermore, the present model appears suitable for CLSM; the penetration of intranuclear dyes for the examination of angiogenesis and apoptosis is also possible. CLSM has previously been employed in the oral mucosa to visualize intraoral mucosal lesions, tumors [12], borders of malignancies, and resection margins [6,16,29].

The jaws are particularly prone to inflammatory complications (e.g., periodontitis or abscess), as they can be sensitively exposed to the external environment in the immediate vicinity of the teeth. The IVM approach can be a particularly valuable tool for the examination of oral inflammatory processes. In consequence of the relatively high penetration depth of laser light, laser-Doppler flowmetry has been used for the detection of mucosal/gingival inflammatory processes. As examples, the consequences of periodontal access flap surgery and inflammation have been detected in the gingiva [18,24] and in the pulpar blood flow [36]. With use of the proposed method, such inflammatory complications could also be examined using the mandibular periosteum.

This study demonstrated certain differences in architecture in the mandibular and the tibial periosteum. Specifically, the venules are proved to be the predominant structures in the examined anteromedial surface of the tibia, whereas arterioles were also detected in the mandible. Differences within the skeletal system were reported by Chanavaz, who found that the jaw microcirculation has a higher number of anastomoses and a greater impact on the centromedullar circulation as opposed to the long bones of the skeleton [8]. A corrosion cast study similarly revealed lower numbers of capillaries and arterioles in the periosteal compartment than in the gingival compartment, which is characterized by a rich capillary network [23]. At the present stage, the impact of our observations cannot be fully assessed and the potential regional differences should also be taken into account: We earlier demonstrated [13] that the anterolateral side of the tibia (which was used for a myocutaneous flap model by Rücker *et al.* [26]) has more capillaries than on the anteromedial side. We consider that the higher density of venules may predispose to microcirculatory inflammatory complications, e.g., the transmigration of neutrophil leukocytes through the postcapillary venules.

In summary, the new microsurgical approach presented provides access to the periosteal microcirculation in the rat mandible. We compared the mandibular microcirculatory variables with those of a standard and stable tibial model by using fluorescence IVM to ascertain that this new technique does not cause microcirculatory disturbances or inflammatory complications. It was demonstrated that this exposure procedure makes the mandibular periosteum accessible for OPS and CLSM examinations. It is anticipated that this model and the investigation of mandibular microcirculatory alterations may contribute to a better understanding of maxillofacial or dentoalveolar diseases.

PERSPECTIVE

The maxillofacial region is particularly prone to inflammatory reactions. The present rat model using IVM techniques should be useful in further studies exploring the periosteal microcirculation, pathophysiological mechanisms of bone regeneration, dentoalveolar diseases, and drug-related complications such as mandibular osteonecrosis.

ACKNOWLEDGMENTS

This publication/presentation is supported by the European Union and cofunded by the European Social Fund. Project title: "Telemedicine-focused research activities in the field of Mathematics, Informatics and Medical Sciences". Project number: TÁMOP-4.2.2.A-11/1/KONV-2012-0073. Further supporting research grants are as follows: TÁMOP 4.2.4.A/2-11-1-2012-0001, TÁMOP-4.2.2.A-11/1/KONV-2012-0035 and OTKA – 109388.

CONFLICT OF INTEREST

The authors declare that they have no conflict of interest.

REFERENCES

1. Abshagen K, Eipel C, Menger MD, Vollmar B. Comprehensive analysis of the regenerating mouse liver: an in vivo fluorescence microscopic and immunohistological study. *J Surg Res* 134: 354–362, 2006.
2. Bauer A, Kofler S, Thiel M, Eifert S, Christ F. Monitoring of the sublingual microcirculation in cardiac surgery using orthogonal polarization spectral imaging: preliminary results. *Anesthesiology* 107: 939–945, 2007.
3. Berggren A, Weiland AJ, Ostrup LT, Dorfman H. Microvascular free bone transfer with revascularization of the medullary and periosteal circulation or the periosteal circulation alone. A comparative experimental study. *J Bone Joint Surg Am* 64: 73–87, 1982.
4. Bhatt R, Lauder I, Finlay DB, Allen MJ, Belton IP. Correlation of bone scintigraphy and histological findings in medial tibial syndrome. *Br J Sports Med* 34: 49–53, 2000.
5. Blazsek J, Dobó Nagy C, Blazsek I, Varga R, Vecsei B, Fejérdy P, Varga G. Aminobisphosphonate stimulates bone regeneration and enforces consolidation of titanium implant into a new rat caudal vertebrae model. *Pathol Oncol Res* 15: 567–577, 2009.
6. Capodiferro S, Maiorano E, Loiudice AM, Scarpelli F, Favia G. Oral laser surgical pathology: a preliminary study on the clinical advantages of diode laser and on the histopathological features of specimens evaluated by conventional and confocal laser scanning microscopy. *Minerva Stomatol* 57: 1–6, 6–7, 2008.

7. Carvalho RR, Pellizzon CH, Justulin L, Jr, Felisbino SL, Vilegas W, Bruni F, Lopes-Ferreira M, Hiruma-Lima CA. Effect of mangiferin on the development of periodontal disease: involvement of lipoxin A4, anti-chemotaxic action in leukocyte rolling. *Chem Biol Interact* 179: 344–350, 2009.
8. Chanavaz M. Anatomy and histophysiology of the periosteum: quantification of the periosteal blood supply to the adjacent bone with 85Sr and gamma spectrometry. *J Oral Implantol* 21: 214–219, 1995.
9. Cox PG, Jeffery N. Reviewing the morphology of the jaw-closing musculature in squirrels, rats, and guinea pigs with contrast-enhanced microCT. *Anat Rec (Hoboken)* 294: 915–928, 2011.
10. De Backer D, Donadello K, Sakr Y, Ospina-Tascon G, Salgado D, Scolletta S, Vincent JL. Microcirculatory alterations in patients with severe sepsis: impact of time of assessment and relationship with outcome. *Crit Care Med* 41: 791–799, 2013.
11. Fayad LM, Kamel IR, Kawamoto S, Bluemke DA, Frassica FJ, Fishman EK. Distinguishing stress fractures from pathologic fractures: a multimodality approach. *Skeletal Radiol* 34: 245–259, 2005.
12. Franz M, Hansen T, Borsi L, Geier C, Hyckel P, Schleier P, Richter P, Altendorf-Hofmann A, Kosmehl H, Berndt A. A quantitative co-localization analysis of large unspliced tenascin-C(L) and laminin-5/gamma2-chain in basement membranes of oral squamous cell carcinoma by confocal laser scanning microscopy. *J Oral Pathol Med* 36: 6–11, 2007.
13. Greksa F, Tóth K, Boros M, Szabó A. Periosteal microvascular reorganization after tibial reaming and intramedullary nailing in rats. *J Orthop Sci* 17: 477–483, 2012.
14. Groner W, Winkelman JW, Harris AG, Ince C, Bouma GJ, Messmer K, Nadeau RG. Orthogonal polarization spectral imaging: a new method for study of the microcirculation. *Nat Med* 5: 1209–1212, 1999.
15. Hartmann P, Erős G, Varga R, Kaszaki J, Garab D, Németh I, Rázga Z, Boros M, Szabó A. Limb ischemia-reperfusion differentially affects the periosteal and synovial microcirculation. *J Surg Res* 178: 216–222, 2012.
16. Haxel BR, Goetz M, Kiesslich R, Gosepath J. Confocal endomicroscopy: a novel application for imaging of oral and oropharyngeal mucosa in human. *Eur Arch Otorhinolaryngol* 267: 443–448, 2010.
17. Horie Y, Wolf R, Miyasaka M, Anderson DC, Granger DN. Leukocyte adhesion and hepatic microvascular responses to intestinal ischemia/reperfusion in rats. *Gastroenterology* 111: 666–673, 1996.
18. Kerdvongbundit V, Vongsavan N, Soo-Ampon S, Hasegawa A. Microcirculation and micromorphology of healthy and inflamed gingivae. *Odontology* 91: 19–25, 2003.
19. Lindeboom JA, Mathura KR, Milstein DM, Ince C. Microvascular soft tissue changes in alveolar distraction osteogenesis. *Oral Surg Oral Med Oral Pathol Oral Radiol Endod* 106: 350–355, 2008.
20. Macnab I, Dehoas WG. The role of periosteal blood supply in the healing of fractures of the tibia. *Clin Orthop* 105: 27–33, 1974.
21. Milstein DM, Cheung YW, Žiūkaitė L, Ince C, van den Akker HP, Lindeboom JA. An integrative approach for comparing microcirculation between normal and alveolar cleft gingiva in children scheduled for secondary bone grafting procedures. *Oral Surg Oral Med Oral Pathol Oral Radiol* 115: 304–309, 2013.
22. Milstein DM, Lindeboom JA, Ince C. Intravital sidestream dark-field (SDF) imaging is used in a rabbit model for continuous noninvasive monitoring and quantification of mucosal capillary regeneration during wound healing in the oral cavity: a pilot study. *Arch Oral Biol* 55: 343–349, 2010.
23. Nobuto T, Yanagihara K, Teranishi Y, Minamibayashi S, Imai H, Yamaoka A. Periosteal microvasculature in the dog alveolar process. *J Periodontol* 60: 709–715, 1989.
24. Retzepi M, Tonetti M, Donos N. Gingival blood flow changes following periodontal access flap surgery using laser Doppler flowmetry. *J Clin Periodontol* 34: 437–443, 2007.
25. Rücker M, Binger T, Deltcheva K, Menger MD. Reduction of midfacial periosteal perfusion failure by subperiosteal versus supraperiosteal dissection. *J Oral Maxillofac Surg* 63: 87–92, 2005.
26. Rücker M, Roesken F, Vollmar B, Menger MD. A novel approach for comparative study of periosteum, muscle, subcutis, and skin microcirculation by intravital fluorescence microscopy. *Microvasc Res* 56: 30–42, 1998.
27. Ruh J, Ryschich E, Secchi A, Gebhard MM, Glaser F, Klar E, Herfarth C. Measurement of blood flow in the main arteriole of the villi in rat small intestine with FITC-labeled erythrocytes. *Microvasc Res* 56: 62–69, 1998.
28. Schaser KD, Zhang L, Haas NP, Mittlmeier T, Duda G, Bail HJ. Temporal profile of microvascular disturbances in rat tibial periosteum following closed soft tissue trauma. *Langenbecks Arch Surg* 388: 323–330, 2003.
29. Scivetti M, Lucchese A, Ficarra G, Giuliani M, Lajolo C, Maiorano E, Favia G. Oral pulse granuloma: histological findings by confocal laser scanning microscopy. *Ultrastruct Pathol* 33: 155–159, 2009.
30. Scoletta M, Arduino PG, Dalmasso P, Broccoletti R, Mozzati M. Treatment outcomes in patients with bisphosphonate-related osteonecrosis of the jaws: a prospective study. *Oral Surg Oral Med Oral Pathol Oral Radiol Endod* 110: 46–53, 2010.
31. Stadelmann VA, Gauthier O, Terrier A, Bouler JM, Pioletti DP. Implants delivering bisphosphonate locally increase periprosthetic bone density in an osteoporotic sheep model. A pilot study. *Eur Cell Mater* 16: 10–16, 2008.
32. Stuehmer C, Schumann P, Bormann KH, Laschke MW, Menger MD, Gellrich NC, Rücker M. A new model for chronic in vivo analysis of the periosteal microcirculation. *Microvasc Res* 77: 104–108, 2009.
33. Top AP, Ince C, de Meij N, van Dijk M, Tibboel D. Persistent low microcirculatory vessel density in nonsurvivors of sepsis in pediatric intensive care. *Crit Care Med* 39: 8–13, 2011.
34. Varga R, Török L, Szabó A, Kovács F, Keresztes M, Varga G, Kaszaki J, Boros M. Effects of colloid solutions on ischemia-reperfusion-induced periosteal microcirculatory and inflammatory reactions: comparison of dextran, gelatin, and hydroxyethyl starch. *Crit Care Med* 36: 2828–2837, 2008.
35. Verdant CL, De Backer D, Bruhn A, Clausi CM, Su F, Wang Z, Rodriguez H, Pries AR, Vincent JL. Evaluation of sublingual and gut mucosal microcirculation in sepsis: a quantitative analysis. *Crit Care Med* 37: 2875–2881, 2009.
36. Verdickt GM, Abbott PV. Blood flow changes in human dental pulps when capsaicin is applied to the adjacent gingival mucosa. *Oral Surg Oral Med Oral Pathol Oral Radiol Endod* 92: 561–565, 2001.
37. Wehrhan F, Stockmann P, Nkenke E, Schlegel KA, Guentsch A, Wehrhan T, Neukam FW, Amann K. Differential impairment of vascularization and angiogenesis in bisphosphonate-associated osteonecrosis of the jaw-related mucoperiosteal tissue. *Oral Surg Oral Med Oral Pathol Oral Radiol Endod* 112: 216–221, 2011.
38. Zhang L, Bail H, Mittlmeier T, Haas NP, Schaser KD. Immediate microcirculatory derangements in skeletal muscle and periosteum after closed tibial fracture. *J Trauma* 54: 979–985, 2003.

II.

Aktuális trendek a gyógyszer indukálta állcsontnecrosis korai felismerése és kezelési stratégiája terén

Janovszky Ágnes dr.[1] ▪ Vereb Tamás dr.[1]
Szabó Andrea dr.[2] ▪ Piffkó József dr.[1]

Szegedi Tudományegyetem, Szent-Györgyi Albert Klinikai Központ, Általános Orvostudományi Kar, 1Arc-, Állcsont- és Szájsebészeti Klinika, 2Sebészeti Műtéttani Intézet, Szeged

A várható élettartam hosszabbodásával egyre gyakoribbak a különféle reumatológiai és onkológiai megbetegedések, amelyek csontszövődményeinek csökkentésére széles körben alkalmaznak különböző per os és intravénás antireszorptív hatású készítményeket (például biszfoszfonátok). Ezek a szerek jótékony hatásuk mellett súlyos szövődményeket is okozhatnak, ilyen például a ma még nem teljesen tisztázott patomechanizmusú állcsontnecrosis. A szerzők célja egy átfogó szakmai tájékoztatás nyújtása a gyógyszer indukálta állcsontnecrosis lehetséges megelőzéséről és terápiájáról. A szakirodalmi áttekintés alapján készült dolgozat azokat a szűrőmódszereket ismerteti (előnyeikkel és limitációikkal együtt), amelyek segítségünkre lehetnek a gyógyszer indukálta állcsontnecrosis korai detektálásában. A szerzők a legújabb sebészi és adjuváns terápiás irányvonalakat is ismertetik. Megállapítják, hogy a patomechanizmus ismeretének hiányában jelenleg még hatékony terápiás modalitás nem áll rendelkezésre, és hangsúlyozzák mind a prevenció, mind a terápia során az interdiszciplináris együttműködés szükségességét és annak fontosságát. Jelenleg ez tűnik a gyógyszer indukálta állcsontnecrosis elleni leghatékonyabb eszköznek. Or. Hetil., 2014, *155*(49), 1960–1966.

Kulcsszavak: antiangiogén terápia, antireszorptív kezelés, biszfoszfonát, osteonecrosis

Current approaches for early detection and treatment of medication-related osteonecrosis of jaw

Owing to the increased life expectancy, the incidence of rheumatoid disorders and oncologic cases with bone metastasis has dramatically increased. Despite the beneficial effects of the applied antiresorptive and antiangiogenic drugs (e.g. bisphosphonates), serious side effects such as jaw osteonecrosis may also develop. The aim of the authors was to summarize present knowledge about the possibilities of prevention and treatment in medication-related osteonecrosis of the jaw. Based on literature data, currently used detection methods for medication-related osteonecrosis of the jaw (including their advantages and limitations) are summarized. In addition, novel trends of surgical and adjuvant therapeutic approaches are also reviewed. The authors conclude that possibilities of prevention and efficacy of therapeutic interventions in this disorder are still limited possibly due to an incomplete knowledge of the underlying pathomechanism. An interdisciplinary cooperation for prevention and attentive monitoring in order to decrease the incidence of iatrogenic oral and maxillofacial complications seems to be particularly important.

Keywords: antiangiogenic therapy, antiresorptiv treatment, bisphosphonate, osteonecrosis

Janovszky, Á., Vereb, T., Szabó, A., Piffkó, J. [Current approaches for early detection and treatment of medication-related osteonecrosis of jaw]. Orv. Hetil., 2014, *155*(49), 1960–1966.

(Beérkezett: 2014. október 3.; elfogadva: 2014. október 30.)

Rövidítések

BIS = biszfoszfonát; BRONJ = (bisphosphonate-related osteonecrosis of the jaw) biszfoszfonát indukálta állcsontnecrosis; CTX = C-terminális telopeptid; LLLT = (low-level laser therapy) alacsony energiájú lézerkezelés; MRONJ = (medication-related osteonecrosis of the jaw) gyógyszer indukálta állcsontnecrosis; VEGF = (vascular endothelial growth factor) endotheliumeredetű növekedési faktor

Antireszorptív és antiangiogén gyógyszerek hatásai és mellékhatásai. A gyógyszer indukálta állcsontnecrosis kockázati tényezői

A különböző hatásmechanizmusú antireszorptív hatású gyógyszerek, legfőképp a biszfoszfonátok (BIS) megjelenése, az osteoporosis és csontmetasztázis kezelésében jelentős mértékben javították mind a terápia sikerességét, mind pedig a betegek életminőségét [1, 2]. Az osteoclast-aktivitást gátló hatásukat kihasználva a csontépítő folyamatok – az osteoblast-osteoclast egyensúly eltolódásával – kerülnek előtérbe, így mára mindezekben a patológiás csontelváltozásokkal járó kórképekben a standard terápia részét képezik [3, 4]. Szemben a BIS-kezelésnek a vázrendszer csontjaiban kifejtett jótékony hatásaival, az állcsontokban ellentétes hatású folyamat léphet fel, amely osteonecrosis kialakulásához vezethet. Egyre több publikáció jelenik meg, hogy nemcsak a BIS, hanem más antireszorptív [5] vagy antiangiogén [6] hatású készítmények mellett is kialakulhat ez a súlyos szövődmény. Ennek megfelelően módosult is az amerikai szakmai ajánlás, amelyben ma már gyógyszer indukálta állcsontnecrosisként (medication-related osteonecrosis of the jaw – MRONJ) definiálja ezt a kórállapotot, a korábbi biszfoszfonát indukálta állcsontnecrosissal szemben (bisphosphonate-related osteonecrosis of the jaw – BRONJ) [4].

Incidenciája kapcsán meglehetősen eltérő adatok érhetők el a nemzetközi szakirodalomban, gyakorisága 0,019–10% között mozog [4]. Az osteonecrosis gyakrabban alakul ki a mandibulában, mint a maxillában (2:1) [3], a molaris régió gyakrabban érintett, mint a praemolaris, illetve frontalis területek [7], valamint fokozódik a kockázat invazív fogászati beavatkozást (fogeltávolítást) követően [3, 4]. Befolyással bír a betegség kialakulására a kezelés indikációja (alapbetegség: osteoporosis, malignus daganat), a BIS beviteli módja (per os vagy intravénás) és időtartama, fennálló szájüregi betegség (periodontalis vagy periapicalis, gyulladásos folyamat), társbetegségek, rossz szájhigiéné, dohányzás [4]. A fő problémát az jelenti, hogy ennek a progrediáló, súlyos elváltozásnak jelenleg nem ismert ténylegesen effektív terápiás megoldása és a nemzetközi ajánlásokban írt kezelési modalitások sem hoznak minden esetben sikert [8, 9].

Mivel a MRONJ pontos patomechanizmusa egyelőre nem ismert, számos kockázati tényező, jelátviteli útvonal és mechanizmus etiológiai szerepe felmerült. Az alap- és klinikai kutatások többsége főként a BIS indukálta gyulladásos és fertőzéses eredet [10], a lokális toxicitás [11], valamint az angiogenesist gátló hatások [12] vizsgálatára fokuszál. A patomechanizmus megértését nehezíti, hogy osteonecrosis néhány évvel a foghúzást követően is kifejlődhet BIS-kezelt páciensekben, ami farmakokinetikai tulajdonságaikra vezethető vissza (hosszú felezési idő) [3].

Ma több mint 200 millióan szenvednek osteoporosisban, illetve annak különböző szövődményeitől világszerte [13]. Németországban nagyjából 8 millió alkalommal írtak fel BIS-származékot az elmúlt évben. Magyarországon megközelítőleg 1 millió regisztrált, osteoporosisban szenvedő betegről tudunk (*Magyar Osteoporosis* és Osteoarthrologiai Társaság). Szintén fokozódik a daganatok előfordulási gyakorisága, amelyek csontáttétei kapcsán gyakran alkalmaznak BIS-készítményeket [14], illetve az angiogenesisgátló biológiai, úgynevezett „target terápiák” is egyre inkább előtérbe kerülnek, ahogy azt a megjelenő publikációk száma is jól mutatja. Amellett, hogy egyre bővül az említett gyógyszercsoportok indikációs köre, valószínű, hogy a MRONJ prevalenciájában is hasonló tendencia lesz megfigyelhető. A fenti adatok jól mutatják, hogy súlyos népegészségügyi problémával állhatunk szemben a későbbiek folyamán, de a komplikációk direkt és indirekt költségei révén a gazdasági vonatkozások sem elhanyagolhatóak.

Az állcsontnecrosis klinikai tünetei és stádiumai

Az „American Association of Oral and Maxillofacial Surgeons” 2014-ben publikált, szakmai ajánlása alapján MRONJ esete állhat fenn, ha az alábbi kritériumok mindegyike igazolható [4]:

– jelenleg is fennálló, vagy az anamnézisben szereplő antireszorptív vagy antiangiogén kezelés;
– legalább 8 hete nem gyógyuló, denudált csontfelszín vagy intra/extra oralis fistula a maxillofacialis régióban;
– kizárható a korábbi irradiáció vagy egyértelmű metasztázis az állcsontok területén.

A MRONJ alábbi 5 stádiuma állapítható meg [4]:

1. *Rizikócsoport:* antireszorptív vagy antiangiogén terápiában (*per os* vagy intravénás) részesült, *tünetmentes* betegek.

2. *Stádium 0: atípusos tünetek* (odontológiai ok nélkül; corpus mandibulae tompa, a temporomandibularis ízületbe sugárzó fájdalma; arcüregfájdalom akár gyulladással és a sinus maxillaris falának elvékonyodásával; megváltozott neuroszenzoros funkciók) vagy *klinikai* (fogvesztés krónikus periodontalis betegség nélkül; periapicalis/periodontalis fistula caries eredetű pulpanecrosis nélkül) és *radiológiai* (alveolaris csonthiány krónikus periodontalis betegség nélkül; trabecularis szerkezet megváltozása az extractio helyén; osteosclerosis az alveolaris régióban; periodontalis ligamentum elvékonyodása) *eltérések klinikailag igazolható osteonecrosis nélkül.*

3. *Stádium 1: denudált,* necroticus *csontfelszín* vagy fistula, lokális *gyulladás nélkül,* alveolaris régióra lokalizált radiológiai eltérésekkel.

4. *Stádium 2: denudált,* necroticus *csontfelszín* vagy fistula, bakteriális *szuperinfekció* és *kísérő tünetei* (fájdalom, erythema, pus), alveolaris régióra lokalizált radiológiai eltérésekkel *(1. ábra).*

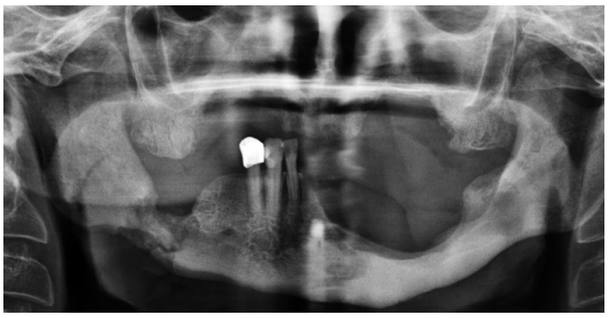

1. ábra | A jobb oldali mandibula necrosisának radiológiai képe

5. *Stádium 3: denudált,* necroticus *csontfelszín* vagy *fistula, fertőzés* és a következő tünetek legalább egyike: alveolaris régión túlterjedő osteonecrosis (mandibula basisa, ramus mandibulae, sinus maxillaris, os zygomaticus), patológiás törés, oro-cutan/oro-nasalis/oro-antralis fistula, osteolysis (mandibula basisa, sinus alap) *(2. ábra)*.

A MRONJ kezelése és progressziójának megelőzési lehetőségei

A legújabb nemzetközi szakmai ajánlás alapján, akár csak a korábbiban, a MRONJ kezelése stádiumspecifikusan történik [4].

- *Stádium 0:* nem specifikus tünetek csökkentése (fájdalomcsillapítás) és konzervatív fogászati kezelés, a betegek *szoros utánkövetése* a potenciális progresszió végett.
- *Stádium 1: fájdalomcsillapítás* és antimikrobiális szájöblögető használata (chlorhexidin 0,12%-os oldata).
- *Stádium 2: fájdalomcsillapítás, szisztémás antibiotikumkezelés,* antimikrobiális szájöblögető (chlorhexidin 0,12%-os oldata) használata.
- *Stádium 3: sebészi debridement vagy a necroticus* állcsontrészlet-reszekció *antibiotikumkezeléssel* egybekötve, illetve a maxillofacialis régió integritásának helyreállítása különböző *rekonstrukciós* módszerekkel jöhet szóba. Ezeknek a technikáknak az eredményességéről még nagyon kevés adat áll rendelkezésünkre *(3. ábra)* [4].

Kiegészítő terápiás lehetőségek

Teriparatid

A teriparatid egy humán rekombináns parathyroid hormon, amelyet *Lee* írt le először a MRONJ kezelése kapcsán [15]. Ugyan a vegyület fokozta a csontdenzitást a csontképződés révén [16], alkalmazása azonban nem haladhatja meg a 2 évet, mivel egyes vizsgálatok szerint fokozza az osteosarcoma kialakulásának esélyét. Így csontmetasztázisok esetén nem is ajánlott [17]. Más szerzők ugyanakkor nem igazolták ezt az összefüggést 15 éves retrospektív klinikai vizsgálatuk során [18].

Pentoxifillin és α-tokoferol

Epstein és mtsai 2010-ben publikálták, hogy az antimikrobiális terápiát pentoxifillinnel és α-tokoferollal kiegészítve 74%-ban csökkenthető a progresszió MRONJ korai stádiumában [19]. Ennek hátterében valószínűleg a pentoxifillin mikrokeringésre kifejtett pozitív és gyulladásos citokinekre gyakorolt gátlóhatása állhat [20], míg az α-tokoferol esetében annak antioxidáns hatása emelendő ki [21].

Alacsony energiájú lézerkezelés (low-level laser therapy – LLLT)

A fentebb említett antibiotikumprofilaxis mellett felmerült az LLLT alkalmazásának lehetősége is a MRONJ kezelése és megelőzése során egyaránt. Hatásai közül kiemelendő sebgyógyulást, angiogenesist, csontregenerációt, kollagén- és fibroblast-proliferációt elősegítő, tehát biostimulatív, valamint fájdalomcsillapító effektusa [22, 23, 24, 25]. Ezek önmagában is igazolhatják az LLLT létjogosultságát a kórkép terápiájában. *Scoletta és mtsai* a MRONJ klinikai lefolyását vizsgálták kiegészítő LLLT-terápia mellett. Vizsgálatuk alapján az LLLT-kezelés hatására az érintett területen csökkent a seb mérete, valamint az oedema és a fájdalom, illetve a genny és fistulák kialakulásának gyakorisága is mérséklődött. Emellett az sem elhanyagolható tény, hogy a betegek az LLLT-kezeléseket jól tolerálták [26].

Ózonterápia és hyperbaricus oxigénterápia

Agrillo és mtsai retrospektív klinikai tanulmányukban beszámoltak az ózonterápia klinikai létjogosultságáról, mint kiegészítő kezelésről a MRONJ standard terápiája mellett [27]. Szintén pozitív hatással volt a MRONJ lefolyására a kiegészítő hyperbaricus oxigénkezelés [28]. Akárcsak az LLLT-nél, itt is a kezelési módszer által indukált biostimulatív hatásokat igyekeznek kihasználni (proliferáció, sebgyógyulás, fájdalomcsillapítás) a terápia során. Az amerikai társaság által kiadott szakmai ajánlás azonban nem támogatja ezt a kiegészítő kezelést, mivel a *Freiberger és mtsai* által közölt tanulmányban kevés esetet vizsgáltak, így azokból nem vonható le statisztikai különbség.

Növekedési faktorok alkalmazása

Felmerült növekedési faktorok terápiás alkalmazhatósága is. *Mozzati és mtsai* kutatásuk során 32 MRONJ-beteg esetében a sebészileg kezelt területre növekedési faktorokban gazdag plazmát juttattak, majd ez után zárták a

2. ábra | Kiterjedt, kétoldali maxillanecrosis klinikai képe

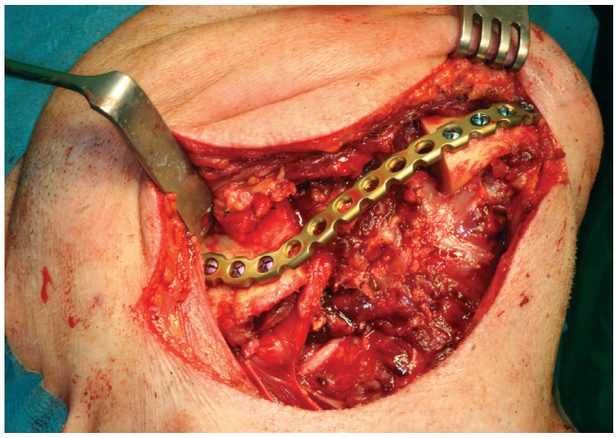

3. ábra | Jobb oldali mandibulanecrosis reszekcióját követő lemezes rekonstrukció intraoperatív képe

nyálkahártyát. Mind a 32 esetben sikeres volt a beavatkozás, 48–50 hónapos utánkövetés során recidíva nem igazolódott [29].

Sebészi lézerek alkalmazása

A nagy energiájú sebészi lézerek szövetek vágására, így például a necroticus csont vaporisatiójára is alkalmasak. A minimálisan invazív technika alkalmazásával nemcsak a műtéti precizitás fokozható, hanem a csontban kialakult mikroperforációk stimulusként hatnak az angiogenesisre, emellett a technika baktericid hatású, javítva ezzel is a posztoperatív felépülést. Összehasonlítva a hagyományos sebészi kezeléssel, sokkal jobb eredmények érhetők el ezt a technikát alkalmazva [17].

Számos alap- és klinikai kutatás irányul újabb kezelési modalitások kidolgozására, azonban magas evidenciájú tudás jelenleg nem áll rendelkezésre, további vizsgálatok szükségesek, amelyet az amerikai ajánlás is hangsúlyoz [4]. Mindezek alapján kiemelkedő jelentőséget kapnak azok az eljárások, amelyek az állcsontnecrosis megelőzését és korai diagnózisát célozzák meg.

Hagyományos eljárások az állcsontnecrosis megelőzése és korai diagnózisa céljából

Kockázatbecslés a terápia megkezdése előtt

Közismert tény, hogy a spontán kialakuló osteonecrosis gyakorisága csekély, az invazív fogászati beavatkozások azonban jelentősen fokozzák a kialakulás rizikóját [30]. A korábban ismertetett egyéb rizikófaktorok (terápia módja, társbetegségek, életkor stb.) mindezt befolyásolhatják, éppen ezért kiemelkedően fontos a terápia megkezdése előtt a fogászati státus ellenőrzése és optimalizálása, a betegek szoros utánkövetése [4], amellyel nagymértékben csökkenthető az osteonecrosis kialakulási esélye. Ugyanakkor a kezelést elrendelő orvosnak is fel kellene hívnia betege figyelmét az esetleges komplikációkra és az esetleges korai tünetek felismerésének fontosságára.

Kockázatbecslés fogászati beavatkozások megkezdése előtt

A kellően átfogó anamnézis segíthet az osteonecrosis megelőzésében. Invazív fogászati beavatkozások előtt tanácsos magára a gyógyszerhasználatra, akár a csontritkulásra is rákérdezni, nemcsak az egyéb, fogászati beavatkozás kapcsán komplikációkat okozó gyógyszerekre. A tervezett fogászati beavatkozás ugyanis módosítható, biztonságosabbá tehető. A BIS-kezelés felfüggesztése – „drug holiday” – kapcsán ellentmondásosak a vélemények, de általánosan elfogadott nézet, hogy egy 2 hónapos gyógyszermentes időszak az invazív fogászati beavatkozás előtt csökkentheti a szövődmények kialakulását BIS-kezelt betegekben [31]. Természetesen ez csak tervezett fogászati beavatkozások esetén az alapbetegség, az onkológiai és/vagy reumatológiai terápia individuális mérlegelése alapján jön szóba.

Az amerikai, a német és a hazai maxillofacialis társaságok szakmai ajánlása alapján a BIS-kezelt betegeknél dentoalveolaris és invazív fogászati beavatkozások során javasolt a profilaktikus antibiotikumkezelés. Elsőként *penicillinszármazékok* választandók (amoxicillin 3×750 mg/nap vagy amoxicillin+klavulánsav 3×625 mg/nap vagy 2×1 g/nap), allergia esetén *quinolonszármazékok*, *macrolidok és lincosamidok* (clarithromycin 2×250 mg/nap, erythromycin, clindamycin 4×300-600 mg/nap), *metronidazol* és *doxycyclin* jöhetnek még számításba. Az antibiotikum adása a beavatkozást megelőzően 1-2 nappal, illetve a primer sebgyógyulásig ajánlott (nagyjából 10 napig), de egyéb indikáció esetén hosszabb ideig is szükséges lehet. A betegség korai stádiumában szintén javulást eredményezhet az antibiotikumkezelés [4, 32, 33].

Laboratóriumi vizsgálómódszerek az állcsontnecrosis korai diagnózisa céljából

A MRONJ esetében egy lokalizált elváltozásról van szó, így a szisztémás paraméterekben nem vagy alig mutatható ki markáns eltérés [4]. Ezért nélkülözhetetlen lenne olyan diagnosztikai eljárások kidolgozása, amelyek révén a prediszponált populáció kiszűrhető még a kezelés megkezdése előtt, vagy az elváltozás hatékonyan kimutatható a korai stádiumban a veszélyeztetett populációban.

Plazma- és szérumminták vizsgálata

A csontokban is megtalálható, főként kollagén I lebomlása során (csontreszorpció) terminális telopeptidek szabadulnak fel, majd a keringésbe kerülnek és további degradáción már nem esnek át. Ezek aminosav-szekvenciái az I. típusú kollagénre erősen specifikusak. Így exkréciója egyenesen arányos a csontreszorpció mértékével [34], valamint vizeletből és vérből (szérum) egyaránt meghatározhatók. A C-terminális (karboxiterminális) telopeptid (CTX), valamint az N-terminális (aminoterminális) telopeptid meghatározása a csontreszorpciót leginkább reprezentáló biokémiai markerek, amelyek az osteoporosiskezelés hatékonyságának követésére is alkalmasak [34, 35]. Számos kutatás vizsgálta a CTX-értékek és MRONJ közötti korrelációt. Egyes kutatási eredmények alapján a CTX szintje, akár szérumból, akár vizeletből mérve, szoros összefüggést mutatott az ostenecrosis kialakulási esélyével, illetve a patológiás elváltozás fennállásával [36, 37]. Az eljárás hátránya, hogy számos tényező befolyásolhatja a mérési eredményeket, ilyen a nem, az étkezési szokások és a gyomor teltségi állapota, az életkor, az évszak, a hormonszintek vagy akár a vesefunkció [34, 38]. *Vescovi és mtsai* szerint nem ad megbízható eredményt a vizsgálat daganatos megbetegedés vagy rheumatoid arthritis kezelését (methotrexat, prednison, raloxafen) követően [17], illetve teljesen normálértékek is detektálhatók MRONJ fennállása esetén, ami megkérdőjelezi a betegség és a szérum-CTX-szint közötti összefüggést [39].

In vitro és *in vivo* tanulmányok alátámasztották egyes intravénásan adagolt BIS-készítmények angiogenesist gátló hatását [40, 41], és ennek a jelenségnek szintén szerepe lehet a kórkép patogenezisében. Ezt támasztják alá azok a közlemények is, amelyekben leírják, hogy bár a malignus tumorok kezelésénél kifejezetten előnyösnek bizonyult az angiogenesist gátló terápia, mégis a BIS és angiogenesist gátló együttes adása mellett a MRONJ incidenciája jelentősen emelkedhet. Egyes retrospektív tanulmányok az osteonecrosisráta megduplázódását írják le [42, 43]. Mivel a MRONJ kialakulása során szignifikáns érendothelium-eredetű növekedési faktor (vascular endothelial growth factor – VEGF) szint csökkenést mértek a szérumban, felmerül a VEGF-szint mérésének szűrésben való felhasználhatósága. Habár felmerült, hogy a VEGF, mint angiogén marker, jó kórjelzője lehet a MRONJ kialakulásának [40], irodalmi adatok – hasonlóan a CTX-méréshez – jelentős eltéréseket mutatnak a mérés szenzitivitásával kapcsolatban [44].

Biomarkerek meghatározása nyálból

Az egyre fejlődő biokémiai módszereknek és technikai megoldásoknak köszönhetően ma már lehetőség van sokfajta biomarker mérésére nyálból, amelyek alkalmasak a csontfolyamatok megítélésére. A BIS-ok ismert osteoclast-aktivitást gátló hatásuknak [3] köszönhetően az osteoblast-tevékenység kerülhet túlsúlyba. A csontspecifikus alkalikus foszfatáz, az osteonectin és osteocalcin az osteoblast-aktivitás jellemző paraméterei, amelyek a szérumban mért értékkel jól korrelálnak [45]. Ez a paraméter MRONJ-ban szenvedő betegek esetében szignifikánsan alacsonyabb értéket mutatott a BIS-sel kezelt, de necrosissal nem rendelkező betegek értékeihez képest [39]. A foghúzáson átesett, BIS-terápiában részesülő betegek szűrése az említett biomarkerek szintjének meghatározásával nem számítanak rutinvizsgálatoknak, kizárólag kutatások tárgyát képezik.

A BIS-ek gyulladást keltő hatásai [46, 47] és a folyamat krónikus volta miatt a gyulladásos mediátorok vizsgálata is szóba jöhet. *Ng és mtsai* az IL-1b, TNF-α, IL-6 szintjét ellenőrizték nyálból, következtetésük alapján ezek szintje jól monitorozza, sőt előre jelzi a periodontalis betegségekre való érzékenységet. A módszer limitációja, hogy a nyálban ezek a mediátorok gyorsan lebomlanak, megnehezítve ezzel az abszolút koncentráció pontos meghatározását [45]. Más tanulmányokban IL-1α-, IL-4-, IL-6-, IL-8-, EGF-, MCP-1-, TNF-α-szintek kerültek detektálásra, amelyekből azt a következtetést vonták le, hogy a gyulladásos paraméterek szintje és ezek változásai eleve eltérhetnek daganatos betegekben a szájüregi folyamatok során [48, 49]. Az egyes citokinszintekben történő változások a MRONJ patogenezise kapcsán még nem teljesen tisztázottak, mivel prospektív vizsgálatok még hiányoznak ebben a tekintetben.

Az oxidoreduktív stresszt jellemző anyagcseretermékek (redukált glutation, malondialdehid, oxidált glutation és 8-oxo-7,8-dihidro-2-deoxiguanozin) mérése szintén jó megközelítése lehet a szájüregi gyulladásos folyamatok detektálásának. *Bagan és mtsai* a fent említett paraméterek vonatkozásában szignifikáns emelkedést mértek BIS-kezelt és osteonecrosisos betegek nyálmintáiban az egészséges páciensek értékeihez képest [50], ezek specificitása/szenzitivitása azonban szintén kérdéses.

Következtetés

A gyógyszer indukálta állcsontnecrosisok prevenciójának és terápiájának egyik legnagyobb hátránya, hogy mind a mai napig nem rendelkezünk magas szintű evidenciaalapú tudással. Éppen ezért kiemelkedő jelentősége van az adatgyűjtés mellett a magas evidenciájú klinikai kutatá-

sok folytatásának. Ehhez elengedhetetlen az interdiszciplináris együttműködés, amely egyben az eredményes kezeléseknek is az alapja. A jelenleg érvényben lévő nemzetközi szakmai ajánlás maximálisan a konzervatív terápia mellett foglal állást, késleltetve a sebészeti intervenciót, amely nem minden esetben hozza meg az elvárt sikert. A kezelés terén beigazolódni látszik a minimálisan invazív sebészi technika szükségessége, amely sok esetben – a betegek előrehaladott alapbetegségét is figyelembe véve – helyi érzéstelenítésben is elvégezhető, ezáltal idősebb és immunszuppresszív terápiában részesült betegeknél is alkalmazható, illetve a sebészi defektus méretének minimalizálásával csökken a sebgyógyulási zavar veszélye is.

Anyagi támogatás: TÁMOP-4.2.2.A-11/1/KONV-2012-0035, TÁMOP 4.2.4.A/2-11-1-2012-0001, OTKA-109388.
Szerzői munkamegosztás: J. Á., V. T.: A kézirat megírása, szakirodalmi adatgyűjtés. Sz. A., P. J.: Szakmai lektorálás. A cikk végleges változatát valamennyi szerző elolvasta és jóváhagyta.

Érdekeltségek: A szerzőknek nincsenek érdekeltségeik.

Irodalom

[1] *Kerschan-Schindl, K., Patsch, J., Kudlacek, S., et al.:* Measuring quality of life with the German Osteoporosis Quality of Life Questionnaire in women with osteoporosis. Wien. Klin. Wochenschr., 2012, *124*(15–16), 532–537.
[2] *Wilson, S., Sharp, C. A., Davie, M. W.:* Health-related quality of life in patients with osteoporosis in the absence of vertebral fracture: a systematic review. Osteoporos. Int., 2012, *23*(12), 2749–2768.
[3] *Brozoski, M. A., Traina, A. A., Deboni, M. C., et al.:* Bisphosphonate-related osteonecrosis of the jaw. Rev. Bras. Reumatol., 2012, *52*(2), 265–270.
[4] *Ruggiero, S. L., Dodson, T. B., Fantasia, J., et al.:* American Association of Oral and Maxillofacial Surgeons position paper on medication-related osteonecrosis of the jaw –2014 update. J. Oral. Maxillofac. Surg., 2014, *72*(10), 1938–1956.
[5] *Aghaloo, T. L., Felsenfeld, A. L., Tetradis, S.:* Osteonecrosis of the jaw in a patient on Denosumab. J. Oral. Maxillofac. Surg., 2010, *68*(5), 959–963.
[6] *Serra, E., Paolantonio, M., Spoto, G., et al.:* Bevacizumab-related osteonecrosis of the jaw. Int. J. Immunopathol. Pharmacol., 2009, *22*(4), 1121–1123.
[7] *Otto, S., Schreyer, C., Hafner, S., et al.:* Bisphosphonate-related osteonecrosis of the jaws – characteristics, risk factors, clinical features, localization and impact on oncological treatment. J. Craniomaxillofac. Surg., 2012, *40*(4), 303–309.
[8] *Marx, R. E.:* Reconstruction of defects caused by bisphosphonate-induced osteonecrosis of the jaws. J. Oral. Maxillofac. Surg., 2009, *67*(5), Suppl. 107–119.
[9] *Vescovi, P., Merigo, E., Meleti, M., et al.:* Surgical approach and laser applications in BRONJ osteoporotic and cancer patients. J. Osteoporos., 2012, *2012,* 585434.
[10] *Mawardi, H., Giro, G., Kajiya, M., et al.:* A role of oral bacteria in bisphosphonate-induced osteonecrosis of the jaw. J. Dent. Res., 2011, *90*(11), 1339–1345.
[11] *Reid, I. R., Bolland, M. J., Grey, A. B.:* Is bisphosphonate-associated osteonecrosis of the jaw caused by soft tissue toxicity? Bone, 2007, *41*(3), 318–320.
[12] *Wood, J., Bonjean, K., Ruetz, S., et al.:* Novel antiangiogenic effects of the bisphosphonate compound zoledronic acid. J. Pharmacol. Exp. Ther., 2002, *302*(3), 1055–1061.
[13] *Schuiling, K. D., Robinia, K., Nye, R.:* Osteoporosis update. J. Midwifery Womens Health, 2011, *56*(6), 615–627.
[14] *Tolia, M., Zygogianni, A., Kouvaris, J. R., et al.:* The key role of bisphosphonates in the supportive care of cancer patients. Anticancer Res., 2014, *34*(1), 23–37.
[15] *Lee, J. J., Cheng, S. J., Jeng, J. H., et al.:* Successful treatment of advanced bisphosphonate-related osteonecrosis of the mandible with adjunctive teriparatide therapy. Head Neck, 2011, *33*(9), 1366–1371.
[16] *Orwoll, E. S., Scheele, W H., Paul, S., et al.:* The effect of teriparatide [human parathyroid hormone (1–34)] therapy on bone density in men with osteoporosis. J. Bone Miner. Res., 2003, *18*(1), 9–17.
[17] *Vescovi, P., Merigo, E., Meleti, M., et al.:* Conservative surgical management of stage I bisphosphonate-related osteonecrosis of the jaw. Int. J. Dent., 2014, *2014,* 107690.
[18] *Andrews, E. B., Gilsenan, A. W., Midkiff, K., et al.:* The US postmarketing surveillance study of adult osteosarcoma and teriparatide: study design and findings from the first 7 years. J. Bone Miner. Res., 2012, *27*(12), 2429–2437.
[19] *Epstein, M. S., Wicknick, F. W., Epstein, J. B., et al.:* Management of bisphosphonate-associated osteonecrosis: pentoxifylline and tocopherol in addition to antimicrobial therapy. An initial case series. Oral Surg. Oral Med. Oral Pathol. Oral Radiol. Endod., 2010, *110*(5), 593–596.
[20] *Delanian, S., Porcher, R., Rudant, J., et al.:* Kinetics of response to long-term treatment combining pentoxifylline and tocopherol in patients with superficial radiation-induced fibrosis. J. Clin. Oncol., 2005, *23*(34), 8570–8579.
[21] *Tousoulis, D., Antoniades, C., Vassiliadou, C., et al.:* Effects of combined administration of low dose atorvastatin and vitamin E on inflammatory markers and endothelial function in patients with heart failure. Eur. J. Heart Fail., 2005, *7*(7), 1126–1132.
[22] *Albertini, R., Villaverde, A. B., Aimbire, F., et al.:* Anti-inflammatory effects of low-level laser therapy (LLLT) with two different red wavelengths (660 nm and 684 nm) in carrageenan-induced rat paw edema. J. Photochem. Photobiol. B, 2007, *89*(1), 50–55.
[23] *Salate, A. C., Barbosa, G., Gaspar, P., et al.:* Effect of In-Ga-Al-P diode laser irradiation on angiogenesis in partial ruptures of Achilles tendon in rats. Photomed. Laser Surg., 2005, *23*(5), 470–475.
[24] *Nicola, R. A., Jorgetti, V., Rigau, J., et al.:* Effect of low-power GaAlAs laser (660 nm) on bone structure and cell activity: an experimental animal study. Lasers Med. Sci., 2003, *18*(2), 89–94.
[25] *Frozanfar, A., Ramezani, M., Rahpeyma, A., et al.:* The effects of low level laser therapy on the expression of collagen type I gene and proliferation of human gingival fibroblasts (Hgf3-Pi 53): in vitro study. Iran J. Basic Med. Sci. 2013, *16*(10), 1071–1074.
[26] *Scoletta, M., Arduino, P. G., Reggio, L., et al.:* Effect of low-level laser irradiation on bisphosphonate-induced osteonecrosis of the jaws: preliminary results of a prospective study. Photomed. Laser Surg., 2010, *28*(2), 179–184.
[27] *Agrillo, A., Filiaci, F., Ramieri, V., et al.:* Bisphosphonate-related osteonecrosis of the jaw (BRONJ): 5 year experience in the treatment of 131 cases with ozone therapy. Eur. Rev. Med. Pharmacol. Sci., 2012, *16*(12), 1741–1747.
[28] *Freiberger, J. J., Padilla-Burgos, R., McGraw, T., et al.:* What is the role of hyperbaric oxygen in the management of bisphosphonate-related osteonecrosis of the jaw: a randomized controlled

trial of hyperbaric oxygen as an adjunct to surgery and antibiotics. J. Oral Maxillofac. Surg., 2012, *70*(7), 1573–1583.
[29] *Mozzati, M., Gallesio, G., Arata, V., et al.:* Platelet-rich therapies in the treatment of intravenous bisphosphonate-related osteonecrosis of the jaw: a report of 32 cases. Oral Oncol., 2012, *48*(5), 469–474.
[30] *Farrugia, M. C., Summerlin, D. J., Krowiak, E., et al.:* Osteonecrosis of the mandible or maxilla associated with the use of new generation bisphosphonates. Laryngoscope, 2006, *116*(1), 115–120.
[31] *Damm, D. D., Jones, D. M.:* Bisphosphonate-related osteonecrosis of the jaws: a potential alternative to drug holidays. Gen. Dent., 2013, *61*(5), 33–38.
[32] *Hungarian Society of Oral and Maxillofacial Surgeons, Hungarian Society of Osteoporosis and Osteoarthrosis, Hungarian Society of Oncologists, Hungarian Rheumatology Association, Hungarian Society of Orthopedic:* Bisphosphonate-induced jaw osteonecrosis prevention and treatment. [Magyar Arc-, Állcsont- és Szájsebészeti Társaság, Magyar Osteoporosis és Osteoarthrologiai Társaság, Magyar Onkológusok Társasága, Magyar Reumatológusok Egyesülete, Magyar Ortopéd Társaság: A biszfoszfonátok által indukált állcsont-osteonecrosisok megelőzése és kezelése.] Orv. Hetil., 2010, *151*(4), 148–149. [Hungarian]
[33] *Deutsche Gesellschaft für Zahn-, Mund- und Kieferheilkunde:* http://www.dgzmk.de/zahnaerzte/wissenschaft-forschung/leitlinien.html
[34] *Chubb, S. A.:* Measurement of C-terminal telopeptide of type I collagen (CTX) in serum. Clin. Biochem., 2012, *45*(12), 928–935.
[35] *Hodsman, A. B., Fraher, L. J., Ostbye, T., et al.:* An evaluation of several biochemical markers for bone formation and resorption in a protocol utilizing cyclical parathyroid hormone and calcitonin therapy for osteoporosis. J. Clin. Invest., 1993, *91*(3), 1138–1148.
[36] *Baim, S., Miller, P. D.:* Assessing the clinical utility of serum CTX in postmenopausal osteoporosis and its use in predicting risk of osteonecrosis of the jaw. J. Bone Miner. Res., 2009, *24*(4), 561–574.
[37] *Pellegrini, G. G., Gonzales Chaves, M. M., Fajardo, M. A., et al.:* Salivary bone turnover markers in healthy pre- and postmenopausal women: daily and seasonal rhythm. Clin. Oral Investig., 2012, *16*(2), 651–657.
[38] *Borromeo, G. L., Tsao, C. E., Darby, I. B., et al.:* A review of the clinical implications of bisphosphonates in dentistry. Aust. Dent. J., 2011, *56*(1), 2–9.
[39] *Lazarovici, T. S., Mesilaty-Gross, S., Vered, I., et al.:* Serologic bone markers for predicting development of osteonecrosis of the jaw in patients receiving bisphosphonates. J. Oral Maxillofac. Surg., 2010, *68*(9), 2241–2247.
[40] *Vincenzi, B., Napolitano, A., Zoccoli, A., et al.:* Serum VEGF levels as predictive marker of bisphosphonate-related osteonecrosis of the jaw. J. Hematol. Oncol., 2012, *5*, 56.
[41] *Ziebart, T., Pabst, A., Klein, M. O., et al.:* Bisphosphonates: restrictions for vasculogenesis and angiogenesis: inhibition of cell function of endothelial progenitor cells and mature endothelial cells in vitro. Clin. Oral Investig., 2011, *15*(1), 105–111.
[42] *Aragon-Ching, J. B., Ning, Y. M., Chen, C. C., et al.:* Higher incidence of Osteonecrosis of the Jaw (ONJ) in patients with metastatic castration resistant prostate cancer treated with anti-angiogenic agents. Cancer Invest., 2009, *27*(2), 221–226.
[43] *Pakosch, D., Papadimas, D., Munding, J., et al.:* Osteonecrosis of the mandible due to anti-angiogenic agent, bevacizumab. Oral Maxillofac. Surg., 2013, *17*(4), 303–306.
[44] *Brozovic, S., Vucicevic-Boras, V., Mravak-Stipetic, M., et al.:* Salivary levels of vascular endothelial growth factor (VEGF) in recurrent aphthous ulceration. J. Oral Pathol. Med., 2002, *31*(2), 106–108.
[45] *Ng, P. Y., Donley, M., Hausmann, E., et al.:* Candidate salivary biomarkers associated with alveolar bone loss: cross-sectional and in vitro studies. FEMS Immunol. Med. Microbiol., 2007, *49*(2), 252–260.
[46] *Senel, F. C., Kadioglu Duman, M., Muci, E., et al.:* Jaw bone changes in rats after treatment with zoledronate and pamidronate. Oral Surg. Oral Med. Oral Pathol. Oral Radiol. Endod., 2010, *109*(3), 385–391.
[47] *Norton, J. T., Hayashi, T., Crain, B., et al.:* Cutting edge: nitrogen bisphosphonate-induced inflammation is dependent upon mast cells and IL-1. J. Immunol., 2012, *188*(7), 2977–2980.
[48] *Citrin, D. E., Hitchcock, Y. J., Chung, E. J., et al.:* Determination of cytokine protein levels in oral secretions in patients undergoing radiotherapy for head and neck malignancies. Radiat. Oncol., 2012, *7*, 64.
[49] *Korostoff, A., Reder, L., Masood, R., et al.:* The role of salivary cytokine biomarkers in tongue cancer invasion and mortality. Oral Oncol., 2011, *47*(4), 282–287.
[50] *Bagan, J., Sáez, G. T., Tormos, M. C., et al.:* Oxidative stress in bisphosphonate-related osteonecrosis of the jaws. J. Oral Pathol. Med., 2014, *43*(5), 371–377.

(Janovszky Ágnes dr.,
Szeged, Kálvária sgt. 57., 6725
e-mail: agnes.janovszky@gmail.com)

III.

Clin Oral Invest
DOI 10.1007/s00784-014-1347-6

ORIGINAL ARTICLE

Periosteal microcirculatory reactions in a zoledronate-induced osteonecrosis model of the jaw in rats

Ágnes Janovszky · Andrea Szabó · Renáta Varga · Dénes Garab · Mihály Boros · Csilla Mester · Nikolett Beretka · Tamás Zombori · Hans-Peter Wiesmann · Ricardo Bernhardt · Imre Ocsovszki · Péter Balázs · József Piffkó

Received: 6 August 2014 / Accepted: 22 October 2014

Abstract
Objectives Nitrogen-containing bisphosphonates induce osteonecrosis mostly in the jaw and less frequently in other bones. Because of the crucial role of periosteal perfusion in bone repair, we investigated zoledronate-induced microcirculatory reactions in the mandibular periosteum in comparison with those in the tibia in a clinically relevant model of bisphosphonate-induced medication-related osteonecrosis of the jaw (MRONJ).
Materials and methods Sprague–Dawley rats were treated with zoledronate (ZOL; 80 i.v. μg/kg/week over 8 weeks) or saline vehicle. The first two right mandibular molar teeth were extracted after 3 weeks. Various systemic and local (periosteal) microcirculatory inflammatory parameters were examined by intravital videomicroscopy after 9 weeks.
Results Gingival healing disorders (~100 %) and MRONJ developed in 70 % of ZOL-treated cases but not after saline (shown by micro-CT). ZOL induced significantly higher degrees of periosteal leukocyte rolling and adhesion in the mandibular postcapillary venules (at both extraction and intact sites) than at the tibia. Leukocyte NADPH-oxidase activity was reduced; leukocyte CD11b and plasma TNF-alpha levels were unchanged.
Conclusion Chronic ZOL treatment causes a distinct microcirculatory inflammatory reaction in the mandibular periosteum but not in the tibia. The local reaction in the absence of augmented systemic leukocyte inflammatory activity suggests that topically different, endothelium-specific changes may play a critical role in the pathogenesis of MRONJ.
Clinical relevance This model permits for the first time to explore the microvascular processes in the mandibular periosteum after chronic ZOL treatment. This approach may contribute to a better understanding of the pathomechanism and the development of strategies to counteract bisphosphonate-induced side effects.

Keywords Mandibular periosteum · Intravital fluorescence videomicroscopy · Leukocytes · Inflammation · Bisphosphonate · Osteonecrosis

Ágnes Janovszky and Andrea Szabó contributed equally to this work.

Á. Janovszky · R. Varga · J. Piffkó
Department of Oral and Maxillofacial Surgery, University of Szeged, Szeged, Hungary

A. Szabó (✉) · D. Garab · M. Boros · C. Mester · N. Beretka
Institute of Surgical Research, University of Szeged, Szőkefalvi-Nagy Béla 6, Szeged H-6720, Hungary
e-mail: szabo.andrea.exp@med.u-szeged.hu

T. Zombori
Department of Pathology, University of Szeged, Szeged, Hungary

H.-P. Wiesmann · R. Bernhardt
Institute of Materials Science, Max Bergmann Center of Biomaterials, TU Dresden, Dresden, Germany

I. Ocsovszki
Department of Biochemistry, University of Szeged, Szeged, Hungary

P. Balázs
Department of Image Processing and Computer Graphics, University of Szeged, Szeged, Hungary

Introduction

Bisphosphonates (BISs) are widely used for the treatment of osteoporosis and tumors with bone metastasis. The therapeutic effect is linked to the inhibition of osteoclast activity, which alters the bone metabolism by inhibiting bone resorption and reducing the bone turnover [1]. Although BIS treatment undoubtedly improves the quality of life of the patients, osteonecrosis is a serious adverse effect in a number of cases [2]. BIS-related osteonecrosis of the jaw (recently termed as

Published online: 30 October 2014

medication-related osteonecrosis of the jaw; MRONJ) occurs mainly after invasive dental procedures, e.g., tooth extraction [3], with an increased incidence particularly after the use of third-generation BISs (e.g., zoledronate, ZOL) [1]. MRONJ most probably has a multifactorial etiology and is influenced by numerous factors, including the administration route and dose, the duration of the therapy, the indication of BIS administration (osteoporosis or oncological reason), co-morbidities, the concomitant use of other drugs (corticosteroids or chemotherapeutics), genetic factors, age, and poor oral hygiene [1, 3]. Local contamination and infection evoked by invasive dental procedures in the presence of BIS treatment have also been emphasized in the development of MRONJ [4]. Osteonecrosis, however, can develop several years later, which may be explained by the long half-lives of these medications [1] and not by the acute infectious induction. Moreover, BIS treatment has been shown to cause sterile inflammatory reactions such as aseptic peritonitis [5, 6] and an enhancement of leukocyte–endothelial cell interactions in the knee joint [7]. These effects may be linked to an upregulation of pro-inflammatory cytokines such as IL-1 and TNF-alpha [6–8] in response to BIS administration. The effects of BISs also exhibit spatial differences, because certain inflammatory reactions are confined to the mandible and not present in the femur [9]. Nevertheless, the exact pathomechanism of MRONJ has not yet been clarified, and the possibilities of its prevention or the use of curative modalities are also limited.

The periosteal perfusion significantly influences bone healing and determines the prognosis of adjacent soft tissue traumas as well [10]. Little, however, is known about the microcirculatory effects of BIS and especially the microcirculation of the mandible. Likewise, to date, no data are available on the periosteal changes after invasive dental procedures involving BIS treatment. In this study, we hypothesized that a disturbed mandibular microcirculation may play a role in the pathogenesis of MRONJ. With this background, we designed an animal model of MRONJ with the possibility of visualizing the mandibular microcirculation by means of an intravital videomicroscopy (IVM) technique. Our aims were to observe and compare the mandibular and tibial periosteal microcirculatory reactions in rats subjected to chronic ZOL treatment with or without tooth extraction.

Materials and methods

All chemicals were purchased from Sigma-Aldrich (St. Louis, MO, USA) unless indicated otherwise. The study was performed in accordance with the Guidelines laid down by the National Institute of Health (NIH) in the USA regarding the care and use of animals for experimental procedures and with the 2010/63/EU Directive and was approved by the Animal Welfare Committee of the University of Szeged (V/1639/2013).

Experimental protocol

Twenty male Sprague–Dawley rats (average initial body weight of 200±10 g) were randomly allocated to saline vehicle-treated control (n=10) or intravenously (i.v.) ZOL-treated (n=10, ZOL) groups. ZOL (zoledronic acid, Zometa, Novartis Europharm, Budapest, Hungary) was administered through the tail vein in a dose of 80 μg/kg once a week for 8 weeks. At the end of the 3rd week of the protocol, the first and second molar teeth on the right side were extracted from the mandible under ketamine and xylazine (i.p. 25 and 75 mg/kg, respectively) anesthesia. The teeth were luxated with an 18G needle, and the extraction was performed with extraction forceps. The roots were also removed with a dental drill under a Zeiss operating microscope (×6 magnification; Carl Zeiss GmbH, Jena, Germany). By these means, the defect was equal in size and severity in all rats. For pain relief, intramuscular ketoprofen (Ketodex Forte; Berlin-Chemie AG, Berlin, Germany; 5 mg/kg) and oral metamizole sodium (Algopyrin; Sanofi-Aventis, Budapest, Hungary; 75 mg/kg) were administered for 3 days. Mucosal healing processes were monitored continuously throughout the experimental period.

Microcirculatory variables were examined on the 9th week of the protocol. The animals were anesthetized intraperitoneally with an initial dose of sodium pentobarbital (45 mg/kg) and placed in a supine position on a heating pad to maintain the body temperature at 36–37 °C. Following cannulation of the trachea, the penile vein was cannulated for the administration of fluid and drugs (supplementary dose of sodium pentobarbital; 5 mg/kg). This was followed by cannulation of the femoral artery on the right side, and blood was drawn for the white blood cell count and determination of the different markers of leukocyte function/activation and inflammation (see later).

The mandibular periosteum was exposed for fluorescence IVM on both sides, in the vicinity of the earlier extraction area and on the contralateral side, between the anterior part of the deep masseter and the anterior superficial masseter muscles, as described elsewhere [11]. Briefly, an incision was made parallel to the incisor tooth in the facial skin and the underlying subcutaneous tissue, and the loose connective tissue between the fascia of the deep masseter and the anterior superficial masseter muscles was carefully cut, using a microsurgical approach under an operating microscope (×6 magnification; Carl Zeiss GmbH, Jena, Germany). By this means, the periosteal membrane covering the corpus of the mandible at the anterior margin of the molar region was reached, laterally/distally to the incisor tooth. To aid better exposure for the microscope objective, retraction was achieved by placing

stitches with 7.0 monofilament polypropylene microsurgical thread into the surrounding masseter muscles. For comparison of the characteristics of the mandibular microcirculation with those of the tibial periosteum, the medial/anterior surface of the left tibia was exposed by complete transection of the anterior gracilis muscle with microscissors and careful atraumatic microsurgical removal of the connective tissue covering the tibial periosteum [12]. After the IVM recordings of the microcirculation, the animals were over-anesthetized with a single overdose of pentobarbital, and the mandibles were removed and placed into 10 % buffered formalin solution for subsequent detection of osteonecrosis of the mandible through micro-CT and histological analyses.

Fluorescence IVM

The exposed periosteal surfaces of the mandible (on both the extracted and intact sides) and of the tibia were consecutively examined by IVM. The exposed surfaces were positioned horizontally on an adjustable stage and superfused with 37 °C saline. The periosteal microcirculation was visualized by IVM (penetration depth: approx. 250 μm; Zeiss Axiotech Vario 100HD microscope; 100-W HBO mercury lamp; Acroplan 20×/0.5 N.A. W, Carl Zeiss GmbH, Jena, Germany). Fluorescein isothiocyanate-labeled erythrocytes (0.2 ml i.v.) were used to stain red blood cells and rhodamine-6G (0.2 %, 0.1 ml i.v.) to stain leukocytes. Images from four to five fields of the mandibular and the tibial periosteum from each rat were recorded with a charge-coupled device video camera (Teli CS8320Bi, Toshiba Teli Corporation, Osaka, Japan) attached to an S-VHS video recorder (Panasonic AG-MD 830; Matsushita Electric Industrial Co., Tokyo, Japan) and a personal computer.

Video analysis

Quantitative evaluation of the microcirculatory parameters was performed off-line by the frame-to-frame analysis of the videotaped images taken for IVM (IVM Software; Pictron Ltd, Budapest, Hungary). Leukocyte–endothelial cell interactions were analyzed in at least four postcapillary venules per rat. Rolling leukocytes were defined as cells moving with a velocity less than 40 % of that of the erythrocytes in the centerline of the microvessel and passing through the observed vessel segment within 30 s and are given as the number of cells per second per vessel circumference. Adherent leukocytes were defined as cells that did not move or detach from the endothelial lining within an observation period of 30 s and are given as the number of cells per square millimeter of endothelial surface, calculated from the diameter and length of the vessel segment. Red blood cell velocity (RBCV, μm/s) was determined by frame-to-frame analysis of five to six consecutive video-captured images taken after labeling of the erythrocytes.

NADPH-oxidase activity of neutrophil leukocytes

The NADPH-oxidase activity of the isolated leukocytes was determined by a modified chemiluminometric method described by Bencsik et al. [13]. Blood was drawn from the femoral artery into EDTA-containing tubes, and the erythrocytes in 100 μl of whole blood were lyzed in a hypotonic solution and centrifuged at 2000 g. The pellet was resuspended and washed twice in a Dulbecco's phosphate-buffered saline solution. Twenty microliters of resuspended pellet was incubated for 3 min at 37 °C in Dulbecco's solution containing lucigenin (1 mM), EGTA (1 mM) and saccharose (140 mM). NADPH-oxidase activity was determined via the NADPH-dependent increase in luminescence elicited by adding 100 mM NADPH (in 20 μl), measured with an FB12 Single Tube Luminometer (Berthold Detection Systems GmbH, Bad Wildbad, Germany). Samples incubated in the presence of nitroblue tetrazolium served as controls. The measurements were performed in triplicates and were normalized for protein content.

Whole blood free radical production

Ten microliters of blood dissolved in Hanks buffer was incubated for 20 min at 37 °C in lucigenin (5 mM; dissolved in Hanks buffer) or luminol (15 mM; dissolved in Hanks buffer) solution in the presence or absence of zymozan (190 μM, dissolved in Hanks buffer). Superoxide and hydrogen peroxide production were estimated via the zymozan-induced increase in chemiluminescence (measured with the above luminometer) and normalized for leukocyte counts in the peripheral blood.

Expression of CD11b adhesion molecule on neutrophil leukocytes

The surface expression of CD11b on the peripheral blood granulocytes was determined by flow cytometric analysis as detailed elsewhere [12], with a CyFlow ML (Partec GmbH, Münster, Germany).

Plasma TNF-alpha content

Blood samples were centrifuged at 13.500 rpm for 5 min at 4 °C and then stored at 70 °C until assayed. Plasma TNF-alpha concentrations were determined in duplicate by means of a commercially available ELISA kit (R&D Systems, Minneapolis, MN, USA).

Evaluation of the gingival lesions

Healing of the gingiva at the end of the study period (6 weeks after the tooth extraction) was determined on the basis of an osteonecrosis staging system provided by the American Association of Oral and Maxillofacial Surgeons [3]; this was adapted for rats (see Table 1). The examination was performed under an operating microscope (×6 magnification; Carl Zeiss GmbH, Jena, Germany) by an independent maxillofacial surgeon. The incidence and the severity of the gingival healing disorder were evaluated simultaneously.

Mandibular osteonecrosis as determined by micro-CT

Mandibles fixed with formaldehyde were used for micro-CT imaging (SCANCO vivaCT 75; Scanco Medical, Brüttisellen, Switzerland); subsequent analysis was performed on 2D sections in the coronal view of the images, the section being chosen that showed the highest degree of tissue defect at the earlier extraction site. The mean density of the bone was estimated via the calculated percentage of the radiolucent area of the alveolar portion of the bone.

Mandibular osteonecrosis as determined by histology

The specimens were fixed in 6 % neutral buffered formalin for 10 days, then rinsed in phosphate-buffered saline and decalcified in 5 % EDTA for 7 days. The decalcified specimens were embedded in paraffin and cut into 20 semi-serial sections with a microtome (Shandon Finesse 325; Thermo Scientific, Waltham, MA, USA), and routine hematoxylin and eosin (H&E) staining was performed. The sections were examined under a light microscope at ×4–40 magnification (Model CHT; Olympus, Hamburg, Germany). The incidence of osteonecrosis of the jaw was determined on the basis of characteristic signs of necrosis, such as missing nuclear staining, the development of sequester formation and inflammatory infiltration.

Table 1 Scoring of macroscopic signs of the bisphosphonate-related healing processes after tooth extraction (adopted from the staging of MRONJ by Ruggiero et al. [3])

Score	Exposed bone	Inflammation/infection	Fistula formation
Score 0	−	−	−
Score 1	+	−	−
Score 2	+	+	−
Score 3	+	+	+

Statistical analysis

The statistical analysis was performed with a statistical software package (SigmaStat for Windows; Jandel Scientific, Erkrath, Germany). For the analysis of microcirculatory parameters, changes in variables within and between groups (with respect to location and treatment, separately) were analyzed by the two-way ANOVA test, followed by the Holm–Sidak test. Differences between groups (other inflammatory parameters and scores) were analyzed with the Student *t* test. Data are presented as mean values and SEM in all Figures and Tables. *P* values <0.05 were considered significant.

Results

Microcirculatory inflammatory reactions

IVM recordings of the microcirculation were performed in a mandibular periosteal region just adjacent to the site of the

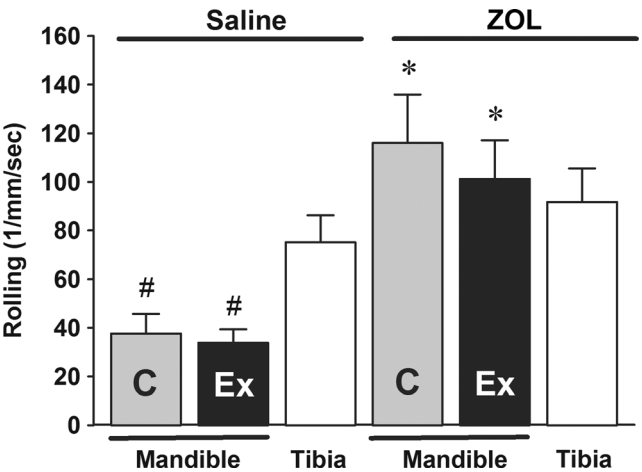

Fig. 1 Periosteal primary leukocyte–endothelial cell interactions (rolling) in saline- and ZOL-treated animals in the postcapillary venules of the mandible on the tooth extraction (*Ex*) and the contralateral (*C*) sides and in the tibia. Data are presented as means±SEM. *Asterisk* indicates $P<0.01$ vs. the corresponding saline-treated group. The *pound sign* indicates $P<0.05$ vs. the tibia. Two-way ANOVA was followed by the Holm–Sidak test

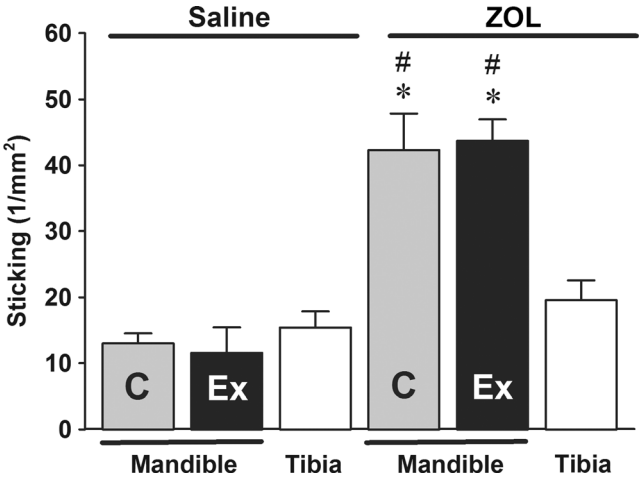

Fig. 2 Periosteal secondary leukocyte–endothelial cell interactions (sticking) in the postcapillary venules of the mandible on the tooth extraction (*Ex*) and the contralateral (*C*) sides and in the tibia in saline- and ZOL-treated animals. Data are presented as means±SEM. *Asterisk* indicates $P<0.01$ vs. the corresponding saline-treated group. The *pound sign* indicates $P<0.01$ vs. the tibia. Two-way ANOVA was followed by the Holm–Sidak test

earlier tooth extraction and also on the contralateral side. Data were compared with those on the tibial periosteum.

In vivo microscopy revealed homogenous microvascular perfusion in all of the periosteal tissues examined; the RBCVs were similar in the mandibular and tibial capillary beds (827.5±30.1 μm/s and 739.0±37.7 μm/s, respectively). The data were similar on the two sides of the mandible and were not influenced by chronic ZOL treatment (data not shown).

However, the leukocyte rolling in the postcapillary venules of the mandible in the ZOL-treated group was significantly higher than in the saline-treated group both at the site of tooth extraction and on the contralateral side; the differences between the sites were not statistically significant (Fig. 1). Similar differences were observed in the leukocyte adhesion values after ZOL, which revealed a statistically significant enhancement in the mandibular periosteum as compared with the tibial periosteum (Fig. 2). ZOL evoked similar rolling and adhesion values irrespectively of the presence of MRONJ (data not shown). The tibial microcirculation was characterized by higher leukocyte rolling but similar adhesion in comparison with the data obtained for the mandible in the saline-treated animals; none of them were influenced by ZOL at this location.

Free radical production of leukocytes

The NADPH-oxidase activity of the neutrophil leukocytes harvested from ZOL-treated animals was significantly lower than that from the control animals (Fig. 3a). The free radical-derived chemiluminescence of the whole blood (as determined by the superoxide and hydroxyl radical-dependent chemiluminescence measurements) indicated no differences between the two experimental groups (Fig. 3b).

Other inflammatory parameters

To exclude the possibility of increased leukocyte counts behind the increased PMN rolling and adhesion after ZOL treatment, the number of PMNs was determined with the conventional Türk solution staining method and using a hemocytometer. As expected, the number of PMN leukocytes was not higher (but rather even lower) in the rats chronically treated with ZOL (Table 2).

As evidenced by the mean fluorescence values of the adhesion molecule CD11b within the leukocyte population (as measured by flow cytometry), no significant differences were detected between the saline- and ZOL-treated animals (Table 2).

There were no differences between the saline- and ZOL-treated experimental groups with respect to the plasma TNF-alpha levels either ($n=6$ and $n=5$, respectively) (Table 2).

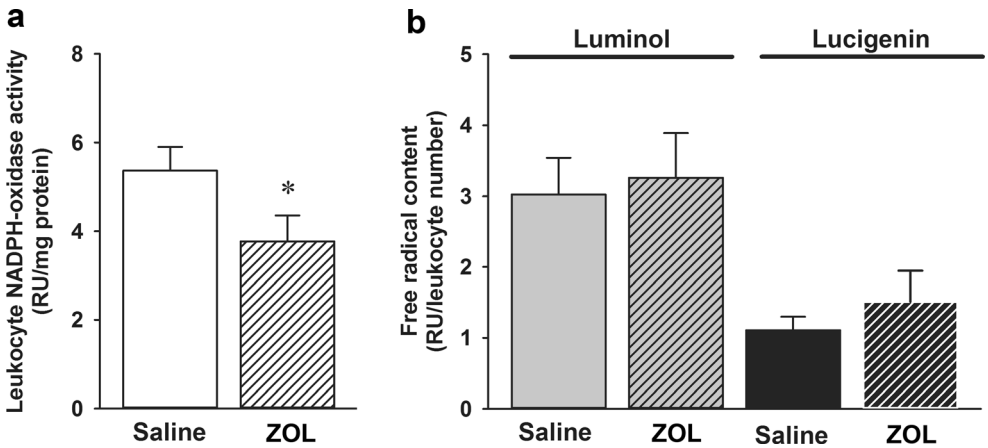

Fig. 3 The effects of chronic ZOL treatment on leukocyte NADPH-oxidase activity (**a**) and whole blood free radical production (**b**) (the latter shown by chemiluminescence in the presence of lucigenin and luminol to detect superoxide anion and hydroxyl radical production, respectively). Data are presented as means±SEM. *Asterisk* indicates $P<0.05$ vs. saline, Student *t*- test

Table 2 The effects of chronic ZOL treatment on the leukocyte count, neutrophil-derived CD11b adhesion molecule expression and plasma TNF-alpha levels

Parameter	Saline	ZOL	*P* values
PMN leukocyte count in the blood (cells/μl)	4513±250	3731±215	<0.05
CD11b expression (mean fluorescence intensity)	1.57±0.21	1.37±0.09	n. s.
TNF-alpha (pg/ml)	2.65±0.49	2.33±0.39	n. s.

Data are presented as mean±SEM. $P<0.05$ vs. saline, Student *t* test

n. s. not significant

Gingival healing after tooth extraction

Six weeks after the tooth extraction, intact mucosa could be observed in 8/10 of the control animals (the average healing score was 0.25±0.25), but different degrees of mucosal healing disorders were detected in all (10/10) of the ZOL-treated animals. The severity of the healing disorders reached a score of 1.83±0.18 in this group ($p<0.01$).

Incidence and severity of mandibular osteonecrosis

Normal bony regeneration with a radiolucent areas of 12.09± 1.91 % of the alveolar bone could be detected at the site of the earlier tooth extraction in all (10/10) of the saline-treated animals. In contrast, a certain degree of discontinuity of the cortical and spongious bone regions was found in 7/10 of the ZOL-treated animals (Fig. 4). This higher incidence of impaired bony regeneration was accompanied by a significantly lower average bone density in this group (39.51±7.18 % of the alveolar area) as compared with that in the saline-treated group ($p<0.01$).

The radiological diagnosis of mandibular osteonecrosis was confirmed by standard histological examinations (Fig. 5). Findings of missing nuclear staining in the osteocytes increased inflammatory infiltration and granulation tissue formation around the necrotic area, and occasional sequester formation were made in 6/10 of the ZOL-treated animals, whereas nearly normal bone regeneration was observed in the other rats.

Discussion

The major aim of the present study was to examine the mandibular periosteal microcirculatory reactions in a rodent model of MRONJ. Through the chronic administration of high i.v. doses of ZOL in combination with an invasive dental intervention, a high prevalence of mucosal healing disorders (~100 %) was achieved together with a relatively high osteonecrosis rate (70 %; as revealed by micro-CT and histological analyses). This protocol was based on a modified literature method [14]. BIS doses in the range 20–2250 μg/kg with different frequencies and different administration routes have been administered by others (for a meta-analysis [15]). The relatively high dose applied here (80 μg/kg/week) is still well tolerated in rats, and although it was also administered in a higher frequency than on human use, it produced symptoms and radiological evidence similar to those observed in humans. Apart from the dose of ZOL, the relatively high incidence of MRONJ in this study can be explained by (1) the triggering effect of the applied dental extraction (the

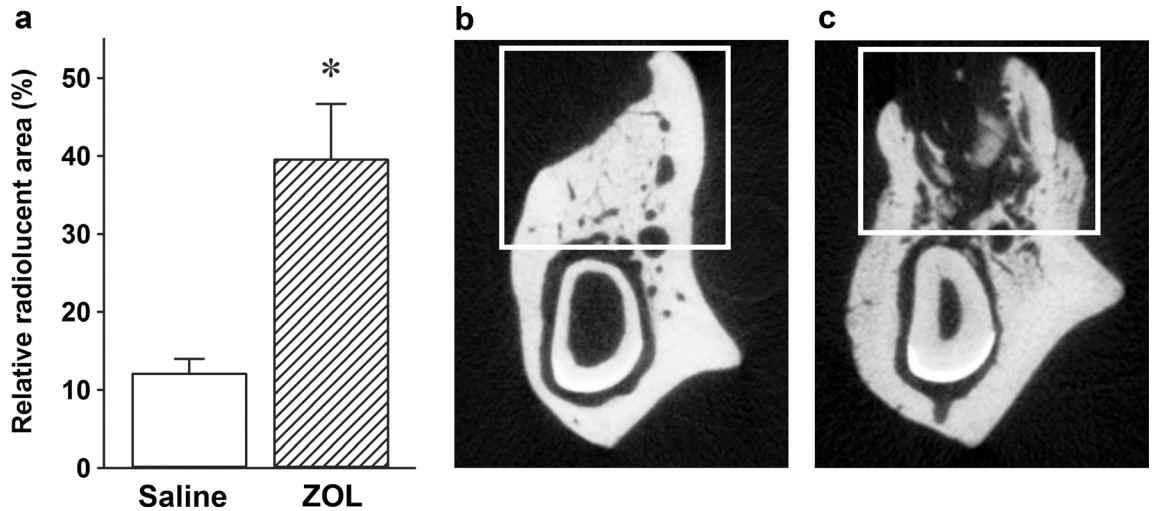

Fig. 4 Bone density differences expressed as a percentage of the radiolucent area of the alveolar bone (marked with a *rectangle*) in saline- and BIS-treated animals 6 weeks after tooth extraction (**a**). Data are presented as means±SEM. *Asterisk* indicates $P<0.05$ vs. saline, Student *t* test. Micro-CT scans show representative images of the mandibular cross-sections in saline- and ZOL-treated rats (**b** and **c**, respectively)

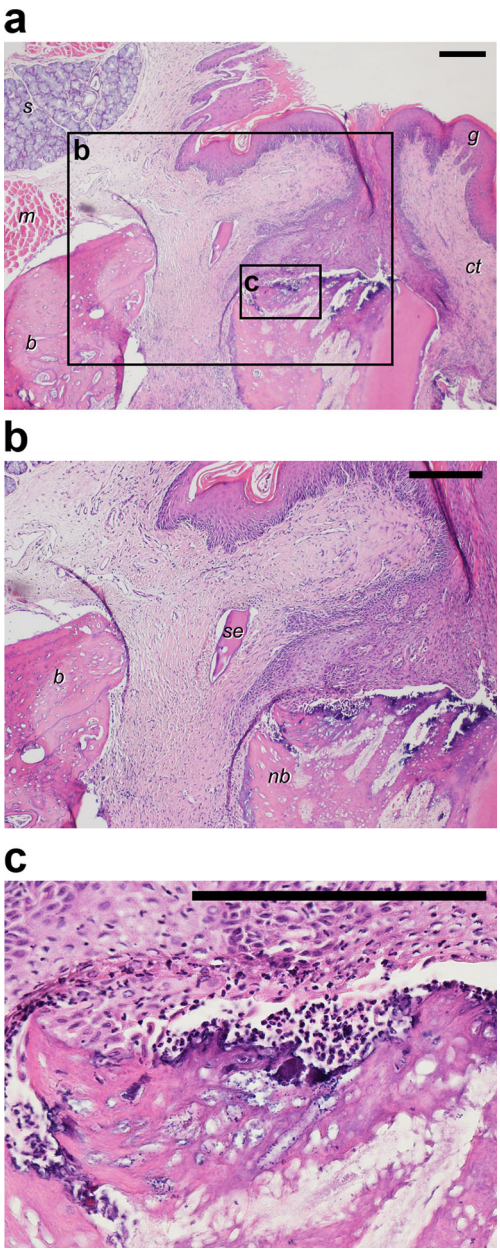

Fig. 5 Representative micrograph (H&E staining) showing regeneration processes in a ZOL-treated animal 6 weeks after tooth extraction (magnification ×4) (**a**). *s* salivary gland, *m* muscle, *b* bone, *g* gingiva, *ct* connective tissue. Sequester formation (*se*) and lack of nuclear staining of the necrotic bone (*nb*) and PMN granulocyte infiltration around the necrotic area (*center* of the section) can be seen at higher magnifications (magnifications ×10 and 40) (**b**, and **c**, respectively). The *bar* denotes 200 μm

importance of which has been demonstrated in MRONJ patients) [3]) and (2) the use of the mandibular site (there is a higher prevalence of osteonecrosis at this localization in humans) [16].

It is reasonable to assume that impaired regeneration processes contribute to the pathophysiology of MRONJ. From a functional aspect, bony regeneration processes depend not only on the functional activity of the osteoblasts and osteoclasts but also on the blood supply and angiogenesis. BISs have been shown to influence all of these processes. As such, the inhibition of osteoclast recruitment to the bone surface [17] and shortening of the osteoclast life span are the main effects of BISs that are brought about directly or indirectly (via the OPG-RANKL pathway) [18]. Accordingly, delayed bone healing [19, 20], together with decreased bone formation and vascularity in the extraction socket, have been detected in ZOL-treated rats [21]. Numerous studies have elucidated the antiangiogenic effects of BIS both in vitro [22] and in vivo [20, 23]. Furthermore, thicker and less connected/ordered blood vessels in the alveolar bone of the mandible were found in ZOL-treated rats after tooth extraction [24]. The aim of the present study was to assess not the structural but the functional aspects of chronic BIS treatment on the microvasculature.

Direct toxic and inflammatory effects of BISs may also contribute to the development of MRONJ. BISs exert toxic effects on many different cell types (fibroblasts, osteoblasts, and endothelial and epithelial cells), manifested in diminished cell proliferation and decreased collagen production, ZOL being the most inhibitory in this respect [25–27]. Furthermore, marked inflammatory reactions are attributed to BISs through the induction of peritonitis via the activation of immunological pathways after intraperitoneal administration [5, 6, 28]. Enhanced leukocyte–endothelial interactions have been demonstrated by means of IVM after BIS treatment in an arthritis model in mice [7]. BIS-associated inflammatory bony changes have also been detected in the mandible [9, 29]. Interestingly, these inflammatory changes were limited to the mandible and were not seen in the femur or the tibia [9, 29]. High-dose ZOL exacerbates the inflammatory response in a periodontitis model, where the bone lesions strikingly resemble MRONJ [21]. In the present study, pro-inflammatory aspects of chronic BIS treatment could also be traced in the mandibular periosteum, and histological analysis supported the infiltration of the tissue by leukocytes in the neighboring necrotic zone.

In this microsurgical model, the periosteal microcirculation of the mandible can be visualized relatively easily in the molar region, which is likewise a cardinal localization of MRONJ [3]. Apart from nutritive considerations, the periosteum is important for its osteoprogenitor cell content during bone regeneration. Although BISs exert effects on osteoblast proliferation, differentiation and migration in the entire skeleton [30], their action seems to depend on the anatomical location, with the jawbones as highly frequent sites of osteonecrosis. After prolonged use, BISs are known to accumulate in the skeleton, reaching the highest concentration in the mandible [25, 31], which may explain their potential toxic effects predominantly in the jawbones. Furthermore, osteoblasts have different proliferation properties at different locations (appendicular vs. axial bones) under physiological circumstances,

and this phenomenon is also critically influenced by BIS treatment [32]. The functional activity of the osteocytes too differs between the mandible and the tibia [33], and the aggravating effects of BISs on bone healing are confined to the jaw [34]. Although the above findings reveal certain potential factors contributing to the higher incidence of osteonecrosis of the jawbones, the exact pathomechanism is unknown.

As opposed to the microcirculatory consequences of bone injury (i.e. fractures) [35], the effects of tooth extraction on the microcirculatory derangement and local inflammation are less commonly described, due to methodological constraints. We focus here on the microcirculatory aspects of chronic ZOL treatment combined with an earlier local trauma of the jaw (tooth extraction). IVM data were obtained in the proximity of the injury and from a contralateral (intact) site on the mandibular periosteum and were compared with those relating to the intact tibia. After chronic ZOL treatment, increased degrees of leukocyte–endothelial interactions (rolling and adhesion) were observed in the mandibular periosteum, both at the site of the earlier tooth extraction and at the contralateral site, but the corresponding interactions in the tibia were less extensive. It is still an unanswered question why the examined cell-to-cell interactions are higher in the postcapillary venules of the mandible, irrespectively of the proximity of the tooth extraction site and the presence of MRONJ in the ZOL-treated group. In preliminary studies, we did not observe inflammatory complications in the mandibular periosteum without tooth extraction, which demonstrated the triggering effect of the trauma in this region. This observation was supported by further findings, when more intense inflammatory reactions of ZOL were evolved in the acute phase after tooth extraction (data not shown). The inflammatory processes were similarly shown in an IVM study to be aggravated by a BIS in an arthritis model in mice [7]. Elevated levels of the pro-inflammatory cytokine TNF-alpha have been reported in human patients in response to certain types of BISs [8] but were not detected after the chronic administration of a BIS in our study. Furthermore, the number and functional activity (free radical-producing capacity) of PMNs were moderately reduced here. Such effects on the free radical-producing potential of PMNs (including NADPH-oxidase activity) have also been demonstrated by others [36, 37]. Favot et al. suggested that the compromised neutrophil functions, too, may be used as potential biomarkers for MRONJ susceptibility [38]. Interestingly, others have found impaired neutrophil chemotaxis after BIS exposure in mice [36] and humans [38], and this parameter is influenced most extensively by ZOL among the different types of BISs [39]. For leukocyte–endothelial interactions (as seen in our study), an enhanced expression of adhesion molecules is required on the surface of the endothelial cells and/or neutrophil leukocytes [40]. Interestingly, expression of the neutrophil-derived adhesion molecule CD11b (responsible for leukocyte adherence) was not found to be influenced by chronic ZOL treatment here or in other studies. The extents of these inflammatory reactions, however, differed in the jaw and the tibial regions. These regional differences might be explained by different degrees of endothelium-derived adhesion molecule expression at the different anatomical locations.

Conclusions

A causative relationship between the microcirculatory inflammatory reactions and the pathogenesis of MRONJ could not be provided in the present study; regional differences in endothelial function/dysfunction, however, may contribute to the explanation of differences in the occurrence of osteonecrosis seen at different anatomical locations.

Acknowledgments This publication is supported by the European Union and co-funded by the European Social Fund. Research grants: TÁMOP 4.2.4. A/2-11-1-2012-0001 "National Excellence Program—Elaborating and operating an inland student and researcher personal support system convergence program;" TÁMOP 4.2.1/B-09/1/KONV-2010-0005; TÁMOP 4.2.2A-11/1/KONV-2012-0035; TÁMOP 4.2.2A-11/1/KONV-2012-0073 "Telemedicine-focused research activities on the field of Mathematics, Informatics and Medical sciences," and OTKA 109388.

Conflict of interest The authors declare that they have no conflict of interest.

References

1. Brozoski MA, Traina AA, Deboni MC, Marques MM, Naclério-Homem Mda G (2012) Bisphosphonate-related osteonecrosis of the jaw. Rev Bras Reumatol 52(2):265–270. doi:10.1590/S0482-50042012000200010
2. Marx RE (2003) Pamidronate (Aredia) and zoledronate (Zometa) induced avascular necrosis of the jaws: a growing epidemic. J Oral Maxillofac Surg 61(9):1115–1117. doi:10.1016/S0278-2391(03)00720-1
3. Ruggiero SL, Dodson TB, Assael LA, Landesberg R, Marx RE, Mehrotra B (2009) Task force on bisphosphonate-related osteonecrosis of the jaws, American Association of Oral and Maxillofacial Surgeons (2009) American Association of Oral and Maxillofacial Surgeons position paper on bisphosphonate-related osteonecrosis of the jaw—2009 update. Aust Endod J 35(3):119–130. doi:10.1111/j.1747-4477.2009.00213.x
4. Wei X, Pushalkar S, Estilo C, Wong C, Farooki A, Fornier M, Bohle G, Huryn J, Li Y, Doty S, Saxena D (2012) Molecular profiling of oral microbiota in jawbone samples of bisphosphonate-related osteonecrosis of the jaw. Oral Dis 18(6):602–612. doi:10.1111/j.1601-0825.2012.01916.x
5. Calligeros D, Douglas P, Abeygunasekera S, Smith G (1993) Aseptic peritonitis in association with the use of pamidronate. Med J Aust 159(2):144
6. Norton JT, Hayashi T, Crain B, Corr M, Carson DA (2011) Role of IL-1 receptor-associated kinase-M (IRAK-M) in priming of immune

and inflammatory responses by nitrogen bisphosphonates. Proc Natl Acad Sci U S A 108(27):11163–11168. doi:10.1073/pnas.1107899108
7. Zysk SP, Dürr HR, Gebhard HH, Schmitt-Sody M, Refior HJ, Messmer K, Veihelmann A (2003) Effects of ibandronate on inflammation in mouse antigen-induced arthritis. Inflamm Res 52(5):221–226. doi:10.1007/s000110300075
8. Anastasilakis AD, Polyzos SA, Makras P, Sakellariou GT, Bisbinas I, Gkiomisi A, Delaroudis S, Gerou S, Ballaouri I, Oikonomou D, Papapoulos SE (2012) Acute phase response following intravenous zoledronate in postmenopausal women with low bone mass. Bone 50(5):1130–1134. doi:10.1016/j.bone.2012.02.006
9. Senel FC, Kadioglu Duman M, Muci E, Cankaya M, Pampu AA, Ersoz S, Gunhan O (2010) Jaw bone changes in rats after treatment with zoledronate and pamidronate. Oral Surg Oral Med Oral Pathol Oral Radiol Endod 109(3):385–391. doi:10.1016/j.tripleo.2009.10.011
10. Schaser KD, Zhang L, Haas NP, Mittlmeier T, Duda G, Bail HJ (2003) Temporal profile of microvascular disturbances in rat tibial periosteum following closed soft tissue trauma. Langenbecks Arch Surg 388(5):323–330. doi:10.1007/s00423-003-0411-5
11. Varga R, Janovszky A, Szabó A, Garab D, Bodnár D, Boros M, Neunzehn J, Wiesmann HP, Piffkó J (2014) A novel method for in vivo visualization of the microcirculation of the mandibular periosteum in rats. Microcirculation (in press) doi: 10.1111/micc.12128
12. Varga R, Török L, Szabó A, Kovács F, Keresztes M, Varga G, Kaszaki J, Boros M (2008) Effects of colloid solutions on ischemia-reperfusion-induced periosteal microcirculatory and inflammatory reactions: comparison of dextran, gelatin, and hydroxyethyl starch. Crit Care Med 36(10):2828–2837. doi:10.1097/CCM.0b013e318186ff48
13. Bencsik P, Kupai K, Giricz Z, Görbe A, Pipis J, Murlasits Z, Kocsis GF, Varga-Orvos Z, Puskás LG, Csonka C, Csont T, Ferdinandy P (2010) Role of iNOS and peroxynitrite-matrix metalloproteinase-2 signaling in myocardial late preconditioning in rats. Am J Physiol 299(2):H512–518. doi:10.1152/ajpheart.00052.2010
14. Biasotto M, Chiandussi S, Zacchigna S, Moimas S, Dore F, Pozzato G, Cavalli F, Zanconati F, Contardo L, Giacca M, Di Lenarda R (2010) A novel animal model to study non-spontaneous bisphosphonates osteonecrosis of jaw. J Oral Pathol Med 39(5):390–396. doi:10.1111/j.1600-0714.2009.00878.x
15. Barba-Recreo P, Del Castillo Pardo de Vera JL, García-Arranz M, Yébenes L, Burgueño M (2013) Zoledronic acid - Related osteonecrosis of the jaws. Experimental model with dental extractions in rats. J Craniomaxillofac Surg pii: S1010-5182(13)00304-1. doi: 10.1016/j.jcms.2013.11.005
16. Marx RE, Cillo JE Jr, Ulloa JJ (2007) Oral bisphosphonate-induced osteonecrosis: risk factors, prediction of risk using serum CTX testing, prevention, and treatment. J Oral Maxillofac Surg 65(12):2397–2410. doi:10.1016/j.joms.2007.08.003
17. Rodan GA, Fleisch HA (1996) Bisphosphonates: mechanisms of action. J Clin Invest 97(12):2692–2696. doi:10.1172/JCI118722
18. Maruotti N, Corrado A, Neve A, Cantatore FP (2012) Bisphosphonates: effects on osteoblast. Eur J Clin Pharmacol 68(7):1013–1018. doi:10.1007/s00228-012-1216-7
19. Yamashita J, Koi K, Yang DY, McCauley LK (2011) Effect of zoledronate on oral wound healing in rats. Clin Cancer Res 17(6):1405–1414
20. Kobayashi Y, Hiraga T, Ueda A, Wang L, Matsumoto-Nakano M, Hata K, Yatani H, Yoneda T (2010) Zoledronic acid delays wound healing of the tooth extraction socket, inhibits oral epithelial cell migration, and promotes proliferation and adhesion to hydroxyapatite of oral bacteria, without causing osteonecrosis of the jaw, in mice. J Bone Miner Metab 28(2):165–175. doi:10.1007/s00774-009-0128-9
21. Aguirre JI, Akhter MP, Kimmel DB, Pingel JE, Williams A, Jorgensen M, Kesavalu L, Wronski TJ (2012) Oncologic doses of zoledronic acid induce osteonecrosis of the jaw-like lesions in rice rats (Oryzomys palustris) with periodontitis. J Bone Miner Res 27(10):2130–2143. doi:10.1002/jbmr.1669
22. Wood J, Bonjean K, Ruetz S, Bellahcène A, Devy L, Foidart JM, Castronovo V, Green JR (2002) Novel antiangiogenic effects of the bisphosphonate compound zoledronic acid. J Pharmacol Exp Ther 302(3):1055–1061. doi:10.1124/jpet.102.035295
23. Pabst AM, Ziebart T, Ackermann M, Konerding MA, Walter C (2014) Bisphosphonates' antiangiogenic potency in the development of bisphosphonate-associated osteonecrosis of the jaws: influence on microvessel sprouting in an in vivo 3D Matrigel assay. Clin Oral Investig 18(3):1015–1022. doi:10.1007/s00784-013-1060-x
24. Guevarra CS, Borke JL, Stevens MR, Bisch FC, Zakhary I, Messer R, Gerlach RC, Elsalanty ME (2013) Vascular alterations in the Sprague-Dawley rat mandible during intravenous bisphosphonate therapy. J Oral Implantol (in press) doi: 10.1563/AAID-JOI-D-13-00074
25. Reid IR, Bolland MJ, Grey AB (2007) Is bisphosphonate-associated osteonecrosis of the jaw caused by soft tissue toxicity? Bone 41(3):318–320. doi:10.1016/j.bone.2007.04.196
26. Scheper MA, Badros A, Chaisuparat R, Cullen KJ, Meiller TF (2009) Effect of zoledronic acid on oral fibroblasts and epithelial cells: a potential mechanism of bisphosphonate-associated osteonecrosis. Br J Haematol 144(5):667–676. doi:10.1111/j.1365-2141.2008.07504.x
27. Açil Y, Möller B, Niehoff P, Rachko K, Gassling V, Wiltfang J, Simon MJ (2012) The cytotoxic effects of three different bisphosphonates in-vitro on human gingival fibroblasts, osteoblasts and osteogenic sarcoma cells. J Craniomaxillofac Surg 40(8):e229–235. doi:10.1016/j.jcms.2011.10.024
28. Yamaguchi K, Motegi K, Iwakura Y, Endo Y (2000) Involvement of interleukin-1 in the inflammatory actions of aminobisphosphonates in mice. Br J Pharmacol 130(7):1646–1654. doi:10.1038/sj.bjp.0703460
29. Yu YY, Lieu S, Hu D, Miclau T, Colnot C (2012) Site specific effects of zoledronic acid during tibial and mandibular fracture repair. PLoS One 7(2):e31771. doi:10.1158/1078-0432.CCR-10-1614
30. Koch FP, Wunsch A, Merkel C, Ziebart T, Pabst A, Yekta SS, Blessmann M, Smeets R (2011) The influence of bisphosphonates on human osteoblast migration and integrin aVb3/tenascin C gene expression in vitro. Head Face Med 7(1):4. doi:10.1186/1746-160X-7-4
31. Wen D, Qing L, Harrison G, Golub E, Akintoye SO (2011) Anatomic site variability in rat skeletal uptake and desorption of fluorescently labeled bisphosphonate. Oral Dis 17(4):427–432. doi:10.1111/j.1601-0825.2010.01772.x
32. Marolt D, Cozin M, Vunjak-Novakovic G, Cremers S, Landesberg R (2012) Effects of pamidronate on human alveolar osteoblasts in vitro. J Oral Maxillofac Surg 70(5):1081–1092. doi:10.1016/j.joms.2011.05.002
33. Çankaya M, Cizmeci Şenel F, Kadioglu Duman M, Muci E, Dayisoylu EH, Balaban F (2013) The effects of chronic zoledronate usage on the jaw and long bones evaluated using RANKL and osteoprotegerin levels in an animal model. Int J Oral Maxillofac Surg 42(9):1134–1139. doi:10.1016/j.ijom.2013.02.008
34. Kuroshima S, Entezami P, McCauley LK, Yamashita J (2014) Early effects of parathyroid hormone on bisphosphonate/steroid-associated compromised osseous wound healing. Osteoporos Int 25(3):1141–1150. doi:10.1007/s00198-013-2570-8
35. Zhang L, Bail H, Mittlmeier T, Haas NP, Schaser KD (2003) Immediate microcirculatory derangements in skeletal muscle and periosteum after closed tibial fracture. J Trauma 54(5):979–985. doi:10.1097/00005373-200305000-00022
36. Kuiper JW, Forster C, Sun C, Peel S, Glogauer M (2012) Zoledronate and pamidronate depress neutrophil functions and survival in mice. Br J Pharmacol 165(2):532–539. doi:10.1111/j.1476-5381.2011.01592.x

37. Yamagishi S, Matsui T, Nakamura K, Takeuchi M (2005) Minodronate, a nitrogen-containing bisphosphonate, inhibits advanced glycation end product-induced vascular cell adhesion molecule-1 expression in endothelial cells by suppressing reactive oxygen species generation. Int J Tissue React 27(4):189–195
38. Favot CL, Forster C, Glogauer M (2013) The effect of bisphosphonate therapy on neutrophil function: a potential biomarker. Int J Oral Maxillofac Surg 42(5):619–626. doi:10.1016/j.ijom.2012.12.011
39. Hagelauer N, Pabst AM, Ziebart T, Ulbrich H, Walter C (2014) In vitro effects of bisphosphonates on chemotaxis, phagocytosis, and oxidative burst of neutrophil granulocytes. Clin Oral Investig (in press) doi: 10.1007/s00784-014-1219-0
40. Eppihimer MJ, Granger DN (1997) Ischemia/reperfusion-induced leukocyte-endothelial interactions in postcapillary venules. Shock 8(1):16–25. doi:10.1097/00024382-199707000-00004

IV.

International Journal of Oral & Maxillofacial Surgery

Official Publication of the International Association of Oral and Maxillofacial Surgeons

IJOMS Editorial Office
Health Sciences, Elsevier Ltd, The Boulevard, Langford Lane, Kidlington, Oxford OX5 1GB, UK
Tel: +44 (0) 1865 843270; Fax: +44 (0) 1865 843992; Email: IJOMS@elsevier.com.
Online manuscript submission: http://ees.elsevier.com/ijoms
Journal homepage: www.ijoms.com

International Association of Oral and Maxillofacial Surgeons
5550 Meadowbrook Drive, Suite 210,
Rolling Meadows, IL 60008, USA.
Tel: 224-232-8737; Fax: 224-735-2965
Email: info@iaoms.org
IAOMS homepage: www.iaoms.org

T3.OR007

Use of antibiotic beads in the management of bisphosphonate-related osteonecrosis of the jaw

M. Esquillo [1,2,3]

[1] *Philippine College Of Oral And Maxillofacial Surgeons, Philippines*
[2] *DLS-STI Medical Center, Philippines*
[3] *Manila Central University, Philippines*

Bisphosphonate Related Osteonecrosis of the Jaw (BRONJ) is a severe complication described as an area of bone in the jaw that has necrosed and been exposed in the mouth for more than eight weeks in a person taking bisphosphonate. Surgical debridement or resection in combination with antibiotic therapy is advised to resolve the acute infection and pain as well as for long-term palliation, particularly for stage 3 cases. The use of antibiotic beads in the management of osteomyelitis, which has similar clinical features with BRONJ, has been described previously. It is hypothesized that the use of antibiotic beads may be beneficial in the management of BRONJ. Two cases diagnosed with stage 3 BRONJ were managed with the use of antibiotic beads. Treatment protocol consists of thorough debridement and curettage to remove infected and necrotic tissue, placement of antibiotic beads, and primary closure of the wound. Removal of the antibiotic beads is then performed after six weeks. Both cases resolved uneventfully. Results suggest that the use of antibiotic beads can be a viable treatment option in the surgical management of stage 3 BRONJ cases. Further clinical and experimental studies are needed to elucidate the exact relationship and mechanisms involved.

Key words antibiotic beads; bisphosphonate; Bronj; osteonecrosis

http://dx.doi.org/10.1016/j.ijom.2013.07.067

T3.OR008

Microcirculatory consequences of chronic bisphosphonate treatment after tooth extraction in a rat model

A. Janovszky [1,*], R. Varga [1], A. Szabó [2], D. Garab [2], M. Boros [2], J. Piffkó [1]

[1] *Department of Oral and Maxillofacial Surgery, Hungary, Europe*
[2] *Institute of Surgical Research, University of Szeged, Szeged, Hungary, Europe*

Background and objectives: Bisphosphonates (BIS) has a beneficial effect in patients whosuffer from osteoporosis and bone metastasis, however, adverse consequences such as osteonecrosis of the jawmayoccur. Our aim was to assess whether inflammatory processes mediated by microcirculatory dysfunction are associated with the development of BIS-related osteonecrosis. This study evaluated themicrocirculatory effects of BIS in the mandibular periosteum after standardizeddental procedures, and in the tibialperiosteum in order to compare the effects of BIS in different osseous locations.

Methods: Sprague-Dawley rats were randomly allotted into vehicle-treated control ($n = 15$) or chronic BIS-treated (ivzoledronate, 80 g/kg once a week, over eight weeks, $n = 20$) groups, respectively. At the end of the chronic treatment, first molarextraction was performed at one side of the mandible. Leukocyte–endothelial interactions were measured at both sides of mandibular periosteum by intravital fluorescence video microscopy as well as in the tibial periosteum. Systemic, inflammatory parameters were measured such as NADPH-oxidase activity of neutrophil leukocytes by luminometry, expression of neutrophil-derived adhesion molecule CD11b by flow cytometry, and plasma levels of TNF-? by ELISA.

Results: Spontaneous osteonecrosis of the jaw could not be revealed by microCT due to BIS. BIS administration increased the leukocyte–endothelial interactionsin the mandibular postcapillary venules compared to the control and tibial periosteum. According to the acute dental procedure, these inflammatory reactions showed a remarkable elevation. NADPH oxidase activity was significantly lower compared to the control. Other parameters were not affected by BIS treatment.

Conclusion: These data provide evidence that chronic BIS treatment is accompanied by characteristic mandibular periosteal microcirculatory inflammatory reactions which are enhanced after an acute dental procedure. This suggests a potential role for leukocytes in the pathogenesis of BIS-induced osteonecrosis.

Grant support: TÁMOP 4.2.4.A/2-11-1-2012-0001, TÁMOP 4.2.2A-11/1/KONV-2012-0035, TÁMOP 4.2.2A-11/1/KONV-2012-0073

Key words: bisphosphonate-related osteonecrosis of the jaw, rat, microcirculatory inflammation, tooth extraction

http://dx.doi.org/10.1016/j.ijom.2013.07.068

T3.OR009

Epidemiological, clinical, histological, radiological and treatment overview of bronj cases from territory of central serbia and montenegro

D. Jelovac [1,*], S. Antic [1], M. Petrovic [1], M. Antunovic [2], M. Gavric [1]

[1] *Faculty of Dental Medicine*
[2] *Faculty of Medicine, Montenegro*

Bisphosphonates are drugs used in treatment of different pathological conditions that affect bones, such as osteoporosis, metastatic bone disease, Paget disease and osteogenesis imperfecta, etc. The aim of the study is to present epidemiological, radiological, clinical, histopathological data and treatment overview of patients with BRONJ in Serbia and Montenegro. From year 2009 to 2012 at the Clinic for Maxillofacial surgery – Faculty of Dentistry, University of Belgrade and Podgorica 9 patients were referred to Clinics due to BRONJ, as non-healing wound in the jaw after tooth extraction. Among them, 8 were oncological (two patients with breast carcinoma (22.2%), three patients with prostate carcinoma (33.3%), two multiple myeloma patients (22.2%) and one patient with MTC (11.1%)) and one suffering from osteoporosis (11.1%), which underwent BPs therapy. Sex, age, underlying diagnosis, type of BPs therapy, dosage, duration and way of administration, additional therapy, location of osteonecrosis, clinical symptoms and dental extraction were analyzed parameters (age range (from 37 to 84 years); male to female ratio was (6:3). Obtained data showed that 8 of 9 our patients received Zometa (88.9%) (Zoledronic acid), except one woman (11.1%) who received Bonviva (Ibandronic acid). Female patient who received Bonviva was the only patient that had no malignancy, and received bisphosphonates orally because of osteoporosis. The time passed between periods of extraction to the period when signs of bone necrosis were observed ranged from 0 to 5 months. Radiographic findings displayed either radiolucent osteolytic zones, or superficial bone defects, that were consonant with bone necrosis. Histological examination excluded malignancy. We performed